

**CHARACTERIZING THE ROLE OF
SECRETORY PHOSPHOLIPASE A₂ GROUP IIA
IN GLIAL CELL-MEDIATED NEUROTOXICITY**

by

Erika Bianca Villanueva

B.Sc., The University of Waterloo, 2008

A THESIS SUBMITTED IN PARTIAL FULFILLMENT OF
THE REQUIREMENTS FOR THE DEGREE OF

MASTER OF SCIENCE

in

The College of Graduate Studies

(Biology)

THE UNIVERSITY OF BRITISH COLUMBIA
(Okanagan)

April 2011

© Erika Bianca Villanueva, 2011

Abstract

Microglia are a type of non-neuronal glial cell that represent the mononuclear phagocyte system and innate immunity in the central nervous system. Astrocytes are another glial cell type. Under pathological circumstances, both glia types are capable of sustaining chronic inflammation in the brain, which results in neuronal death.

Immune response involves glial secretion of pro-inflammatory mediators. Phospholipases A₂ (PLA₂) convert cell membrane glycerophospholipids into arachidonic acid, which in turn is a precursor to several pro-inflammatory eicosanoids that are released by glial cells. It is well established that secretory PLA₂ group IIA (sPLA₂IIA) is a pro-inflammatory mediator, however little is known about the role this enzyme plays in neurodegeneration. This thesis focuses on sPLA₂IIA and its role in chronic inflammation underlying neurodegenerative disorders such as Alzheimer's and Parkinson's diseases.

Activated astrocytes have been shown to secrete sPLA₂IIA. However, no information is available on sPLA₂IIA expression and regulation in microglia. This thesis hypothesizes that sPLA₂IIA is a toxin secreted by activated glial cells, which causes neuronal death. If sPLA₂IIA contributes to neurotoxicity, then agents that inhibit, modify, or remove sPLA₂IIA from extracellular space should reduce the cytotoxic effects of glial secretions.

The following human cells were used to study sPLA₂IIA expression, secretion and functions: microglia-like promonocytic THP-1 cells, U-373 MG astrocytoma cells, primary human astrocytes and neuroblastoma SH-SY5Y cells. Reverse transcriptase polymerase chain reaction (RT-PCR) revealed that stimulation by pro-inflammatory mediators induced sPLA₂IIA mRNA expression by glial cells. Stimulated glial cell

supernatants were toxic to neuronal SH-SY5Y cells. Stimulation caused increased sPLA₂IIA protein concentrations in supernatants from all three types of glial cells. Despite observing increased sPLA₂IIA-specific enzymatic activity in stimulated glial cell supernatants, neither specific nor non-specific PLA₂ inhibitors exhibited anti-cytotoxic effects. However, the removal of sPLA₂IIA from supernatants by immunosorbents resulted in significantly increased neuronal survival, suggesting that sPLA₂IIA neurotoxicity relies on a non-enzymatic mechanism.

Based on *in vitro* experiments and a literature review, potential sPLA₂IIA neurotoxicity mechanisms are proposed. The data obtained provide valuable information toward a more detailed mechanistic understanding of neuroinflammation and may guide future research toward more effective therapeutic agents for neurodegenerative disorders.

Preface

To date, none of my research on sPLA₂IIA has been published. To experiment with primary human astrocytes, I obtained approval to work with Biosafety Level 2 materials (certificate # B08-0040).

I am responsible for all experimental data and writing presented in this thesis, except for the publication presented in Appendix B. For this publication, I was involved with obtaining fresh porcine tissues and developing the extraction technique for porcine glial cells, in addition to writing parts of the manuscript. V.A. Ionescu was the primary author of the manuscript and was also involved with developing the extraction technique for porcine glial cells. M. Bahniwal was responsible for the tumor necrosis factor- α enzyme-linked immunosorbent assay data, in addition to characterizing the effects of cytokine-stimulated porcine astrocyte supernatants on neuronal SH-SY5Y cells. S. Hashioka produced the immunostaining images of porcine glial cells. A. Klegeris designed the study, wrote a significant portion of the manuscript and is the corresponding author for this study.

Table of Contents

Abstract.....	ii
Preface.....	iv
Table of Contents.....	v
List of Tables.....	ix
List of Figures.....	x
List of Abbreviations and Symbols.....	xii
Acknowledgements.....	xvi
Dedication.....	xvii
1 Introduction.....	1
1.1 Neurodegeneration.....	1
1.1.1 Cells of the Central Nervous System (CNS).....	1
1.1.2 Intercellular Communication between Glial Cells and Neurons.....	1
1.1.2.1 Glia to Glia Communication.....	1
1.1.2.2 Glia to Neuron Interactions.....	2
1.1.3 Neurodegenerative Disorders.....	3
1.1.3.1 Alzheimer’s Disease.....	3
1.1.3.2 Parkinson’s Disease.....	5
1.1.4 Inflammatory Hypothesis of Neurodegeneration.....	6
1.1.5 Cell Culture Models of Neurodegeneration.....	6
1.2 Phospholipases A₂ and Inflammation.....	9
1.2.1 Phospholipase A ₂ Isoforms.....	10
1.2.2 Secretory Phospholipases A ₂ (sPLA ₂).....	11
1.3 sPLA₂IIA.....	12
1.3.1 Structure of sPLA ₂	12
1.3.2 Enzymatic Activity and Known Inhibitors of sPLA ₂	13
1.3.3 Non-Enzymatic Activity of sPLA ₂ IIA.....	15

1.3.4	Pathologies involving sPLA ₂ IIA	16
1.3.4.1	Rheumatoid Arthritis	16
1.3.4.2	Atherosclerosis.....	17
1.3.4.3	Cancer	17
1.3.4.4	Neurodegenerative Disease.....	18
1.3.5	sPLA ₂ IIA Regulation.....	19
1.3.6	Neurotoxic Mechanisms of sPLA ₂ IIA.....	20
1.4	Research Overview and Hypotheses	24
2	Materials and Methods.....	26
2.1	Chemicals and Reagents.....	26
2.2	Equipment	28
2.3	Cell Culture Models.....	29
2.4	Collecting Glial Cell Supernatants.....	30
2.5	Plating SH-SY5Y Cells for Experiments	31
2.6	Cytotoxicity Assays: Lactate Dehydrogenase (LDH)	31
2.7	Cytotoxicity Assays: MTT.....	32
2.8	Cytotoxicity Assays: Live/Dead Immunofluorescence	33
2.9	Immunosorbent Experiments	35
2.10	Enzyme-Linked Immunosorbent Assay (ELISA).....	36
2.11	RNA Isolation and Reverse Transcription (RT).....	37
2.12	Polymerase Chain Reaction (PCR)	40
2.13	PCR Primer Design and Restriction Analyses	41
2.14	Neurotoxicity of Exogenous sPLA₂	43
2.14.1	Bee Venom sPLA ₂ type III (sPLA ₂ III).....	43
2.14.2	Human rsPLA ₂ IIA	43
2.14.3	Bacterial Lipopolysaccharide (LPS).....	44
2.15	Experiments with Enzyme Inhibitors and Receptor Antagonists.....	44
2.15.1	Specific sPLA ₂ Inhibitors	44
2.15.2	Non-Specific PLA ₂ Inhibitors and PGE ₂ Receptor Antagonists	45
2.16	Measurement of PLA₂ Enzymatic Activity.....	46

2.17 Potential Mechanisms of sPLA₂IIA Neurotoxicity	48
2.17.1 Effects of sPLA ₂ IIA on SH-SY5Y Cells Pre-Treated with H ₂ O ₂	48
2.17.2 sPLA ₂ IIA Regulation via PPAR α	49
2.17.3 Non-Enzymatic Complex between sPLA ₂ IIA and Neuronal TLR4	49
2.18 Statistical Analysis	50
3 Results.....	52
3.1 Inflammatory Stimuli Evoke Neurotoxic Glial Cell Response	52
3.2 Neurotoxicity of sPLA₂ Isoforms.....	54
3.3 sPLA₂IIA mRNA Expression by Human Cell Lines and Astrocytes.....	59
3.4 Concentrations of sPLA₂IIA in Glial Cell Supernatants	61
3.5 PLA₂ Enzymatic Activity in Cell Supernatants	62
3.6 Effects of Specific sPLA₂ Inhibitors on Neurotoxicity of Stimulated Glial Cell Supernatants	66
3.7 Removal of sPLA₂IIA from Cell Supernatants.....	70
3.8 Effects of Non-Specific PLA₂ Inhibitors and PGE₂ Receptor Antagonists on THP-1 Cytotoxicity Toward SH-SY5Y Cells.....	73
3.9 Possible Mechanisms of sPLA₂IIA Toxicity	79
3.9.1 Effect of rsPLA ₂ IIA on H ₂ O ₂ -Induced Neurotoxicity	79
3.9.2 Experiments with the PPAR α Antagonist MK886	81
3.9.3 Effects of the Anti-TLR4/MD-2 Antibodies on sPLA ₂ IIA Toxicity Toward SH-SY5Y Cells	84
4 Discussion.....	86
4.1 Neurotoxins Secreted by Stimulated Glial Cells	86
4.1.1 Stimulated Glial Cells Secrete Neurotoxic sPLA ₂ IIA.....	86
4.1.2 Comparison of sPLA ₂ IIA Protein Concentrations in Cell Culture Supernatants with Exogenous sPLA ₂ IIA Concentrations Required to Induce Neurotoxicity.....	87
4.2 Inhibition of sPLA₂IIA Enzymatic Activity	87
4.2.1 sPLA ₂ IIA Enzymatic Activity is Significantly Higher in Stimulated than Unstimulated THP-1 and U-373 MG Cell Supernatants.....	88
4.2.2 sPLA ₂ IIA-Specific Inhibitor Failed to Protect SH-SY5Y Cells from rsPLA ₂ IIA Toxicity or Glial Cell-Induced Neurotoxicity.....	90

4.3 Removal of sPLA₂IIA and PGE₂ from Stimulated Glial Cell Supernatants Significantly Decreased Neuronal Death	91
4.4 Non-Specific PLA₂ Inhibitors and PGE₂ Receptor Antagonists Failed to Protect SH-SY5Y Cells from Glial Cell-Induced Toxicity	92
4.5 Non-Enzymatic Mechanisms of sPLA₂IIA Neurotoxicity	95
4.5.1 H ₂ O ₂ -Induced Neuronal Apoptosis Does Not Enhance rsPLA ₂ IIA Toxicity	96
4.5.2 sPLA ₂ IIA Regulation Through PPAR α Cannot be Confirmed Due to Cytotoxicity of Receptor Antagonist MK886	97
4.5.3 Neuronal TLR4 Does Not Mediate sPLA ₂ IIA Neurotoxicity	98
5 Conclusions.....	100
5.1 Strengths and Limitations of this Study	100
5.2 Future Directions	101
5.3 Significance of Findings.....	103
References.....	105
Appendices.....	116
Appendix A: RNA Purity Values.....	116
Appendix B: Publication	117

List of Tables

Table 1.1:	Classification of PLA ₂ Isoforms	10
Table 2.1:	Non-Specific PLA ₂ Inhibitor and PGE ₂ Receptor Antagonist Targets and their Concentrations Used in Experiments	46

List of Figures

Figure 1.1:	Events Surrounding the Pathological Activation of Glial Cells and Related Neuronal Death	5
Figure 1.2:	Human Cell Culture Model of Neuroinflammation	9
Figure 1.3:	Proposed PLA ₂ Pathways Leading to the Up-Regulation of Endogenous sPLA ₂ IIA mRNA.....	21
Figure 2.1:	Typical Calibration Curve for the sPLA ₂ IIA-Specific ELISA.....	38
Figure 3.1:	Neurotoxicity of Stimulated Glial Cell Models	53
Figure 3.2:	Neurotoxicity of Bee venom sPLA ₂ III.....	55
Figure 3.3:	Neurotoxicity of Human rsPLA ₂ IIA	56
Figure 3.4:	Neurotoxicity of Bacterial LPS and Human IFN- γ at Concentrations Used in Experiments.....	58
Figure 3.5:	sPLA ₂ IIA mRNA Expression in Stimulated and Unstimulated Glial Cells.....	60
Figure 3.6:	sPLA ₂ IIA Protein Concentrations in Stimulated and Unstimulated Glial Cell Supernatants.....	61
Figure 3.7:	PLA ₂ Enzymatic Activity in Stimulated and Unstimulated Glial Cell Supernatants.....	62
Figure 3.8:	Effects of the Specific sPLA ₂ Inhibitors on rsPLA ₂ IIA-Specific Enzymatic Activity.....	63
Figure 3.9:	Effects of the Specific sPLA ₂ Inhibitors on PLA ₂ Enzymatic Activity in Stimulated THP-1 cell Supernatants	64
Figure 3.10:	rsPLA ₂ IIA-Specific Enzymatic Activity in Stimulated and Unstimulated Glial Cell Supernatants	65
Figure 3.11:	Effects of the Specific sPLA ₂ Inhibitors on the Neurotoxicity of Exogenous rsPLA ₂ IIA.....	67
Figure 3.12:	Effects of the Specific sPLA ₂ Inhibitors on the Neurotoxicity of Stimulated THP-1 Cell Supernatants	68
Figure 3.13:	Neuroprotective Effects of the Specific sPLA ₂ Inhibitors	69
Figure 3.14:	Effects of sPLA ₂ IIA- or PGE ₂ -Specific Immunosorbents on Stimulated THP-1 Cell Supernatant Neurotoxicity (LDH and MTT Assays)	71
Figure 3.15:	Effects of sPLA ₂ IIA- or PGE ₂ -Specific Immunosorbents on Stimulated THP-1 Cell Supernatant Neurotoxicity (Live/Dead Immunofluorescence).....	72

Figure 3.16: Effects of sPLA ₂ IIA- or PGE ₂ -Specific Immunosorbents on Stimulated U-373 MG Cell or Human Astrocyte Supernatant Neurotoxicity)	74
Figure 3.17: Cytotoxicity of Non-Specific PLA ₂ Inhibitors Toward THP-1 Cells	75
Figure 3.18: Effects of Non-Specific PLA ₂ Inhibitors on the Neurotoxicity of Stimulated THP-1 Cell Supernatants	77
Figure 3.19: Neuroprotective Effects of Non-Specific PLA ₂ Inhibitors.....	78
Figure 3.20: Effect of rsPLA ₂ IIA on H ₂ O ₂ -Induced Neurotoxicity.....	80
Figure 3.21: Cytotoxicity of PPAR α Antagonist MK886 toward THP-1 Cells.....	82
Figure 3.22: Effects of PPAR α Antagonist MK886 on the Neurotoxicity of Stimulated THP-1 Cell Supernatants	83
Figure 3.23: Neuroprotective Effects of Anti-TLR4/MD-2 mAb	85

List of Abbreviations and Symbols

$\alpha 5\beta 3$	Alpha-5-beta-3 integrin
A β	Amyloid beta (Alzheimer's disease hallmark protein)
AD	Alzheimer's disease
AH6809	6-isopropoxy-9-oxoxanthene-2-carboxylic acid; antagonizes prostaglandin E ₂ receptors 1, 2 and 3
AM	Acetoxymethyl ester (of calcein)
ANOVA	Analysis of variance
α -syn	Alpha-synuclein (Parkinson's disease hallmark protein)
β -NAD	Beta-nicotinamide adenine dinucleotide
bp	Base pair
BPPA	5-(4-benzyloxyphenyl)-4S-(7-phenylheptanoylamino) pentanoic acid; phospholipase A ₂ inhibitor
cAMP	Cyclic adenine monophosphate
cDNA	Complementary deoxyribonucleic acid
CNS	Central nervous system
ConA	Concanavalin A
COX	Cyclooxygenase
cPLA ₂	Cytosolic phospholipase A ₂
d	Difference
DNA	Deoxyribonucleic acid
DMDA	7,7-dimethyl-5,8-eicosadienoic acid; phospholipase A ₂ inhibitor
DMEM-F12	Dulbecco's Modified Eagle's Medium - nutrient mixture Ham's F12
DMF	N,N-dimethylformamide
DMSO	Dimethyl sulfoxide

EDTA	Ethylenediaminetetraacetic acid
ELISA	Enzyme-linked immunosorbent assay
EP ₁₋₄	Prostaglandin E ₂ receptors. (4 known isoforms: EP ₁ , EP ₂ , EP ₃ and EP ₄)
ERK _{1/2}	Extracellular signal-regulated kinases 1 and 2
EthD-1	Ethidium homodimer-1
EtOH	Ethanol
F5	Dulbecco's Modified Eagle's Medium - nutrient mixture Ham's F12 with 5% added fetal bovine serum
F10	Dulbecco's Modified Eagle's Medium - nutrient mixture Ham's F12 with 10% added fetal bovine serum
Fas L	Fas ligand
FBS	Fetal bovine serum
FITC	Fluorescein isothiocyanate
GPCR	Guanine nucleotide-binding protein-coupled receptor
IC ₅₀	Half-maximal inhibitory concentration; the amount of compound required to reduce the effect of a biological process by half
IFN- γ	Interferon-gamma
IL	Interleukin
IL-1 β	Interleukin-1 beta
IL-6	Interleukin-6
INT	Iodonitrotetrazolium chloride
iPLA ₂	Calcium-independent phospholipase A ₂
L-161,982	N-[[4'-[[3-butyl-1,5-dihydro-5-oxo-1-[2-(trifluoromethyl)phenyl]-4H-1,2,4-triazol-4-yl]methyl][1,1'-biphenyl]-2-yl]sulfonyl]-3-methyl-2-thiophenecarboxamide; antagonizes prostaglandin E ₂ receptor 4
LDH	Lactate dehydrogenase (measured as indicator of cell death)
LPS	Lipopolysaccharide
LSD	Least significant difference

mAb	Monoclonal antibody
MAFP	Methyl arachidonyl fluorophosphonate; phospholipase A ₂ inhibitor
MAPK	Mitogen activated protein kinase
MD-2	Lymphocyte antigen 96; associated with toll-like receptor 4 to form a complex targeted by bacterial lipopolysaccharide
Me-indoxam	Secretory phospholipase A ₂ group IIA-specific inhibitor
MK886	Peroxisome proliferator-activated receptor-alpha antagonist
mRNA	Messenger ribonucleic acid
MTT	Formazan dye (measured as indicator of cell viability)
NF-κB	Nuclear factor-kappa-B
NFT	Neurofibrillary tangle (Alzheimer's disease hallmark aggregate)
NFW	Nuclease-free water
OD	Optical density
OPHAO	4-[(1-oxo-7-phenylheptyl)amino]-(4R)-octanoic acid; non-specific PLA ₂ inhibitor
PBS	Phosphate-buffered saline
PCR	Polymerase chain reaction
PD	Parkinson's disease
PG	Prostaglandin
PGE ₂	Prostaglandin E ₂
PGPM	1-hexadecanoyl-2-(1-pyrenedecanoyl)-sn-glycero-3-phosphomethanol; substrate for phospholipase A ₂ enzyme activity assay
PKC	Protein kinase C
PLA ₂	Phospholipase A ₂
PPARα	Peroxisome proliferator-activated receptor-alpha

Ras	Guanine triphosphatase involved in signal transduction; originally identified as a rat sarcoma oncogene product
RO032107	Secretory phospholipase A ₂ group IIA-specific inhibitor
RO041709	Inactive control compound to RO032107
RO092906	Secretory phospholipase A ₂ group X-specific inhibitor
ROS	Reactive oxygen species
RNA	Ribonucleic acid
RNS	Reactive nitrogen species
rsPLA ₂ IIA	Recombinant sPLA ₂ IIA
RT	Reverse transcription
RT-PCR	Reverse transcription polymerase chain reaction
S-2427	Non-steroidal anti-inflammatory compound
SDS	Sodium dodecyl sulfate
SH-SY5Y	Human dopaminergic neuroblastoma cell line (neuron model)
sPLA ₂	Secretory phospholipase A ₂
sPLA ₂ IIA	Secretory phospholipase A ₂ group IIA
sPLA ₂ III	Secretory phospholipase A ₂ group III (found in bee venom)
sPLA ₂ V	Secretory phospholipase A ₂ group V
sPLA ₂ X	Secretory phospholipase A ₂ group X
STAT-3	Signal transducer and activator of transcription type 3
SYBR safe	Deoxyribonucleic acid stain
THP-1	Human immortalized promonocytic leukemia cell line (microglia model)
TLR4	Toll-like receptor 4
TNF- α	Tumor necrosis factor-alpha
U-373 MG	Human immortalized astrocytoma cell line (astrocyte model)
YM-26734-1	Secretory phospholipase A ₂ group IIA-specific inhibitor

Acknowledgements

My sincerest gratitude and utmost respect are offered to my supervisor, Dr. Andis Klegeris, whose wisdom, patience and leadership has taught me the value of perseverance (particularly when faced with embarrassingly difficult super quizzes). Thank you so much for the opportunity to learn from and work with you.

Thank you to Dr. Mark Rheault's laboratory for the use of equipment. Thanks to Drs. Michael Gelb and Rob Oslund for providing samples of rsPLA₂IIA and the specific sPLA₂ inhibitors that were key in the completion of this study. I thank my colleagues at the Laboratory of Cellular and Molecular Pharmacology, whose jovial and honourable spirits motivated me to carry on through both favourable and frustrating circumstances. Thanks to my committee members Dr. Bruce Mathieson and Dr. Mark Rheault, whose leadership helped me maintain perspective from day one of this project. I thank Dr. Jason Loepky for advice with statistical methods and Dr. Mary Forrest for restriction enzymes. In addition, I thank the faculty and staff of the University of British Columbia Okanagan Department of Biology for their continued support and cheerful personalities.

Special thanks are offered to my Parents, my brother Karl, friends and family for steadying my perpetual state of confusion and helping me through my addiction to higher learning despite the temporal, spatial and financial challenges faced. Finally, I thank Andrew, my better half, whose love continues to be my utmost inspiration.

*In loving memory of my grandmother (1920-2010),
whose departure set her free from Alzheimer's disease.*

1 Introduction

1.1 Neurodegeneration

1.1.1 Cells of the Central Nervous System (CNS)

The CNS consists of the brain and the spinal cord. Cellular populations in the brain include approximately 15% neurons and 85% glial cells (Hickey 2001; Rock *et al.* 2004). Neurons are excitable cells that respond to stimuli, communicate with other cells and conduct impulses. Among other functions, glial cells support neurons with vital nutrients and protection. In the CNS, glial cells include: a) oligodendrocytes, which wrap neuronal processes with a myelin sheath allowing rapid conduction of electrical signals within the CNS; b) astrocytes, which are star-shaped glial cells that provide nutrients for neurons; and c) microglia, which represent the innate immune system of the CNS (Aloisi 2001; Hume 2006). This study focuses on microglial, astrocytic and neuronal interactions in the brain; therefore, the terms “glia” and “glial cell” refer to microglia and astrocytes only.

1.1.2 Intercellular Communication between Glial Cells and Neurons

1.1.2.1 Glia to Glia Communication

Microglia are macrophages that belong to the mononuclear phagocyte system; they are derived from progenitor cells in the bone marrow and are thought to have migrated to the CNS during embryonic development (Hume 2006; Rock 2009). Microglia are essential for defense against pathological events that may occur in the CNS (Aloisi 2001; Bessis *et al.* 2007). Astrocytes play a role in potassium homeostasis in the CNS

and communicate to other astrocytes through intercellular gap junctions (Peuchen *et al.* 1997).

Pathological formations (such as amyloid-beta (A β) plaques in Alzheimer's disease (AD)) have been shown to activate both types of glial cells, which release mediators that function to dispose of the formations (Streit *et al.* 2004). Specific pro-inflammatory mediators include cytokines in addition to eicosanoids such as PGE₂ (Town *et al.* 2005), all of which trigger the activation and proliferation of other microglia; these events lead to increased and accelerated neuronal death. Pro-inflammatory cytokines endogenous to the central nervous system include tumor necrosis factor alpha (TNF- α), interleukin (IL)-1 β and IL-6. These pro-inflammatory signals activate other surrounding microglia and astrocytes, ultimately amplifying the immune response (Aloisi 2001; Hashioka *et al.* 2009). The activation and multiplication of glial cells in a way that is detrimental to neurons form basis of neuroinflammation (Mattson 2000; Streit *et al.* 2004).

1.1.2.2 Glia to Neuron Interactions

At rest, glial cells function as support structures for neurons (Rock *et al.* 2004). Microglia are thought to be responsible for scavenging cellular debris produced as a result of physiological tissue renewal and remodeling in addition to playing a neurotrophic (supporting neuronal survival) role in the developing brain; however, in the adult brain, the role of resting microglia is poorly understood (Rock *et al.* 2004). Astrocytes provide neurons with nutrients such as lactate and growth factors such as nerve growth factor (Peuchen *et al.* 1997; Wagner *et al.* 2006).

Neurons die as a part of the normal aging process; however, in neurodegenerative disorders such as AD and Parkinson's disease (PD), the rate of neuronal death is accelerated and the magnitude of neuronal loss is increased (Cummings 2004; McNaught and Olanow 2006; Rock 2009). Several studies have suggested that microglia and/or astrocytes initiate inflammation in response to either pathologic substances that are present in AD and PD, or neuronal cell death (Bessis *et al.* 2007; Kermer *et al.* 2004; Mattson 2000; Nakajima and Kohsaka 2001; Streit *et al.* 2004; Wang *et al.* 2005). During inflammation, glial cells initiate several processes that can cause substantial neuronal death, including: a) production of free radicals including reactive oxygen and nitrogen species; and b) release of toxins such as lysozymes, glutamate and proteases (Block *et al.* 2007; Coyle and Puttfarcken 1993). Because neurons depend on glial cells for survival, it has been theorized that these imbalanced interactions between glial cells and neurons exacerbate neurodegenerative diseases (Aschner *et al.* 1999; Block and Hong 2007; Parpura and Haydon 2000).

1.1.3. Neurodegenerative Disorders

1.1.3.1 Alzheimer's Disease

A major cause of neurodegeneration is AD, which is devastating to the quality of life of patients. Sadly, there is neither an effective treatment nor a cure for this disorder. The risk of developing neurodegenerative conditions including AD increases with age; therefore, an increasing number of aging North Americans are at risk for neurodegenerative disorders (Bird, 2008). Research on treatment and preventative

therapy against neurodegeneration is necessary in order to properly facilitate the health care needs of the aging population (Cummings 2004).

The characteristic symptoms of patients at advanced stages of AD include severe memory loss and the inability to independently carry out daily tasks (Cummings 2004). In AD, neuronal death occurs mainly in the hippocampus and cerebral cortex (Coyle *et al.* 1983). Acetylcholine-releasing (cholinergic) neurons are affected first, which ultimately leads to loss of memory and cognition (Coyle *et al.* 1983; Kar *et al.* 2004). Research has revealed the following three hallmarks of AD: neurofibrillary tangles (NFT), A β plaques and chronic inflammation (Bird 2008; Cummings 2004; Sastre *et al.* 2006). Though NFT and A β plaques are found in healthy non-AD brains, the number of NFT and A β plaques is significantly higher in brains of individuals with AD (Cummings 2004). Several studies suggest that chronic neuroinflammation in the brain can lead to increased numbers of both formations, which in turn perpetuates inflammation (LaFeria *et al.* 2007; Moses *et al.* 2006; Sastre *et al.* 2006). It is not known what triggers the initial inflammation, although several factors including gene mutations and environmental factors are being rigorously studied. Figure 1.1 depicts the cyclic nature of glial cell-mediated inflammation that may contribute to neurodegeneration in AD.

Several major factors impede the discovery of successful treatment for AD, one of which is the complex mechanism of neurodegeneration. Biochemical pathways thought to be involved in neurodegeneration are complex and multifaceted, making it necessary to study the finer details of each mechanism in order to discover more effective therapeutic treatments. Another hurdle to therapy development is that there are no species, other than humans, that can model all aspects of AD pathophysiology. Because it

is challenging to study human AD brains *in vivo*, research on potential *in vitro* and animal models of neurodegeneration will aid tremendously in the effort towards confirming the mechanisms of neurodegeneration and eventually finding a cure.

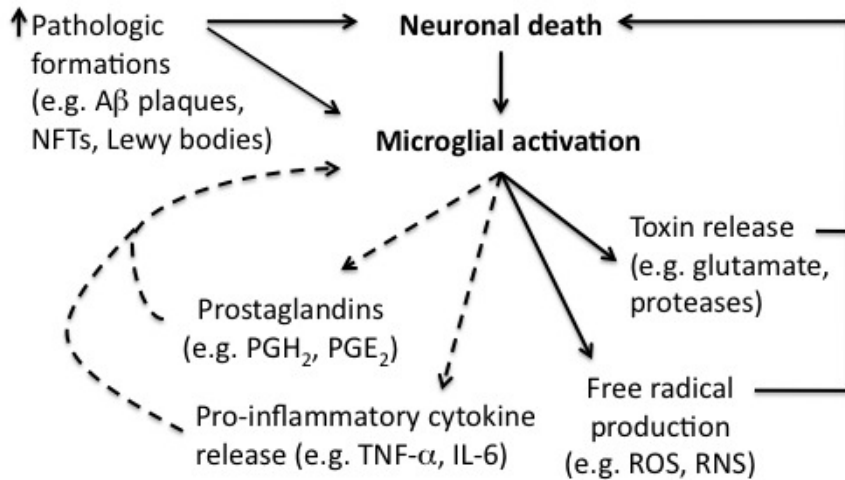


Figure 1.1: Glial cells (microglia and astrocytes) are activated by pathological formations ($A\beta$ and NFTs in AD; Lewy bodies in PD) and as a result of neuronal death. Glial cell activation leads to the production of pro-inflammatory mediators including several prostaglandins (e.g. PGH_2 , PGE_2) and cytokines (e.g. TNF -alpha, IL -6). In addition, activated glial cells can release toxins (e.g. glutamate and proteases) and free radicals (e.g. reactive oxygen species (ROS) and reactive nitrogen species (RNS)), which are directly neurotoxic. Broken line arrows highlight possible feedback pathways of activated glial cell mediators, which activate other glial cells.

1.1.3.2 Parkinson's Disease

Like AD, a hallmark of PD pathology is chronic inflammation caused by activated glial cells (McNaught and Olanow 2006). Another hallmark of PD is the presence of intracellular proteinaceous Lewy bodies composed of alpha-synuclein (α -syn) aggregates (McNaught and Olanow 2006; Moore *et al.* 2005). In PD-affected brains, there is significant death of pigmented dopaminergic neurons in the substantia nigra of the mid-brain. Oxidative stress and free radical production contribute to the loss of

neurons in this region (Moore *et al.* 2005). The resulting symptoms of PD pathology include tremor, rigidity, loss of balance, and impaired motor control.

1.1.4. Inflammatory Hypothesis of Neurodegeneration

Though different regions of the brain are affected by AD (cholinergic neurons of the hippocampus and cerebral cortex) and PD (dopaminergic neurons of the substantia nigra and other areas), increasing evidence suggests that these two neurodegenerative illnesses share the same underlying symptom, which is chronic inflammation (Hirsch and Hunot 2009). Increased pro-inflammatory cytokine levels have been found in AD brains compared to unaffected brains. Brain tissue contains no pain receptors; therefore, people experiencing chronic inflammation in their brain cannot feel its detrimental effects.

Research in neurodegenerative diseases has begun to investigate the effects of anti-inflammatory compounds to combat the inflammation; however, conventional steroidal and non-steroidal anti-inflammatory compounds both have severe side-effects if taken long term, and can ultimately pose a greater risk to the patient than neurodegeneration itself (Klegeris and McGeer 2005b). It has therefore become important to study the biochemical mechanisms of chronic inflammation in order to design more efficacious anti-inflammatory drugs.

1.1.5 Cell Culture Models of Neurodegeneration

Though primary human astrocytes are relatively easy to culture and are able to proliferate *in vitro*, human microglia and neurons are limited in their ability to survive post-mortem conditions. Therefore, alternative methods of studying neuroinflammation

exist, including the use of immortalized human and murine (e.g. rat or mouse) cell lines as well as primary animal cell cultures.

Immortalized human cell lines are cells that have been extracted from various source tissues and have acquired ability to proliferate indefinitely. Culturing and maintaining cell lines are relatively simple and inexpensive compared to *in vivo* animal models; thus, use of cell lines makes conducting numerous experiments relatively easy. The downside to using human cell lines is that their original morphologies and functions may differ from the original source tissue depending on the cell type.

Animal primary cells are much easier to obtain than human primary cells due to the relative availability of animal post-mortem tissue. Though murine primary cell lines are readily accessible for a variety of research purposes and are good models of the CNS, the physiological differences between human and murine cells are difficult to account for; therefore, an animal model more closely related to humans is preferred where available. Before our laboratory gained access to primary human astrocytes, we developed a technique to culture porcine glia from fresh adult pig brain tissues (Ionescu *et al.* 2011, see Appendix B for the publication). The comparison of microglia-neuron interactions in two different species (human and pig) can determine whether porcine glial cells can serve as good models for human glial cells. The use of porcine cells and tissues to study human physiology is widespread, since many physiological mechanisms in pigs and humans are similar (Hu *et al.* 1996; Ibrahim *et al.* 2006). The techniques that we have developed may provide other researchers with valuable methodology on how to extract and culture glial cells from adult porcine brains (see Appendix B).

The following human cell lines were used to construct an *in vitro* neuroinflammatory model for this thesis: THP-1 promonocytic leukemia cells, U-373 MG astrocytoma cells and SH-SY5Y neuroblastoma cells. All three immortalized cell lines have been used extensively in neuroinflammatory studies to model microglia, astrocytes and neurons (Combs *et al.* 2001; Hashioka *et al.* 2009; Klegeris *et al.* 2005; Klegeris and McGeer 2000; Xie *et al.* 2010). In 2000, Klegeris and McGeer determined that the combination of exogenous pro-inflammatory bacterial lipopolysaccharide (LPS) and human interferon-gamma (IFN- γ) can be used on THP-1 cells to induce a cytotoxic response that models the pathological activation of microglia (Klegeris and McGeer 2000). Stimulation with IFN- γ alone activates both U-373 MG cells and human astrocytes to produce similar cytotoxic responses (Hashioka *et al.* 2009). Though neither LPS nor IFN- γ is endogenous to the CNS, they induce a similar activation response in THP-1 cells, U-373 MG cells and human astrocytes as endogenous pro-inflammatory TNF- α , IL-6 and IL-1 β , but in a significantly more robust manner (Hashioka *et al.* 2009; Klegeris *et al.* 2005). Stimulating model glial cells allows us to assess the pro-inflammatory and cytotoxic compounds released as a result of activation. This model can also be used to screen various compounds for their anti-cytotoxic or neuroprotective properties. Figure 1.2 depicts the *in vitro* neuroinflammatory model that will be used in this study. Experiments and end-point analyses are described in more detail in the Methods section.

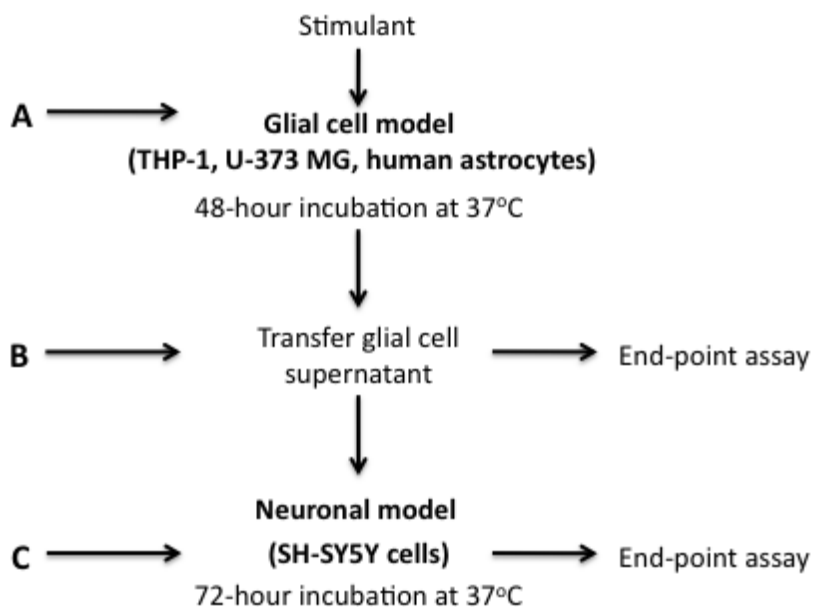


Figure 1.2: Human cell culture model of neuroinflammation. A glial cell model (either microglia-like THP-1 cells, astrocytic U-373 MG cells or human astrocytes) is stimulated with bacterial LPS and human IFN- γ for 48 h at the average human body temperature, 37°C. Supernatants from the glial cell model are then transferred to neuron-like SH-SY5Y cells, which are incubated for another 72 h at 37°C. Adding compounds at point A assesses their anti-cytotoxic properties (i.e. whether they are capable of preventing glial cell cytotoxicity). Adding compounds at point B assesses whether the compounds are neuroprotective by acting on various mediators in the glial cell supernatant before being added to SH-SY5Y cells. Finally, adding compounds at point C assesses the neuroprotective capabilities of compounds by acting directly on the SH-SY5Y cells. End-point analyses are conducted on both the glial cell model and on SH-SY5Y cells during the times indicated in the figure.

1.2 Phospholipases A₂ and Inflammation

All known phospholipase A₂ (PLA₂) isoforms convert cell membrane glycerophospholipids into arachidonic acid, which in turn is a substrate for cyclooxygenases (COX) and lipoxygenases (Farooqui and Horrocks 2006). When converted by COX-1 or COX-2, arachidonic acid yields prostaglandin (PG) H₂, the

precursor of pro-inflammatory PGE₂ (Dennis 1994; Farooqui and Horrocks 2006). When converted by lipoxygenases, arachidonic acid yields several leukotrienes (Dennis 1994; Farooqui and Horrocks 2006). Both PGs and leukotrienes act as intracellular messengers that mediate either anti- or pro-inflammatory responses (Dennis 1994).

1.2.1 Phospholipase A₂ Isoforms

There are three main isoforms of phospholipase A₂: cytosolic PLA₂ (cPLA₂), secretory or secreted PLA₂ (sPLA₂), and Ca²⁺-independent PLA₂ (iPLA₂) (Dennis 1994; Lambeau and Gelb 2008). Each type of PLA₂ has a number of isozymes, and therefore they are considered “groups” (see Table 1.1), which are generally classified based on nucleotide sequences and order of discovery (Dennis 1994; Lambeau and Gelb 2008).

Table 1.1: Classification of PLA₂ Isoforms (previously published in Cummings *et al.* 2000)

Type	Groups	Molecular Mass	Location
cPLA ₂	IVA–B	85–100 kDa	Cytosol
sPLA ₂	IA–B, IIA–C, III, V, IX, X	14–18 kDa	Secreted
iPLA ₂	IVC, VI, VIIB, VIII	29–85 kDa	Cytosol and membrane

It is currently under debate as to which PLA₂ isoform contributes in the greatest extent to arachidonic acid production in inflammatory events; however, it is generally accepted that cPLA₂α (also known as PLA₂IVA) is the major contributor to inflammatory eicosanoid production (Han *et al.* 2003). Ca²⁺ release from mitochondrial stores has been shown to rely on Ca²⁺-independent PLA₂β (also known as iPLA₂β or PLA₂VIA), which is important for the constriction of major arteries (Park *et al.* 2008). Physiological functions of extracellular PLA₂s known as sPLA₂s are discussed below.

1.2.2 Secretory Phospholipases A₂ (sPLA₂)

Earlier studies on phospholipases have shown that sPLA₂, specifically group IIA (sPLA₂IIA), are secreted by macrophages in human synovial fluid in rheumatoid arthritis and may mediate pathogenic inflammation in atherosclerosis (Bobik 2009; Casserly and Topol 2004; Ibeas *et al.* 2009; Mathisen *et al.* 2007; Piek and de Winter 2003). There are currently nine forms of sPLA₂ expressed in humans, each coded by separate genes (Lambeau and Gelb 2008). Some forms of sPLA₂ that are structurally similar to those found in humans have been described in other animals such as rodents, pigs, snakes and bees (Lambeau and Gelb 2008). Thus far, it has been shown that sPLA₂IIA, sPLA₂ group X (sPLA₂X) and sPLA₂ group V (sPLA₂V) contribute most to human inflammatory events (Lambeau and Gelb 2008).

The exogenous addition of recombinant (r) sPLA₂IIA has been shown to induce death in rat cortical neurons (Yagami *et al.* 2002). There is also evidence that the neurotoxic sPLA₂ forms found in bee venom (sPLA₂III) and rattlesnake venom (sPLA₂IIA) are structurally similar to human sPLA₂III and sPLA₂IIA, respectively (Dennis 1994). Studying both exogenous and recombinant forms of pro-inflammatory sPLA₂s may lead to insights as to the mechanism of sPLA₂IIA neurotoxicity (Burke and Dennis 2009; Lambeau *et al.* 1991; Mounier *et al.* 2001; Pluckthun and Dennis 1985). Since microglia are a type of macrophage, the stimulation of microglia is hypothesized to result in the secretion of sPLA₂IIA, which would subsequently induce neurotoxicity.

Furthermore, there is growing evidence that sPLA₂IIA plays a key role in neurodegeneration (Moses *et al.* 2006; Saegusa *et al.* 2008; Yagami *et al.* 2002). One study found that levels of sPLA₂IIA are elevated in the post-mortem brain tissues of AD

patients (Moses *et al.* 2006). Isozymes of sPLA₂ are also thought to contribute to reactive oxygen species production and oxidative stress found in PD pathology (Wei *et al.* 2003; Yagami *et al.* 2002). Other studies have suggested that sPLA₂IIA may have a non-enzymatic role in inflammation (Birts *et al.* 2008; Saegusa *et al.* 2008), which is discussed in detail below.

Little is known about the relationship between microglial cells and sPLA₂IIA. It has been shown that astrocytes release sPLA₂IIA (Lin *et al.* 2004; Oka and Arita 1991); however, it is not known whether microglia secrete sPLA₂IIA, or whether glial sPLA₂IIA contributes to glial-cell mediated neurotoxicity in the brain. Therefore, the role of sPLA₂IIA in human neurotoxicity is the primary focus of this project.

1.3 sPLA₂IIA

1.3.1 Structure of sPLA₂

All extracellular PLA₂ isoforms are interfacial enzymes, which are enzymes that function at the interface of water and lipid surfaces (Berg *et al.* 2001; Bezzine *et al.* 2002). Interfacial enzymes, including sPLA₂IIA, have distinct catalytic (enzymatic substrate-binding) and interfacial (cell surface-binding) sites (Berg *et al.* 2001). Ca²⁺ is required at the sPLA₂IIA catalytic site for catalysis; however, it has been recently noted that sPLA₂IIA interfacial binding occurs with more frequency in the absence of Ca²⁺ (Olson *et al.* 2010). Upon membrane binding, the interface between sPLA₂IIA and the cell membrane usually spans between 30-40 glycerophospholipid molecules (Bezzine *et al.* 2002).

Because human sPLA₂IIA is considered a low molecular weight protein (~16 kDa (Lambeau and Gelb 2008)), it is possible that sPLA₂IIA is secreted through a specific channel; however, there is no current evidence suggesting the existence of PLA₂-specific channels in cell membranes. Cells must therefore use exocytosis in order to release sPLA₂IIA into the extracellular environment (Lambeau and Gelb 2008). Similarly, the internalization of sPLA₂IIA may involve pinocytosis or phagocytosis following its binding to either membrane phospholipids or cell surface proteins (Boilard *et al.* 2003).

The surface composition of the sPLA₂IIA protein includes many arginine and lysine residues, making sPLA₂IIA uniquely cationic compared to other PLA₂ isoforms (Bezzine *et al.* 2002). The catalytic active site of sPLA₂IIA has a high affinity for anionic glycerophospholipids such as phosphatidylethanolamine and phosphatidylserine. For this reason, sPLA₂IIA does not bind well to zwitterionic phosphatidylcholine-rich mammalian cell membranes under physiological circumstances (Bezzine *et al.* 2002); however, the ability of sPLA₂IIA to bind to mammalian cell membranes increases during apoptosis (Boilard *et al.* 2003). Upon membrane blebbing, the bi-layered cell membrane inverts, exposing the layer normally positioned facing the cytosol; the inner membrane layer contains phosphatidylserine, which sPLA₂IIA has a higher affinity for (Boilard *et al.* 2003).

1.3.2 Enzymatic Activity and Known Inhibitors of sPLA₂

All PLA₂s, including sPLA₂IIA, are capable of producing arachidonic acid by hydrolyzing membrane glycerophospholipids. The catalytic site of sPLA₂IIA comprises an aspartate-histamine diad and Ca²⁺ bound by a peptide loop, which is conserved in all

active sites of mammalian sPLA₂s (Lambeau and Gelb 2008). Membrane binding increases the efficiency of substrate binding to the catalytic site, as well as overall catalytic efficiency (Lambeau and Gelb 2008).

Several sPLA₂ and specific sPLA₂IIA inhibitors have been developed within the past decade. The compound named 'sPLA₂IIA inhibitor 1' (a cyclic pentapeptide) is effective at micromolar concentrations (Church *et al.* 2001); however, it has been suggested that inhibitors with potency in this concentration range may have limited specificity due to an increased chance of non-specific binding at such high concentrations (Lambeau and Gelb 2008). YM-26734-1 is a natural derivative from the fruit of *Horsfieldia amygdaline* and is highly specific for human sPLA₂IIA with nanomolar potency (Miyake *et al.* 1992). Indoxam (LY315920) and its derivative Me-indoxam are also sPLA₂IIA-specific inhibitors and were found to be more potent than YM-26734-1 (Oslund *et al.* 2008).

In 2008, Drs. Rob Oslund and Michael Gelb synthesized an indoxam derivative RO032107 (14b in Oslund *et al.* 2008) that exhibited greater potency at lower nanomolar concentrations than indoxam (Oslund *et al.* 2008). Another compound, RO041709 (15b in Oslund *et al.* 2008), was designed as a methylated control compound to RO032107, meaning that it contains an N-methyl group that prevents a key hydrogen bond from occurring between the inhibitor and a histidine or aspartate residue in the catalytic site of sPLA₂IIA. RO041709 has at least 30-fold lower IC₅₀ (half-maximal inhibitory concentration) than RO032107 (Oslund *et al.* 2008). A third inhibitor, RO092906 (11h in Oslund *et al.* 2008), was synthesized to specifically inhibit sPLA₂X.

1.3.3 Non-Enzymatic Activity of sPLA₂IIA

Due to its cationic surface, sPLA₂IIA exhibits potent bactericidal effects in several ways: 1) sPLA₂IIA has a strong affinity for anionic peptidoglycans, which represent a large component of bacterial cell membranes (Lambeau and Gelb 2008; Wei *et al.* 2003; Wu *et al.* 2010); 2) sPLA₂IIA is also basic and electrostatically attracted to acidic lipoteichoic acids present in Gram-positive bacterial cell walls and hydrolyzes the underlying plasma membrane (Birts *et al.* 2009; Lambeau and Gelb 2008; Wei *et al.* 2003); and 3) sPLA₂IIA disrupts the LPS-containing coat and increases the permeability of Gram-negative bacterial cell walls, which enables it to hydrolyze the underlying cell wall (Lambeau and Gelb 2008). In addition, it has been shown that the cationic surface of sPLA₂IIA allows it to bind with high affinity to anionic heparin sulfate proteoglycans, which are expressed on cell surfaces and may serve as sPLA₂IIA interfacial-binding sites (Boilard *et al.* 2003). The use of heparin and heparinase III to block sPLA₂IIA from binding to heparin sulfate proteoglycans only partially prevented sPLA₂IIA from binding to apoptotic cells, which suggests that sPLA₂IIA may also bind to other membrane proteins (Boilard *et al.* 2003).

Beck *et al.* (2003) hypothesized that sPLA₂IIA interacted with the muscle (M)-type receptor, which is one of the two types of cell surface receptors that binds to neurotoxic snake venom sPLA₂S (Lambeau *et al.* 1995). Another sPLA₂-binding receptor, the neuronal (N)-type receptor, is expressed in rabbit brain, heart and kidney and may be involved in sPLA₂IIA-mediated mechanisms (Kolko *et al.* 2002; Lambeau *et al.* 1995; Lambeau *et al.* 1991). Recently however, it was discovered that the sPLA₂IIA-M-type receptor interaction is species specific, and that human sPLA₂IIA does not bind

effectively to human M-type receptors (Lambeau and Gelb 2008).

The global cationic structure of sPLA₂IIA contributes to its ability to aggregate with anionic lipid vesicles and may contribute to cellular uptake and removal of cellular debris (Birts *et al.* 2008). Upon investigating cellular uptake of sPLA₂IIA and an enzymatically inactive mutant of sPLA₂IIA using confocal microscopy, it was found that once sPLA₂IIA was inside the cell, it was targeted to the nucleus and somehow escaped proteolysis during and after endocytic uptake (Birts *et al.* 2008). It is possible that by binding to cell surface heparin sulfate proteoglycans (Boilard *et al.* 2003), the cell initiates either phagocytosis or pinocytosis to internalize sPLA₂IIA and its bound liposome (Birts *et al.* 2008).

1.3.4 Pathologies involving sPLA₂IIA

Increased levels of sPLA₂IIA have been detected in various inflammatory conditions such as rheumatoid arthritis, atherosclerosis, cancer, AD and PD. It is still debated as to whether the role of sPLA₂IIA is to exacerbate or resolve inflammation; however, current studies on sPLA₂IIA function suggest that the action of sPLA₂IIA may be tissue and/or disease specific.

1.3.4.1 Rheumatoid Arthritis

Rheumatoid arthritis is characterized by chronic inflammation in the joints, leading to pain and damage to joint cartilage and bone (Choy and Panayi 2001). Human sPLA₂IIA was originally isolated from inflamed synovial joint fluid of rheumatoid arthritis patients (Bidgood *et al.* 2000; Masuda *et al.* 2005). It has been consistently

shown that the sPLA₂IIA concentration in rheumatoid-arthritic synovial joints is significantly higher than in non-arthritic joints (Bryant *et al.* 2010; Jamal *et al.* 1998; Masuda *et al.* 2005). Several studies have linked TNF- α -induced sPLA₂IIA with increased cPLA₂/COX-2-coupled production of pro-inflammatory PGE₂ in synovial joint fluid (Bidgood *et al.* 2000; Bryant *et al.* 2010), a relationship that has also been demonstrated in TNF- α -stimulated rat mesangial cells (Beck *et al.* 2003; Han *et al.* 2003).

1.3.4.2 Atherosclerosis

Atherosclerosis is the thickening of arterial walls by cholesterol-laden plaques. Several studies have shown high concentrations of sPLA₂IIA within the serum plasma of atherosclerotic patients compared to patients with no history of cardiovascular problems (Ghesquiere *et al.* 2005). It has been reported that sPLA₂IIA contributes to atherosclerosis both in an enzymatic (catalytic) and non-enzymatic manner. Enzymatically, sPLA₂IIA hydrolyzes oxidized low-density lipoproteins, which releases fatty acids and lysophospholipids that can be further metabolized into inflammatory mediators (Divchev and Schieffer 2008). Due to its uniquely anionic surface, sPLA₂IIA binds to proteoglycans in the extracellular matrix, which has been linked to increased collagen deposition and development of atherosclerotic plaques.

1.3.4.3 Cancer

The over-expression of sPLA₂IIA has been found in many cancerous tissues. Inhibitors of sPLA₂IIA were found to suppress the growth of esophageal adenocarcinoma

cells (Mauchley *et al.* 2009). It was also found that sPLA₂IIA attenuated colorectal cancer tumorigenesis in a manner independent of the adenomatous polyposis coli tumor suppressor gene. Research on both prostate cancer and colorectal cancer has found that sPLA₂IIA contributes to cancerous cell survival (Jiang *et al.* 2002). sPLA₂IIA-induced astrocytoma proliferation through Ras (guanine triphosphatase involved in signal transduction; originally identified as a rat sarcoma oncogene product) activation and promoted mitochondria-independent accumulation of reactive oxygen species (ROS) (Hernandez *et al.* 2010; Martin *et al.* 2009; Mathisen *et al.* 2007). Such evidence suggests that sPLA₂IIA participates in cell regulation by acting through the nuclear factor-kappa-B (NF-κB) pathway and mitogen-activated protein kinase (MAPK) cascade (Martin *et al.* 2009). It has been demonstrated that depending on the cell type sPLA₂IIA could either promote or inhibit cell growth (Dong *et al.* 2010).

1.3.4.4 Neurodegenerative Disease

One study found that levels of sPLA₂IIA are elevated in the post-mortem brain tissues of AD patients compared to patients with no dementia (Moses *et al.* 2006). The enzymatic activity of sPLA₂IIA is also thought to be responsible for free radical production and oxidative stress that contributes to PD pathology (Chiricozzi *et al.* 2010; Wei *et al.* 2003; Yagami *et al.* 2002). The combined evidence of several *in vitro* studies that showed sPLA₂IIA-induced neuronal apoptosis (Chiricozzi *et al.* 2010; Yagami *et al.* 2002) and the presence of increased levels of sPLA₂IIA in AD and ischemic brains prompted a recent review to conclude that sPLA₂IIA exacerbates neuronal death in neurodegenerative diseases (Schaeffer *et al.* 2010).

1.3.5 sPLA₂IIA Regulation

Numerous studies have reported that various pro-inflammatory compounds including TNF- α , IL-1 β , IFN- γ and exogenous LPS induce sPLA₂IIA mRNA expression in a number of different cell types (Lin *et al.* 2004; Massaad *et al.* 2000). In rat cortical astrocytes, TNF- α induction of sPLA₂IIA was mediated by cyclic adenosine monophosphate (cAMP), while the induction of sPLA₂IIA by LPS involved protein kinase C (PKC) (Oka and Arita 1991). IFN- γ induced sPLA₂IIA mRNA in human arterial smooth muscle cells, which appeared to be cell type specific and involved STAT (signal transducer and activator of transcription)-3 activation (Peilot *et al.* 2000). Extracellular signal-regulated kinase (ERK)_{1/2} and PKC had to be activated in order for sPLA₂IIA and sPLA₂V to enhance the effect of H₂O₂-induced arachidonic acid release in mouse mesangial cells; sPLA₂IIA amplified cPLA₂ activity and its coupling with COX enzymes (Han *et al.* 2003; Jensen *et al.* 2009).

The first study to document the astrocytic production of group II sPLA₂ was published in 1991 (at the time of the study, group II sPLA₂ was not yet differentiated into subtypes e.g. sPLA₂IIA): inflammatory cytokines TNF- α , IL-1 β and IFN- γ were found to enhance the expression of sPLA₂IIA mRNA in cultured rat astrocytes (Oka and Arita 1991). In a more recent study, the up-regulation of sPLA₂IIA mRNA was found in reactive astrocytes after transient focal cerebral ischemia in rat brain tissue (Lin *et al.* 2004).

Several studies have concluded that sPLA₂ and cPLA₂ isozymes regulate each other during inflammation (Beck *et al.* 2003; Kuwata *et al.* 2000; Murakami *et al.* 1999). It was also suggested that cPLA₂ isozymes contribute to membrane hydrolysis and

arachidonic acid release during inflammatory events to a greater extent than sPLA₂ isozymes (Han *et al.* 2003; Lambeau and Gelb 2008). Figure 1.3 illustrates a proposal by Beck *et al.* (2003), which states that, upon cPLA₂-mediated generation of eicosanoids, the peroxisome proliferator-activated receptor alpha (PPAR α) up-regulates sPLA₂IIA mRNA production.

Because sPLA₂IIA is involved in numerous inflammatory diseases, it is difficult to characterize a single sPLA₂IIA function, target or contributing pathway. Therefore, the next section will focus primarily on evidence supporting either an enzymatic or non-enzymatic mechanism of sPLA₂IIA-induced neurotoxicity, though it is likely that the protein engages in both actions.

1.3.6 Neurotoxic Mechanisms of sPLA₂IIA

In 2002, it was found that exogenous application of human recombinant sPLA₂IIA (rsPLA₂IIA) to rat cortical neurons resulted in significant neuronal death (Yagami *et al.* 2002). Rat cortical neurons undergoing apoptosis were found to exhibit a change in membrane phospholipids; specifically, upon increased exposure to oxidants during oxidative stress, phospholipid composition of plasma membrane shifted to containing more arachidonic acid. cPLA₂ α has been shown to provide the majority of arachidonic acid liberated from cell membranes (Han *et al.* 2003). Even though sPLA₂IIA has a low affinity for mammalian cell membranes, it still may act on neuronal membranes that have been pre-damaged by H₂O₂ (Han *et al.* 2003). Cell membrane hydrolysis via sPLA₂ isozymes increases during apoptotic or necrotic cell death, partially due to the cell losing its normal resistance to membrane hydrolysis (Olson *et al.* 2010).

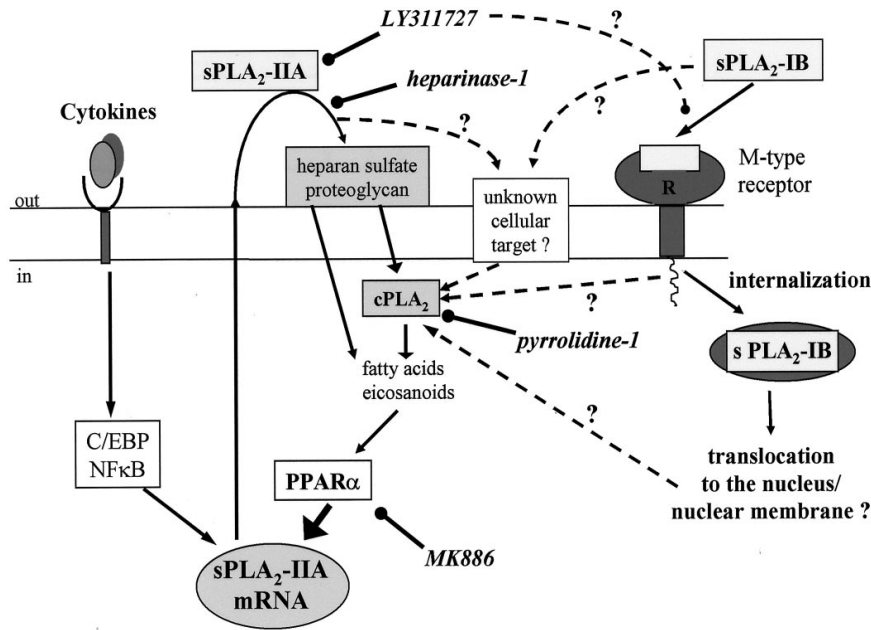


Figure 1.3: Proposed PLA₂ pathways leading to the up-regulation of endogenous sPLA₂IIA mRNA (previously published in Beck *et al.* 2003). Once the activation of cPLA₂ produces eicosanoids, the nuclear receptor PPAR α up-regulates sPLA₂IIA mRNA. Cytokines such as TNF- α and IL-1 β can directly increase sPLA₂IIA mRNA production. Once sPLA₂IIA is produced and secreted by the cell, it may contribute to its own positive feedback loop by binding to heparin sulfate proteoglycans on the cell membrane surface, which activates cPLA₂ and PPAR α , and results in further sPLA₂IIA up-regulation.

Bee venom-derived sPLA₂ type III can potentiate glutamate-induced Ca²⁺ increase causing subsequent neuronal death in prenatal rat neurons (DeCoster *et al.* 2002). Snake venom sPLA₂IIA binds to N-type receptors and potentiates glutamate-induced neuronal death (Kolko *et al.* 2002; Lambeau *et al.* 1995). Glutamate ionotropic N-methyl-D-aspartic acid and α -amino-3-hydroxyl-5-methyl-4-isoxazole-propionate receptors have both been implicated in snake venom sPLA₂-mediated neuronal death (Kolko *et al.* 2002). Glutamate ionotropic N-methyl-D-aspartic acid and α -amino-3-hydroxyl-5-methyl-4-isoxazole-propionate receptor antagonists have exhibited

neuroprotective effects, particularly in ischemia and epilepsy (Kolko *et al.* 2002). sPLA₂IIA inhibitor 1 has been found to reduce glutamate-mediated reactive oxygen species proliferation in rat granular neurons (Mathisen *et al.* 2007). Therefore it is possible that sPLA₂IIA enzymatic activity contributes to glutamate-induced excitotoxicity.

Ca²⁺ homeostasis may be affected by the up-regulation of sPLA₂IIA; it has been demonstrated that sPLA₂IIA enhances Ca²⁺ intake into rat cortical neurons via the L-type voltage-gated Ca²⁺ channel (Yagami *et al.* 2003). An influx of intracellular Ca²⁺ is required for glutamate ionotropic receptor-mediated long-term potentiation (Pineau and Lacroix 2009). Low concentrations of bee venom sPLA₂III potentiated glutamate-stimulated intracellular Ca²⁺ increase in rat cortical neurons (DeCoster *et al.* 2002). It is possible that sPLA₂IIA may contribute to the regulation of Ca²⁺ channels in a similar way. The glutamate ionotropic N-methyl-D-aspartic acid receptor antagonist MK-801 attenuated the effects of both human sPLA₂IIA and bee venom sPLA₂III on glutamate signaling (Putz *et al.* 2007).

Mitochondria purified from rat brain astrocytes, neuron-like PC-12 cells and U-251 astrocytoma cells were found to store sPLA₂IIA (Macchioni *et al.* 2004). Reduced membrane potential and oxidative stress caused mitochondria from rat brain astrocytes to release sPLA₂IIA into the cytosol; this not only may activate cPLA₂-driven arachidonic acid production (see Fig. 3.1), but may also contribute to neuronal death by hydrolyzing the inner layer of the plasma membrane (Macchioni *et al.* 2004). The localization of sPLA₂IIA in mitochondria may be a result of prior internalization through binding with heparin sulfate proteoglycans (Boilard *et al.* 2003; Macchioni *et al.* 2004).

Mitochondrially-located sPLA₂IIA may also regulate intra-neuronal Ca²⁺ concentrations because neurons have intracellular stores of Ca²⁺ in both the endoplasmic reticulum and mitochondria. As a result, the neurotoxic mechanism of sPLA₂IIA may be attributed to its binding to neuronal surface receptors and initiating cell death pathways or to disrupting Ca²⁺ regulation and contributing to glutamate-induced neuronal excitotoxicity (Yagami *et al.* 2003).

A more recent model of the non-enzymatic sPLA₂IIA neurotoxicity involves its interaction with the cell surface integrins. In 2008, it was shown that sPLA₂IIA had high affinity for the integrin alpha-5-beta-3 ($\alpha 5\beta 3$) and that binding of sPLA₂IIA to this receptor induced proliferation of U937 human monocytic lymphoma cells (Saegusa *et al.* 2008). Affiliation with integrin receptors indicates that sPLA₂IIA may regulate the cell signaling pathways responsible for activating monocytes. Since microglia are a type of tissue macrophage that originates from monocytes, it is possible that sPLA₂IIA may also contribute the activation of microglia.

Another possible sPLA₂IIA receptor may be the toll-like receptor 4 (TLR4) that is expressed by both neuronal and glial cells (Tang *et al.* 2008). LPS binding to TLR4 complexed with MD-2 (lymphocyte antigen 98) induces the NF- κ B cascade in microglia-like THP-1 cells (Zhang *et al.* 1999). As sPLA₂IIA has been shown to initiate the NF- κ B cascade (Alaoui-El-Azher *et al.* 2002; Martin *et al.* 2009), it may do so by binding to TLR4. By blocking sPLA₂IIA from binding to TLR4 on neurons, it may be possible to attenuate sPLA₂IIA-induced neuronal death.

If the sPLA₂IIA neurotoxicity is due to its enzymatic activity, then the addition of sPLA₂IIA-specific inhibitors to cytotoxic glial cell supernatants should result in reduced

neuronal death; however, if sPLA₂IIA-specific inhibitors fail to reduce cytotoxicity of glial secretions, then the non-enzymatic activity of sPLA₂IIA should be suspected. Therefore, if sPLA₂IIA is secreted by glial cells upon stimulation with inflammatory factors and induces neurotoxicity in a non-enzymatic manner, it can be hypothesized that either 1) removing sPLA₂IIA from the glial supernatants, or 2) blocking sPLA₂IIA from forming complexes with potential cell surface receptors should result in reduced neuronal death.

1.4 Research Overview and Hypotheses

Studying the role of sPLA₂IIA in glial cell-neuron interactions may offer more insight as to its function in neuroinflammation. Previous work has shown that sPLA₂IIA may function as an intercellular mediator or neurotoxin during inflammation; therefore, studies are needed to better understand the sPLA₂IIA-mediated cellular processes that occur during neuroinflammation. Though the association between sPLA₂IIA and astrocytes has been investigated before, no information is available about the relationship between microglia and sPLA₂IIA. Furthermore, the contribution of sPLA₂IIA enzymatic activity to glia-mediated neuroinflammation has not been studied before.

Activated (stimulated) microglia and astrocytes contribute to neuroinflammation by releasing a plethora of pro-inflammatory mediators and neurotoxins. The following neurotoxins released from stimulated glial cells have been identified: the excitotoxic amino acid glutamate (Moriguchi *et al.* 2003; Parpura and Haydon 2000), soluble Fas ligand (Fas L) (Ciesielski-Treska *et al.* 2001), tissue plasminogen activator (Flavin *et al.*

2000), cathepsin B (Gan *et al.* 2004; Kingham and Pocock 2001), and several proteases including metalloproteases (Harris *et al.* 2007) and chymotrypsin-like proteases (Klegeris and McGeer 2005a). A number of unidentified soluble neurotoxic proteins have also been observed to originate from activated glial cells (Flavin *et al.* 1997; Giulian *et al.* 1993); these unidentified neurotoxins may include extracellular phospholipases such as sPLA₂IIA.

The central hypothesis of this study is that sPLA₂IIA is a toxin secreted by activated glial cells, which causes neuronal death. Human cell lines THP-1 promonocytic leukemia cells, U-373 MG astrocytoma cells and SH-SY5Y neuroblastoma cells are used to model microglia, astrocytes and neurons, respectively. Human primary astrocytes are also used to confirm processes studied in U-373 MG cells. The selective sPLA₂IIA inhibitor RO032107 is used to assess the contribution of sPLA₂IIA enzymatic activity to glial cell neurotoxicity. The effect of sPLA₂IIA on neuronal cells pre-damaged by hydrogen peroxide is examined, as well as the regulatory role of PPAR α in sPLA₂IIA-induced neurotoxicity. The effect of using a sPLA₂IIA-specific immunosorbent to remove it from stimulated cell supernatants is also investigated. Outcomes of this thesis may contribute to the development of drugs that disrupt the pro-inflammatory and cytotoxic effects of sPLA₂IIA in neuroinflammation.

2 Materials and Methods

2.1 Chemicals and Reagents

The following reagents were supplied by Cayman Chemical Company (Ann Arbor, MI, USA): 1-[(4-chlorophenyl)methyl]-3-[(1,1-dimethylethyl)thio]- α,α -dimethyl-5-(1-methylethyl)-1H-indole-2-propanoic acid sodium salt (MK885, Cat#10133), 4-[(1-oxo-7-phenylheptyl)amino]-(4R)-octanoic acid (OPHAO, Cat#13181), 7,7-dimethyl-5,8-eicosadienoic acid (DMDA, Cat#70500), 6-isopropoxy-9-oxoxanthene-2-carboxylic acid (AH6809, Cat# 14050), bee venom sPLA₂III (Cat#60500), methyl arachidonyl fluorophosphonate (MAFP, Cat#70660), mouse anti-PGE₂ immunosorbent (Cat#414020), mouse anti-human PGE₂ monoclonal antibody (Cat# 414013), mouse anti-human sPLA₂ type IIA (sPLA₂IIA) monoclonal antibody (Cat#160500), mouse anti-human sPLA₂IIA immunosorbent (Cat#485009), N-[[4'-[[3-butyl-1,5-dihydro-5-oxo-1-[2-(trifluoromethyl)phenyl]-4H-1,2,4-triazol-4-yl]methyl][1,1'-biphenyl]-2-yl]sulfonyl]-3-methyl-2-thiophenecarboxamide (L-161,982, Cat#10011565), and sPLA₂IIA enzyme-linked immunosorbent assay (ELISA) kit (Cat#585000).

The following reagents were purchased from Fisher Scientific (Ottawa, ON, Canada): bovine serum albumin (BSA), diethanolamine, Dulbecco's modified Eagle medium nutrient mixture F-12 Ham (DMEM-F12), ethanol (EtOH), ethylenediaminetetraacetic acid (EDTA) sodium salt, glycine, HCl, H₂O₂, NaCl, N,N-dimethylformamide (DMF), sodium acetate, sodium borate, sodium dodecyl sulfate (SDS), SYBR safe dye, and tris(hydroxymethyl)aminomethane (Tris).

The following reagents were obtained from Sigma-Aldrich (Oakville, ON, Canada): 3-(4,5-dimethylthiazol-2-yl) 2,5-diphenyl 21 tetrazolium bromide (MTT), 5-(4-

benzyloxyphenyl)-4S-(7-phenylheptanoylamino) pentanoic acid (BPPA, Cat#S3319), agarose, beta-nicotinamide adenine dinucleotide (β -NAD), $\text{CaCl}_2 \cdot 2\text{H}_2\text{O}$, diaphorase (from *Clostridium kluyveri*), dimethyl sulfoxide (DMSO), iodonitrotetrazolium chloride (INT), lipopolysaccharide (LPS, from *Escherichia coli* 055:B5), sodium L-lactate (lactate), oxamic acid, and Triton X-100.

IDSol Pre-mixed 30% acrylamide:Bis (29:1) solution (Cat# IS003) was supplied by Dgel Electrosystem Inc. (Montreal, QC, Canada). Concanavalin A (ConA, a tetrameric metalloprotein extracted from the jack bean *Canavalia ensiformis*) sepharose 4B (Cat#17-0440-03) was obtained from GE Healthcare (Baie d'Urfe, QC, Canada). sPLA₂IIA forward and reverse primers were ordered from Integrated DNA Technologies (IDT, San Diego, CA, USA). The live/dead mammalian cell viability/cytotoxicity assay kit (Cat# L-3224) was purchased from Invitrogen (Burlington, ON, Canada). Penicillin (100,000 U/ml) and streptomycin (100,000 $\mu\text{g}/\text{ml}$) dual antibiotic solution was obtained from MP Biomedicals (Solon, OH, USA). Human IFN- γ was ordered from PeproTech (Ottawa, ON, Canada). The SV Total RNA Isolation System (50 preparations, Cat#Z3100), Improm-II Reverse Transcription (RT) System (100 reactions, Cat#A3802), GoTaq Green Master Mix kit, 100 bp and 1 kb ladders were purchased from Promega (Madison, WI, USA). Trypsin/EDTA solution and fetal bovine serum (FBS) were obtained from Thermo Scientific (Waltham, MA, USA). Phosphate-buffered saline (PBS) tablets were purchased from Takara Bio Incorporated (Madison, WI, USA). Mary Forrest of the Department of Biology, University of British Columbia Okanagan, in Kelowna, BC, Canada generously provided the restriction enzymes *Bam*HI and *Dde*I.

Michael Gelb and the Laboratory of Medicinal Enzymology, University of

Washington, in Seattle, WA, USA generously provided RO032107, RO041709, and RO092906 inhibitors as well as a sample of human recombinant sPLA₂IIA (rsPLA₂IIA). Another human rsPLA₂IIA sample was obtained from ProSpec (East Brunswick, NJ, USA, Cat#ENZ-290). Mouse antibodies against human toll-like receptor 4 (TLR4)/MD-2 complex (Cat#HM2246) were purchased from Hycult Biotech (Burlington, ON, Canada). 10-(1-Pyrenyl)-decanoic acid (1-pyrenedecanoic acid, Cat#5236) and 1-hexadecanoyl-2-(1-pyrenedecanoyl)-sn-glycero-3-phosphomethanol (PGPM, Cat#2276) were purchased from Genolite Biotek (Portland, OR, USA)

2.2 Equipment

Tissue culture dishes (10 cm) and 96-well sterile plastic plates (Corning Inc., Corning, NY, USA) were used where the experiment involved collection of large volumes of supernatants or treatments in small volumes, respectively. The rest of cell culture experiments were conducted by using sterile 24-well plastic cell culture plates (Corning). Cell cultures were grown in T-75 flasks (Sarstedt, Montreal, QC, Canada) in a Steri-Cycle HEPA Class 100 carbon dioxide (CO₂) incubator (Model#370, Thermo Scientific). A hemocytometer (ChangBioscience, Castro Valley, CA, USA) was used to count cells. The Sorvall RT1 Centrifuge (Cat#75002384, Thermo Scientific) was used to centrifuge cell samples for supernatant collection or for use in the experiments.

The C1000 Thermal Cycler (Model#185-1048) used to conduct polymerase chain reactions (PCR) and the Mini-PROTEAN Tetra Cell System with HC Power Supply (Cat#165-8001 and 164-5070, respectively) used for casting polyacrylamide gels and

running electrophoresis were purchased from Bio-Rad (Philadelphia, PA, USA). The Eppendorf Biophotometer Plus (Cat# 952000006) spectrophotometer was used to estimate mRNA concentrations. PCR products in polyacrylamide gels were visualized and digitally photographed using the AlphaView imaging system (Model FluorChem HD2) purchased from Alpha Innotech (Santa Clara, CA, USA).

The Fluostar Omega microplate reader was purchased from BMG Labtech (Nepean, ON, Canada). Fluorescence images from the live/dead assay were visualized and digitally photographed using an inverted microscope with epi-fluorescence attachment (Model AE31) from Motic (Richmond, BC, Canada). Black 96-well plates (Cat#655076) used in the fluorescent enzyme activity assay were obtained from Grenier Bio-One (Monroe, NC, USA).

2.3 Cell Culture Models

The SH-SY5Y dopaminergic neuroblastoma cell line was used as a neuronal model, while THP-1 promonocytic cell line was used as a microglial model. Primary human astrocytes prepared from surgically dissected human epilepsy tissues and the U-373 MG astrocytoma cells were used as astrocyte models. All cell lines and human astrocyte cultures were obtained from the Kinsmen Laboratory of Neurological Research at the University of British Columbia, Vancouver, Canada. Cultures were grown in DMEM-F12 with 10% FBS, penicillin (100 U/ml) and streptomycin (100 µg/ml). Cultures were incubated in a CO₂ incubator set at 37°C with 5% added CO₂ and 100% humidity.

2.4 Collecting Glial Cell Supernatants

10 ml of THP-1 cells were seeded onto a 10 cm culture dish at 0.5 million cells/ml. After 15 min incubation in a CO₂ incubator at 37°C, THP-1 cells were stimulated with a combination of LPS (0.5 µg/ml) and IFN-γ (150 U/ml) and incubated for 48 h at 37°C in a CO₂ incubator. Supernatant was carefully collected and any remaining cells removed by centrifugation at 250 g for 10 min.

Adherent U-373 MG astrocytoma cells were harvested from T-75 flasks by discarding supernatant and incubating cells with 1.5 ml of 0.05% trypsin/EDTA solution for 2 min at 37°C. The trypsin was then inactivated by adding 10 ml DMEM-F12 medium with 10% FBS (F10). U-373 MG cells were then counted with a hemocytometer, centrifuged and reconstituted with fresh DMEM-F12 plus 5% FBS (F5) to a concentration of 0.25 million cells/ml in 10 ml. The cells were seeded onto a 10 cm culture dish and incubated at 37°C in a CO₂ incubator. After incubation for 24 h, medium was replaced with fresh F5 and cells were stimulated with IFN-γ (150 U/ml) and incubated for an additional 48 h at 37°C in a CO₂ incubator. Supernatant was carefully collected via aspiration into a sterile plastic 50 ml tube and any remaining cells removed by centrifugation at 250 g for 10 min.

Adherent primary human astrocytes were harvested from T-75 flasks by removing cell supernatant and incubating cells with 1.5 ml of 0.25% trypsin/EDTA solution for 2 min at 37°C. From this point, the protocol described above for collecting U-373 MG cell supernatants was followed, except that human astrocytes were plated at a density of 0.2 million cells/ml in 10 ml.

Experiments with THP-1 and U-373 MG cell supernatants were performed on at least three independently grown batches of cells. Human astrocytes prepared from three different surgical cases were used. All supernatants were tested for toxicity on SH-SY5Y cells before sorbent and other experiments were initiated.

2.5 Plating SH-SY5Y Cells for Experiments

Adherent SH-SY5Y cells were detached from T-75 flasks by removing supernatant and incubating with 1.5 ml of 0.05% trypsin/EDTA for 2 min. Trypsin was then inactivated with 10 ml F10. SH-SY5Y cells were counted with a hemocytometer, centrifuged, and reconstituted with fresh F5 to a concentration of 0.2 million cells/ml. The cells were then seeded onto 24-well plates at 0.4 ml/well and incubated for 24 h at 37°C in a CO₂ incubator before use in experiments.

2.6 Cytotoxicity Assays: Lactate Dehydrogenase (LDH)

LDH enzymatic activity was measured to estimate the percent cell death as compared to a 100% lysed cell control where all cells were lysed by adding 1% Triton X-100. LDH is a stable enzyme that catalyzes the conversion of lactate to pyruvate, which is a reaction that is important for cell survival. LDH is present in the cytosol and is released from cells with damaged membranes. Conversion of lactate to pyruvate by LDH requires the reduction of beta-nicotinamide adenine dinucleotide (β -NAD), which can be coupled with the diaphorase-catalyzed reduction of iodinitrotetrazolium (INT) dye to a purple

formazan. (Decker and Lohmann-Matthes 1988). The optical density of INT is linearly correlated with the concentration of LDH in the sample (Nachlas *et al.* 1960).

Cell supernatant (0.1 ml) was collected from each experimental sample and transferred to a 96-well plate. INT was added to each well to a concentration of 260 $\mu\text{g/ml}$, and an initial measurement of optical density (OD) at 490 nm was performed. A reaction mixture containing lactate (750 $\mu\text{g/ml}$ in sample), β -NAD (60 $\mu\text{g/ml}$ in sample) and diaphorase (55 $\mu\text{g/ml}$ in sample) in PBS was added to each well and the reaction was allowed to proceed for 20-30 min until it was terminated by the addition of oxamic acid (1.5 mg/ml in sample). An end point measurement of OD at 490 nm was performed after the addition of oxamic acid, and percent cell death for each sample was determined by using the following two-step equation:

$$(1) A_{\text{final}} - A_{\text{initial}} = dA_n$$

$$(2) [(dA_n - dA_{\text{medium}})/(dA_{\text{lysis}} - dA_{\text{medium}})] \times 100 = \% \text{ death,}$$

where A_{initial} represents initial absorbance, A_{final} represents final absorbance, dA_n represents the difference between A_{initial} and A_{final} for experimental samples (i.e. each well containing 0.1 ml cell supernatant), dA_{medium} represents dA_n for the medium control, and dA_{lysis} represents dA_n for the lysed cell control.

2.7 Cytotoxicity Assays: MTT

MTT is a yellow formazan dye that is reduced by metabolically active mitochondria into purple crystals. The optical density of MTT is linearly correlated with the concentration of live cells in the sample (Hansen *et al.* 1989; Mosmann 1983). After

collecting 0.1 ml supernatant for LDH assay from each experimental well, 30 μ l of 5 mg/ml MTT solution was added to the remaining 0.3 ml cell culture medium and plates incubated at 37°C in CO₂ incubator for 1 h. Subsequently, 0.4 ml of a 20% SDS/50% DMF solution in deionized water was added and the plates incubated overnight at 37°C to solublize the crystals. To measure OD of the samples, 0.1 ml from each well was transferred to a 96-well plate and absorbances at 570 nm were measured using a microplate reader. Percent cell viability (% viability) for each well was determined using the following two-step equation:

$$(3) A_n - A_{\text{medium}} = dA_n$$

$$(4) [dA_n / dA_{\text{untreated}}] \times 100\% = \% \text{ viability},$$

where A_n represents the absorbance value for the sample in question, dA_n is the difference between A_n and A_{medium} , A_{medium} represents the absorbance value for the medium control and $dA_{\text{untreated}}$ represents the difference between $A_{\text{untreated}}$ (absorbance value for the untreated control) and A_{medium} .

2.8 Cytotoxicity Assays: Live/Dead Immunofluorescence

The live/dead assay uses two fluorescent dyes to differentiate living cells from dead cells. Non-fluorescent calcein acetoxymethyl ester (AM) is permeable to intact cell membranes and is converted by ubiquitous intracellular esterases into fluorescent calcein, which causes viable cells to fluoresce green. Ethidium homodimer-1 (EthD-1), though impermeable to intact cell membranes, is able to enter cells with damaged membranes.

EthD-1 is non-fluorescent until it binds to nucleic acids, which causes dead cells to fluoresce red.

The viability of SH-SY5Y cells used in immunosorbent experiments (see section 2.9) was assessed using the live/dead assay. Supernatants were removed and 0.2 ml of 1 μ M calcein AM and 1 μ M EthD-1 in PBS was added to each well. The plate was incubated at 37°C in CO₂ incubator for 5-10 min before visualizing the cells on an inverted microscope. Live cells were visualized through a fluorescein isothiocyanate (FITC) fluorescence set of filters, while dead cells were visualized through a Texas Red fluorescence set of filters.

Digital photographs were taken of each experimental well at 100x total magnification. A 4 x 6 grid containing 4.5 cm x 4.2 cm rectangles was overlaid on each photograph. Cell counts were conducted in a blinded fashion in that the counter did not know which images represented which treatments. The counter chose 3 random rectangles from which to count live (green) and dead (red) cells, and determined the average (\bar{x}) for each sample (i.e. average cells per well). The percentages of live and dead cells were determined using the following equations:

$$(5) \% \text{ Live cells} = \bar{x}_{\text{live cells}} / [\bar{x}_{\text{live cells}} + \bar{x}_{\text{dead cells}}] \times 100\%$$

$$(6) \% \text{ Dead cells} = \bar{x}_{\text{dead cells}} / [\bar{x}_{\text{live cells}} + \bar{x}_{\text{dead cells}}] \times 100\%,$$

where $\bar{x}_{\text{live cells}}$ represents the average number of live cells in the sample and $\bar{x}_{\text{dead cells}}$ represents the average number of dead cells in the sample. At least 170 cells were counted for each sample.

2.9 Immunosorbent Experiments

Immunosorbents for sPLA₂IIA and PGE₂ were composed of sepharose 4b beads coated with mouse anti-human sPLA₂IIA or mouse anti-human PGE₂ antibodies, respectively. Both sorbents were supplied as a 1:1 (v/v) suspension in PBS. ConA-coated sepharose, also containing sepharose 4b beads, was used as a control for the sepharose 4b matrix used in both sPLA₂IIA and PGE₂ sorbents.

The initial 1:1 sorbent aliquots (total volume 0.1 ml each) were centrifuged at 500 g for 1 min and reconstituted at a ratio of 1:20 v/v by replacing the supernatant with 1 ml PBS. Each aliquot underwent one regeneration cycle before use in experiments, which consisted of rinses with four different solutions in the following order: 1 x 1 ml HCl-glycine buffer (pH 4), 1 x 1 ml 100% molecular-grade EtOH, 2 x 1 ml PBS, and 1 x 1 ml serum-free DMEM-F12. Prior to each solvent rinse, sorbent aliquots were centrifuged at 500 g for 1 min to sediment the sorbent before proceeding to the next solvent. After each centrifugation step, supernatant was discarded and the sorbent was gently pipetted up and down 5x to disperse sorbent before subsequent rinsing.

After rinsing, 1 ml cell culture supernatant was added to each sorbent aliquot, dispersed via pipetting, and incubated on a bench-top rocker for 10 min at room temperature. Sorbent-treated samples were then centrifuged at 500 g for 1 min, the sorbent-free supernatants transferred to SH-SY5Y cells and cultures were incubated at 37°C in a CO₂ incubator. LDH and MTT assays were performed on the SH-SY5Y cells cultures after 72 h incubation.

2.10 Enzyme-Linked Immunosorbent Assay (ELISA)

The ELISA was conducted exactly as specified in Cayman Chemical Company's protocol. Briefly, the assay utilized a double-antibody "sandwich" technique, allowing any sPLA₂IIA in cell supernatant samples to first bind with a primary antibody immobilized to the well surface. The secondary antibody was an acetylcholinesterase:antigen-binding fragment conjugate that bound selectively to an alternative epitope on the sPLA₂IIA protein, forming an immobilized sPLA₂IIA "sandwich" between the primary and secondary antibodies. After rinsing the plate from excess supernatant and antibodies, Ellman's reagent was added, which contained substrate for acetylcholinesterase causing production of a yellow colour upon being converted by acetylcholinesterase. The optical density of the samples at 405 nm was measured and the concentration of sPLA₂IIA derived by using samples containing known concentrations of rsPLA₂IIA.

Cell supernatants (0.1 ml) and eight ELISA standards of known rsPLA₂IIA concentration were transferred to a 96-well plate pre-coated with mouse anti-human sPLA₂IIA antibodies, after which 0.1 ml of acetylcholinesterase:antigen-binding fragment conjugate was added to each well except one blank well. The plate was covered and incubated for 24 h at 4°C. After incubation, plate contents were discarded and the plate was washed 5x with wash buffer provided with the kit. 0.2 ml Ellman's reagent was added to each well, after which the plate was incubated in the dark on an orbital rotator for 2 h. Absorbance at 405 nm was measured using the microplate reader, and concentrations of sPLA₂IIA in each sample (i.e. each well containing 0.2 ml Ellman's reagent) were determined using the following equations:

$$(7) A_n - A_{\text{blank}} = dA_n$$

$$(8) [dA_n - Y \text{ intercept}] / \text{slope} = \text{sPLA}_2\text{IIA concentration (pg/ml)}$$

where A_n represents the absorbance of the sample in question, A_{blank} is the absorbance of the blank sample, and dA_n is the difference between A_n and A_{blank} . The Y intercept and slope values were determined from an equation derived by plotting the absorbance versus concentration for the rsPLA₂IIA standards (for an example of the calibration curve, see Figure 2.1). All resulting values were then converted from pg/ml to pmol/L (sPLA₂IIA molecular weight =16 kDa). The detection limit of the assay (pmol/L) was determined by multiplying the standard deviation of all blank absorbance values by 2 and calculating the corresponding sPLA₂IIA concentration.

2.11 RNA Isolation and Reverse Transcription (RT)

RNA from both stimulated and unstimulated THP-1 cells, U-373 MG cells, and human astrocytes was isolated using the SV RNA isolation kit from Promega. Procedures were performed as specified in the manufacturer's protocols. All reagents listed in this section were provided in the kits with the following exceptions: LPS, human IFN- γ and 100% molecular-grade EtOH.

Briefly, 10 ml of a 0.5 million cells/ml solution of each cell type were seeded on separate 10 cm tissue culture dishes. THP-1 cells were incubated at 37°C in a CO₂ incubator for 15 min before stimulation with LPS (0.5 μ g/ml) and human IFN- γ (150 U/ml). U-373 MG cells and human astrocytes were allowed to adhere for 24 h before stimulation with IFN- γ (150 U/ml). THP-1 cells were stimulated for 4, 24 and 48 h, after

which cells were harvested into separate 1.5 ml microtubes and centrifuged at 250 g for 10 min. U-373 MG cells were stimulated with IFN- γ for 24 h, after which supernatants were removed and cells were detached by using 0.05% trypsin/EDTA solution, collected into 1.5 ml microtubes and centrifuged at 250 g for 10 min. Human astrocytes were stimulated for 48 h with human IFN- γ , after which supernatants were removed and cells were detached with 0.25% trypsin/EDTA solution, collected into 1.5 ml microtubes and centrifuged at 250 g for 10 min.

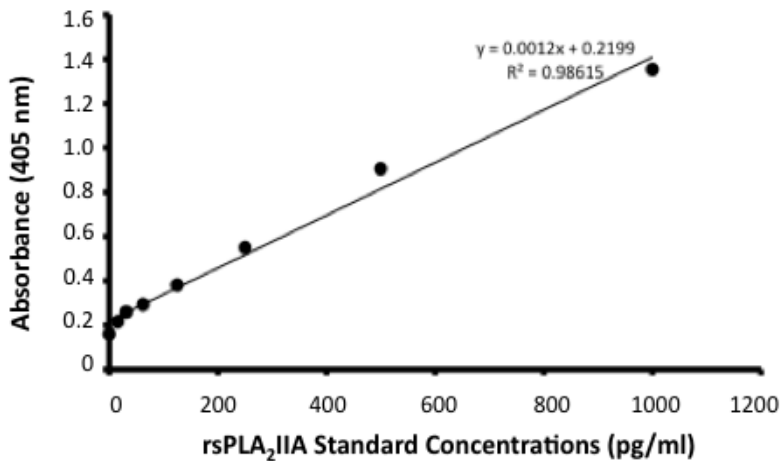


Figure 2.1: A typical calibration curve for the sPLA₂IIA ELISA. Standard concentrations for the sPLA₂IIA ELISA were linearly correlated with the absorbance values at 405 nm. The slope equation in addition to the R² value for the linear relationship is shown on the graph.

After centrifugation, supernatants were removed and the remaining cells were treated with 175 μ l RNA lysis buffer (4 M guanidine thiocyanate, 0.01 M Tris at pH 7.5 and 1% v/v β -mercaptoethanol) and 350 μ l RNA dilution buffer (6x saline-sodium citrate buffer at pH 7 containing 0.9 M NaCl and 0.09 M sodium citrate, 10 mM Tris-HCl at pH 7.4, 1 mM EDTA and 0.25% w/v SDS). The microtubes were placed in a heating block at

70°C for 3 min and subsequently centrifuged for 10 min at 13,000 g. The resulting supernatant was collected into a spin column assembly (consisting of a filter nested within a 2 ml collection tube) and mixed thoroughly with 200 µl 100% molecular-grade EtOH. The spin column assembly was centrifuged for 1 min at 13,000 g, after which the collection tube was emptied and 600 µl of RNA wash solution (162.8 mM potassium acetate and 27.1 mM Tris-HCl at pH 7.5) was added to each assembly. After centrifugation for 1 min at 13,000 g, 40 µl yellow core buffer (22.5 mM Tris at pH 7.5, 1.25 M NaCl and 0.0025% w/v yellow dye), 10 µl 0.09 M MnCl₂•4H₂O and 10 µl DNase I enzyme were added to each assembly and left to incubate at room temperature for 15 min. 200 µl DNase stop solution was added to each assembly and centrifuged at 13,000 g for 1 min. After emptying the collection tube, filters were rinsed twice with RNA wash buffer: 600 µl with centrifugation at 13,000 g for the first rinse, and 250 µl with centrifugation at 16,000 g for the second rinse. Collection tubes beneath the filters were replaced with fresh 1.5 ml microtubes for the collection of mRNA. To collect THP-1 and U-373 MG mRNA, 100 µl nuclease-free water (NFW) was added to each filter and assemblies were centrifuged at 13,000 g for 1 min. For human astrocyte RNA, only 50 µl NFW was added before centrifugation to obtain more concentrated RNA samples. RNA concentrations in all samples were estimated using a spectrophotometer and were within the acceptable 260/280 range of 1.7 to 2.3 (see Appendix A for RNA purity values). More concentrated samples were diluted with NFW to match the lowest concentration per cell type.

The Promega Improm 2 RT kit was used to convert mRNA samples to cDNA as specified in the manufacturer's protocol. Random hexamer (1 µl) was added to 4 µl of

mRNA samples and the mixture was heated to 70°C for 5 min. Samples were placed on ice for 5 min, after which 15 µl of a solution containing RT, 6 mM MgCl₂, deoxynucleotide triphosphates, reaction buffer (250 mM Tris-HCl (pH 8.3 at 25°C), 250 mM KCl, 50 mM MgCl₂, 2.5 mM spermidine and 50 mM dithiothreitol) and NFW was added. Samples were incubated at room temperature for 5 min, then at 40°C for 1 h. The RT reaction was stopped by heating each sample at 70°C for 15 min.

2.12 Polymerase Chain Reaction (PCR)

PCR amplification of cDNA was performed using GoTaq Green Master Mix (400 µM each of deoxyadenosine triphosphate, deoxyguanosine triphosphate, deoxycytidine triphosphate and deoxythymidine triphosphate, as well as 3 mM MgCl₂ in Green GoTaq reaction buffer at pH 8.5) from Promega. Each PCR sample was prepared by mixing 1.5 µl 10 µM forward primer, 1.5 µl 10 µM reverse primer, 4 µl cDNA, 12.5 µl GoTaq Green Master Mix, and 5.5 µl NFW, for a total sample volume of 25 µl. The thermal cycler program for amplification of THP-1 cell and human astrocyte cDNA using sPLA₂IIA-specific primers consisted of an initial 95°C denaturation step for 2 min, followed by 40 cycles of 30 sec denaturation at 95°C, 30 sec annealing at 62°C and 1 min extension at 74°C for 1 min, with the final extension step lasting 5 min. For amplification of U-373 MG cell cDNA using sPLA₂IIA-specific primers, only 30 cycles of 30 sec denaturation were performed; otherwise the program was the same. The thermal cycler program for the amplification of all glial cell cDNA using both housekeeping primers (see next section) was the same as for sPLA₂IIA primers except it continued for 35 cycles

and the annealing temperature was 55°C. PCR products were separated using electrophoresis on a 6% polyacrylamide gel and visualized by staining with SYBR safe dye. Digital photographs of the gels were taken with the AlphaView imaging system and software for image analysis.

2.13 PCR Primer Design and Restriction Analyses

All primers were obtained from IDT and were designed using the Primer 3 software. sPLA₂IIA-specific primers (Genbank accession NM000300.3) were designed to amplify a product to span at least two introns so that any resulting genomic DNA product would be much larger than the expected cDNA-amplified products. Homologous sequences in other genes for each primer were ruled out using a nucleotide Basic Local Alignment Search Tool (BLAST, <http://blast.ncbi.nlm.nih.gov/Blast.cgi>).

Two PCR primer pairs were used to amplify sPLA₂IIA cDNA. The first pair of primers (S1) contained: forward, 5' AGGAAAGGAAGCCGCACTCAGTTA 3'; and reverse, 5' AGAGAGGGAAATTCAGCACTGGGT 3'. The second pair of primers (S2) contained: forward, 5' AGGAAAGGAAGCCGCACTCAGTTA 3'; and reverse, 5' AGGCTGGAAATCTGCTGGATGTCT 3'. These primer pairs were designed to produce 386 base pair (bp) and 514 bp fragments, respectively.

To ensure the identity of the PCR products, restriction enzyme analysis was conducted on PCR products obtained by the sPLA₂IIA mRNA-specific primers. The restriction enzymes *Bam*HI and *Dde*I were used because they have recognition sequences common to both S1 and S2 PCR products. S1 PCR products (386 bp) were digested by

*Bam*HI into 357 and 29 bp fragments, and by *Dde*1 into 312 and 74 bp fragments. S2 PCR products (514 bp) were digested by *Bam*HI into 452 and 62 bp fragments, and by *Dde*1 into 497 and 17 bp fragments. Digested PCR products were separated on a 6% polyacrylamide gel and visualized by staining with SYBR safe dye. All digestion products were of the expected sizes (data not shown).

Cyclophilin and glyceraldehyde-3-phosphate dehydrogenase (G3PDH) were used as housekeeping genes on each sample because both cyclophilin and G3PDH are expressed in nearly all cells due to their roles in basic cellular metabolism (Zhong and Simons, 1999). Primers for the cyclophilin gene were designed to produce a 206 bp product and contained: forward, 5' ATGGTCAACCCACCGTGTCTTCG 3'; and reverse, 5' CGTGTGAAGTCACCACCCTGACACA 3'. Primers for the G3PDH gene were designed to produce a 215 bp product and contained: forward, 5' CCATGTTCGTCATGGGTGTGAACCA 3'; and reverse, 5' GCCAGTAGAGGCAGGGATGATGTTC 3'. Both housekeeping primer pairs were previously used by Klegeris and McGeer (2000). All primer pairs, including S1 and S2, were optimized for annealing temperature using a gradient between 50 and 65°C (data not shown).

2.14 Neurotoxicity of Exogenous sPLA₂

2.14.1 Bee Venom sPLA₂ type III (sPLA₂III)

To verify the effect of exogenous sPLA₂ isozymes on SH-SY5Y neuroblastoma cells, bee venom-derived sPLA₂III was used in similar concentrations at which human sPLA₂IIA was reported to be neurotoxic (Yagami *et al.* 2002). Lyophilized sPLA₂III (molecular weight = 14 kDa) was reconstituted in sterile deionized water to a stock concentration of 100 µM. The sPLA₂III stock was serially diluted with deionized water before adding to SH-SY5Y cells to achieve the final concentrations of 1, 0.5, 0.1, 0.05, and 0.01 µM. SH-SY5Y cells were then incubated in a CO₂ incubator at 37°C for 72 h before LDH and MTT assays were conducted.

2.14.2 Human rsPLA₂IIA

The protocol for plating SH-SY5Y cells to test the cytotoxicity of human rsPLA₂IIA (molecular weight = 16 kDa) differed only in that the cells were seeded on to a sterile 96-well plate rather than a 24-well plate in order to conserve rsPLA₂IIA stock. In addition, the well volumes were 0.1 ml rather than 0.4 ml. Samples of rsPLA₂IIA were obtained from two independent sources. The lyophilized human rsPLA₂IIA from ProSpec was reconstituted in 0.2 ml sterile PBS (pH 7.5) to a stock concentration of 3 µM. Serial dilutions of the ProSpec rsPLA₂IIA stock were made in PBS before adding the protein to SH-SY5Y cells such that the final concentrations of 1, 0.5, 0.1, 0.05 and 0.01 µM were achieved. SH-SY5Y cells were then incubated in a CO₂ incubator at 37°C for 72 h before LDH and MTT assays were conducted.

Another sample of 0.9 mg/ml (56.3 μ M) rsPLA₂IIA in 5 mM tris (pH 8) buffer was provided by Dr. Michael Gelb. Serial dilutions of rsPLA₂IIA were made in tris (pH 8) before adding the protein to SH-SY5Y cells such that the final concentrations of 1, 0.5, 0.1, 0.05 and 0.01 μ M were achieved. SH-SY5Y cells were then incubated in a CO₂ incubator at 37°C for 72 h before LDH and MTT assays were conducted.

2.14.3 Bacterial Lipopolysaccharide (LPS)

Because both rsPLA₂IIA samples were produced in bacteria, it was necessary to exclude the possibility that chance residual bacterial lipopolysaccharide (LPS) was cytotoxic to SH-SY5Y cells. LPS was added directly to SH-SY5Y cells to achieve the final concentrations of 1, 0.5, 0.1, 0.05 and 0.01 μ g/ml. SH-SY5Y cells were then incubated in a CO₂ incubator at 37°C for 72 h before LDH and MTT assays were conducted.

2.15 Experiments with Enzyme Inhibitors and Receptor Antagonists

2.15.1 Specific sPLA₂ Inhibitors

Two specific sPLA₂ inhibitors and their pharmacologically inactive derivative were kindly provided by Drs. Michael Gelb and Rob Oslund. RO032107 is a novel inhibitor highly selective for sPLA₂IIA. RO041709 is a methylated control compound for RO032107, which is inactive towards sPLA₂IIA. RO092906 is a novel inhibitor selective for sPLA₂ type X (sPLA₂X). Because of the specificity of these inhibitors towards secreted (extracellular) forms of PLA₂, they were either 1) incubated with THP-1

supernatants from cells that had been stimulated with LPS and IFN- γ for 48 h before transfer to SH-SY5Y cells; 2) directly added to SH-SY5Y cells immediately after transfer of supernatants from cells that had been stimulated with LPS and IFN- γ for 48 h; or 3) added to SH-SY5Y cells treated with 1 μ M rsPLA₂IIA. SH-SY5Y cells were incubated at 37°C for 72 h in CO₂ incubator before assessing cell viability with LDH and MTT assays. For each experiment, all three compounds were tested at 10, 5, 1, 0.5, and 0.1 μ M, while keeping the DMSO content in each well at 0.5% v/v. In addition, a DMSO solvent control was included in each experiment

2.15.2 Non-Specific PLA₂ Inhibitors and PGE₂ Receptor Antagonists

Four non-specific PLA₂ inhibitors and two PGE₂ receptor antagonists were tested for their 1) effects on THP-1 cytotoxicity, and 2) neuroprotective properties. To test the effects of the compounds on THP-1 cytotoxicity, THP-1 cells were plated onto 24-well plates at a density of 0.5 million cells/ml, 0.8 ml/well. Drugs were added to THP-1 cells 15 min before stimulation with the combination of LPS (0.5 μ g/ml) and IFN- γ (150 U/ml). Plates were incubated at 37°C in CO₂ incubator for 48 h and then supernatants were transferred to SH-SY5Y cells. After 72 h incubation at 37°C in CO₂ incubator SH-SY5Y cell viability was assessed by using the LDH and MTT assays.

To determine whether drugs had neuroprotective properties, they were added to SH-SY5Y cells immediately after the transfer of supernatants from stimulated THP-1 cells. The SH-SY5Y cells were then incubated at 37°C for 72 h in CO₂ incubator before assessing cell viability by using the LDH and MTT assays.

All six compounds were dissolved in DMSO. The DMSO content in each well was kept at 0.5% v/v, and a DMSO solvent control was included in each experiment. Drug targets and concentrations used in experiments are listed in Table 2.1.

Compound	Target(s)	Concentration Gradient (μM)
<i>PLA₂ Inhibitors</i>		
MAFP	cPLA ₂ and iPLA ₂	10, 5, 1, 0.5, 0.1
BPPA	sPLA ₂ isoforms	10, 5, 1, 0.5, 0.1
DMDA	cPLA ₂	100, 50, 10, 5, 1
OPHAO	sPLA ₂ isoforms	100, 50, 10, 5, 1
<i>PGE₂ Receptor Antagonists</i>		
AH6809	EP ₄ receptor	100, 50, 10, 5, 1
L-161,982	EP ₁ , EP ₂ , and EP ₃ receptors	10, 5, 1, 0.5, 0.1

Table 2.1: Non-Specific PLA₂ Inhibitor and PGE₂ Receptor Antagonist Targets and their Concentrations Used in Experiments.

2.16 Measurement of PLA₂ Enzymatic Activity

This assay was used to determine sPLA₂IIA enzymatic activity in cell-free supernatants from stimulated and unstimulated THP-1 cells, U-373 MG cells and human astrocytes. The rate at which sPLA₂ enzymatically altered the substrate PGPM was measured. PGPM is a glycerophospholipid that has 1-pyrenedecanoic acid bound to the PLA₂ target sn-2 position of the glycerol (Pernas *et al.* 1991). While bound, the fluorescence of 1-pyrenedecanoic acid is quenched. In the presence of enzymatically active PLA₂, the 1-pyrenedecanoic acid is released; therefore, stronger fluorescent signals

are indicative of higher levels of PLA₂ enzymatic activity (Pernas *et al.* 1991). Substrate buffer used to dilute PGPM consisted of 50 mM tris base, 500 mM NaCl, and 20 mM CaCl₂, pH 8.5. Samples of rsPLA₂IIA at 0.1 μM was used as positive controls. Since PGPM acts as a substrate for several sPLA₂ isoforms, the sPLA₂IIA-selective inhibitor RO032107 and the sPLA₂X-selective inhibitor RO092906 were used at 10 μM to differentiate sPLA₂IIA- and sPLA₂X-specific activity.

50 μl samples of supernatants from stimulated and unstimulated THP-1 cells, U-373 MG cells and human astrocytes were transferred to a black, top-read 96-well plate. The 1-pyrenedecanoic acid standard was diluted in F10 to achieve 10, 5, 2.5, and 1.25 μM concentrations after the addition of 50 μl substrate buffer to 50 μl of standard. To initiate the assay, 50 μl of substrate buffer was added to each supernatant sample, and fluorescence was read in a microplate reader for 5 min. A substrate blank, which consisted of 50 μl of F10 and 50 μl of substrate, was included with each plate. The microplate reader was programmed to measure fluorescence at 320 nm excitation and 405 nm emission every 30 sec for 5 min, orbitally shaking the plate for 3 sec before each measurement. The rate of sPLA₂ enzyme activity for each supernatant sample (n) was determined using the following equations:

$$(9) [F_{ave_n} - F_{ave_{blank}}] = dF_n$$

$$(10) dF_n \times \text{conversion factor} = \text{sPLA}_2 \text{ enzyme activity (pmol/min)},$$

where F_{ave_n} represents the average fluorescence of sample n, $F_{ave_{blank}}$ represents average fluorescence of the blank, and dF_n represents the difference between F_{ave_n} and $F_{ave_{blank}}$ in relative fluorescence units (RFU)/min. The conversion factor (pmol/RFU) represents 1/slope, where the slope was determined by plotting absorbance versus concentration for

the 1-pyrenedecanoic acid standards. To determine sPLA₂IIA-specific activity, the calculated sPLA₂ enzyme activity for samples treated with RO032107 was subtracted from the values obtained from samples treated with DMSO. Similarly, sPLA₂X-specific activity was calculated by subtracting sPLA₂ activity for samples treated with RO092906 from values obtained from samples treated with DMSO.

sPLA₂IIA-specific inhibitor RO032107, sPLA₂X-specific RO092906 and control compound RO041709 were also tested for their effects on rsPLA₂IIA activity. 1 µM of either compound or the corresponding volume of DMSO solvent was added to 50 µl of 0.1 µM rsPLA₂IIA in F5 in a 96-well black plate. The plate was incubated at room temperature for 10 min before adding the substrate and reading the fluorescence over a 5 min period at the emission and excitation settings described above.

2.17 Potential Mechanisms of sPLA₂IIA Neurotoxicity

2.17.1 Effects of sPLA₂IIA on SH-SY5Y Cells Pre-Treated with H₂O₂

It is possible that sPLA₂IIA becomes more toxic to cells with disrupted membranes; therefore, H₂O₂ was used to pre-damage SH-SY5Y cells before the addition of rsPLA₂IIA. The experiment followed the protocol for testing 1 µM rsPLA₂IIA toxicity on SH-SY5Y cells except that, 5 min prior to sPLA₂IIA addition, 250 µM H₂O₂ was added to the well. SH-SY5Y cells were incubated at 37°C for 72 h in CO₂ incubator before their viability was assessed by using the LDH and MTT assays.

2.17.2 sPLA₂IIA Regulation via PPAR α

Certain cPLA₂ products may stimulate PPAR α and contribute to sPLA₂IIA up-regulation in glial cells. MK886 was used to test whether antagonizing PPAR α would affect THP-1 cytotoxicity. MK886 was dissolved in DMSO. THP-1 cells were seeded onto a 24-well plate at 0.5 million cells/ml in 0.8 ml/well. Cells were incubated at 37°C in CO₂ incubator for 15 min, after which MK886 was added to achieve the final concentrations of 10, 5, 1, 0.5 and 0.1 μ M, keeping the DMSO concentration at 0.5% v/v in each well. From this point the experiment was carried on exactly as described for testing the non-specific PLA₂ inhibitors on THP-1 cytotoxicity (section 2.15.2).

2.17.3 Non-Enzymatic Complex between sPLA₂IIA and Neuronal TLR4

To test the hypothesis that glial cell-derived sPLA₂IIA cytotoxicity is caused by binding to neuronal TLR4, the anti-TLR4/MD-2 monoclonal antibody (mAb) was used to interfere with the hypothetical sPLA₂IIA-TLR4 complex. Anti-TLR4/MD-2 mAb at 2, 1, 0.2, 0.1 or 0.02 ng/ml in sterile PBS (pH 7.5) was either 1) incubated with supernatants from THP-1 cells that had been stimulated for 48 h with LPS and IFN- γ before transfer to SH-SY5Y cells, or 2) directly added to SH-SY5Y cells immediately after transfer of supernatants from THP-1 cells that had been stimulated for 48 h with LPS and IFN- γ . SH-SY5Y cells were then incubated at 37°C for 72 h in CO₂ incubator before their viability was assessed by using LDH and MTT assays.

2.18 Statistical Analysis

SPSS software (version 16.0; IBM SPSS, Chicago, IL, USA) was used to conduct statistical analyses of the data. Experiments were designed to allow pairwise comparisons or use of randomized block design analysis of variance (ANOVA) for statistical analysis, which lessened the impact of variability between experimental days by assigning each day as a block. Randomized block design ANOVA was performed with data obtained from the experiments involving concentration gradients, followed by the Fisher's Least Significant Difference (LSD) post hoc test, which was used to assess all possible comparisons for significant differences. The Fisher's LSD test is the least stringent post hoc test and was chosen in order to avoid overlooking any small (but significant) effects.

Student's T-test for paired observations was used to assess the differences between the effects of unstimulated and stimulated glial cell supernatants. Data on all figures are presented as means \pm the standard error of the mean (SEM). A probability (P) value less than 0.05 was considered statistically significant, though cases that were less than 0.01 were also indicated for transparency. All cases where Fisher's LSD test or paired Student's t-test showed statistically significant differences are identified on the figures as either *P<0.05 or **P<0.01.

Randomized block design ANOVAs were conducted separately on LDH and MTT data sets. The dependent variable for the ANOVA was the LDH or MTT values, the independent variable was the compound concentration from 0 (solvent only value) to the highest compound concentration tested, and the random variable used to define the blocks was the day the experiment took place. Though the Fisher's LSD test analyzed

each possible comparison within a data set, only comparisons made between the solvent only value and all other compound concentrations were reported on figures.

3 Results

3.1 Inflammatory Stimuli Evoke Neurotoxic Glial Cell Response

The following experiments were conducted to test the central hypothesis that sPLA₂IIA is 1) neurotoxic, and 2) produced and secreted by microglia-like cells and astrocytes upon stimulation with inflammatory factors. The toxicity of microglia and astrocytes toward neurons after stimulation with inflammatory factors has been demonstrated by several studies (Cameron and Landreth 2009; Zhang *et al.* 1999; Klegeris *et al.* 2003; Hashioka *et al.* 2009). A preliminary experiment was conducted to reproduce these experiments in our laboratory and confirm that monocytic THP-1 cells, U-373 MG astrocytoma cells, and primary human astrocytes become neurotoxic after 48 h of stimulation with pro-inflammatory IFN- γ alone or in combination with LPS.

Cell-free supernatants from stimulated and unstimulated THP-1 cells, U-373 MG cells or human astrocytes were incubated with neuronal SH-SY5Y cells for 72 h, after which SH-SY5Y cell death and viability was determined using the LDH and MTT assays, respectively (Fig. 3.1). Student's T-tests for paired observations were conducted to compare the effects of stimulated and unstimulated cell supernatants of each glial cell type. For all three glial cell types, stimulated supernatants showed a significantly higher toxicity towards SH-SY5Y cells, increasing cell death by at least 30% compared to the untreated control according to the LDH assay (Fig. 3.1.A). Similarly, MTT values showed that stimulated supernatants had significantly increased detrimental effects on SH-SY5Y cell viability compared to unstimulated supernatants (Fig. 3.1.B). LDH and MTT values for SH-SY5Y cells treated with unstimulated supernatants were not significantly different from values obtained from medium-treated SH-SY5Y cells.

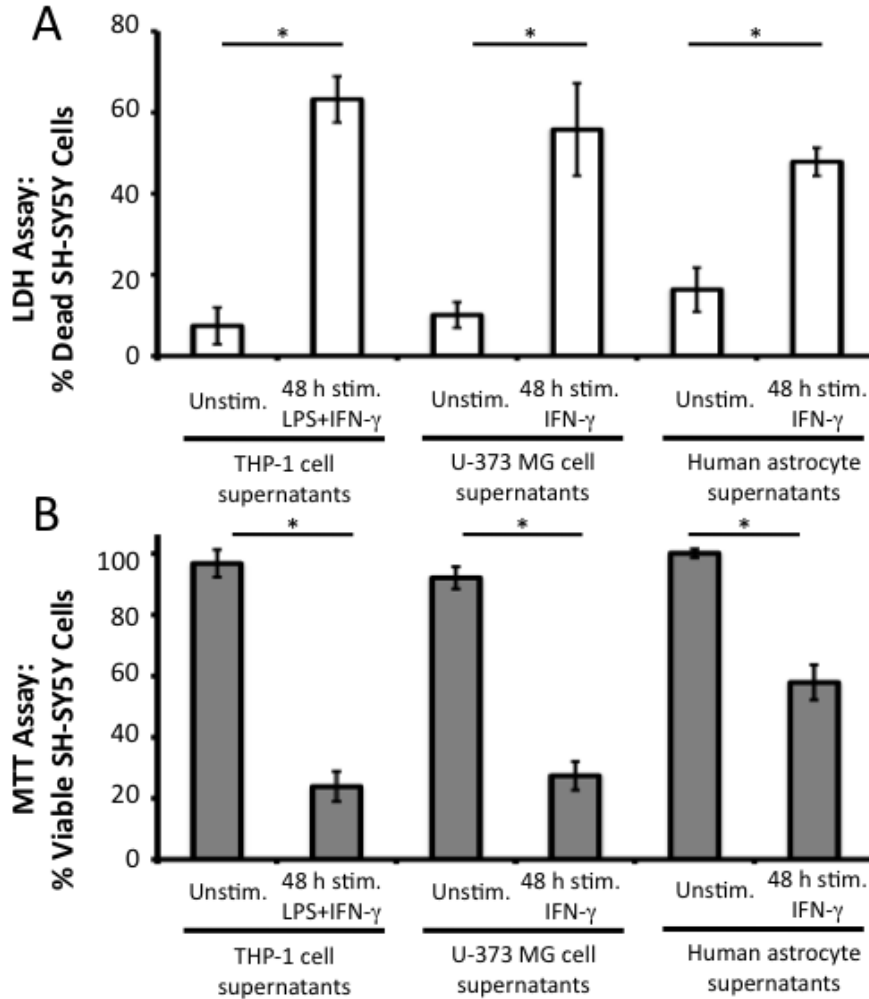


Fig. 3.1: Supernatants from stimulated human THP-1 cells, U-373 MG cells and astrocytes were toxic to human SH-SY5Y neuroblastoma cells. LDH (A, white bars) and MTT (B, shaded bars) assays were used to determine the effect of treating human SH-SY5Y neuroblastoma cells with supernatants from either unstimulated (Unstim.) or stimulated cells. THP-1 cell were stimulated with LPS (0.5 $\mu\text{g/ml}$) and IFN- γ (150 U/ml), U-373 MG cell and human astrocytes were stimulated with IFN- γ (150 U/ml) only for 48 h. (A) The LDH assay was used to measure cell death after each treatment; results are expressed as a percentage of a 100% lysed cell control. (B) The MTT assay was used to measure cell viability; results are expressed as a percentage of the values obtained from medium-only treated SH-SY5Y cell control. Data from 5 independent experiments are presented as means. Pairwise comparisons were made between stimulated and unstimulated samples respective of each cell type using Student's T-test for paired observations, showing significance where * $P < 0.05$.

3.2 Neurotoxicity of sPLA₂ Isoforms

It is known that bee venom is neurotoxic (Dennis 1994). An active ingredient of the bee venom, sPLA₂III, is structurally similar to human sPLA₂IIA. The neurotoxicity of sPLA₂III was verified by using human SH-SY5Y neuroblastoma cells. Figure 3.2 illustrates that as the amount of sPLA₂III added increased, the viability of SH-SY5Y cells decreased. 1 μ M sPLA₂III caused a significant increase in SH-SY5Y cell death (Fig. 3.2.A) and a decrease in cell viability (Fig. 3.2.B).

Next we studied the effects of human rsPLA₂IIA. Recombinant protein samples obtained from Prospec and the University of Washington were used. Similar to experiments with sPLA₂III, the viability of SH-SY5Y cells decreased with increasing concentrations of added rsPLA₂IIA. Figure 3.3.A shows significant enhancement of LDH release from SH-SY5Y cells treated with 1 μ M rsPLA₂IIA (Prospec) compared to the 100% lysed cell control. Figure 3.3.B shows that the addition of 1 μ M rsPLA₂IIA significantly decreased SH-SY5Y cell compared to the untreated SH-SY5Y cell viability. Because experiments with rsPLA₂IIA were conducted in 96-well plates, the spontaneous death rate for untreated SH-SY5Y cells was higher than for untreated SH-SY5Y cells plated in 24-well plates (see untreated SH-SY5Y cell values in Fig. 3.2.A vs. Fig. 3.3.A). rsPLA₂IIA from the University of Washington was tested in the same manner and also found to be significantly toxic to SH-SY5Y cells at 1 μ M (data not shown).

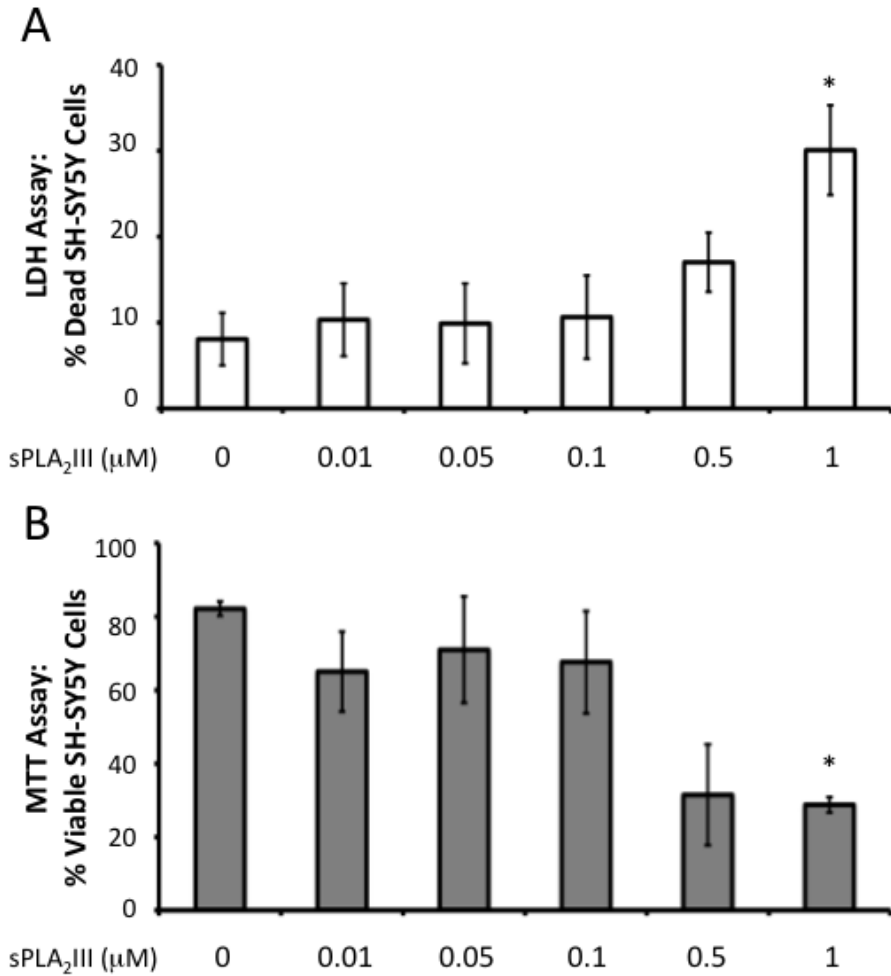


Figure 3.2: Bee venom sPLA₂III was toxic toward human SH-SY5Y neuroblastoma cells at 1 μM. LDH (A) and MTT (B) assays were used to measure the survival of SH-SY5Y cells, which were treated with either medium only or with various concentrations of sPLA₂III. (A) Cell death for each treatment is expressed as a percentage of a 100% lysed cell control. (B) Cell viability is expressed as a percentage of the values obtained from medium only-treated SH-SY5Y cells. Data from 3-5 independent experiments are presented as means. All values were compared using randomized block design ANOVA, followed by the Fisher's Least Significant Difference (LSD) test, where *P<0.05 if significantly different from the medium only treated control.

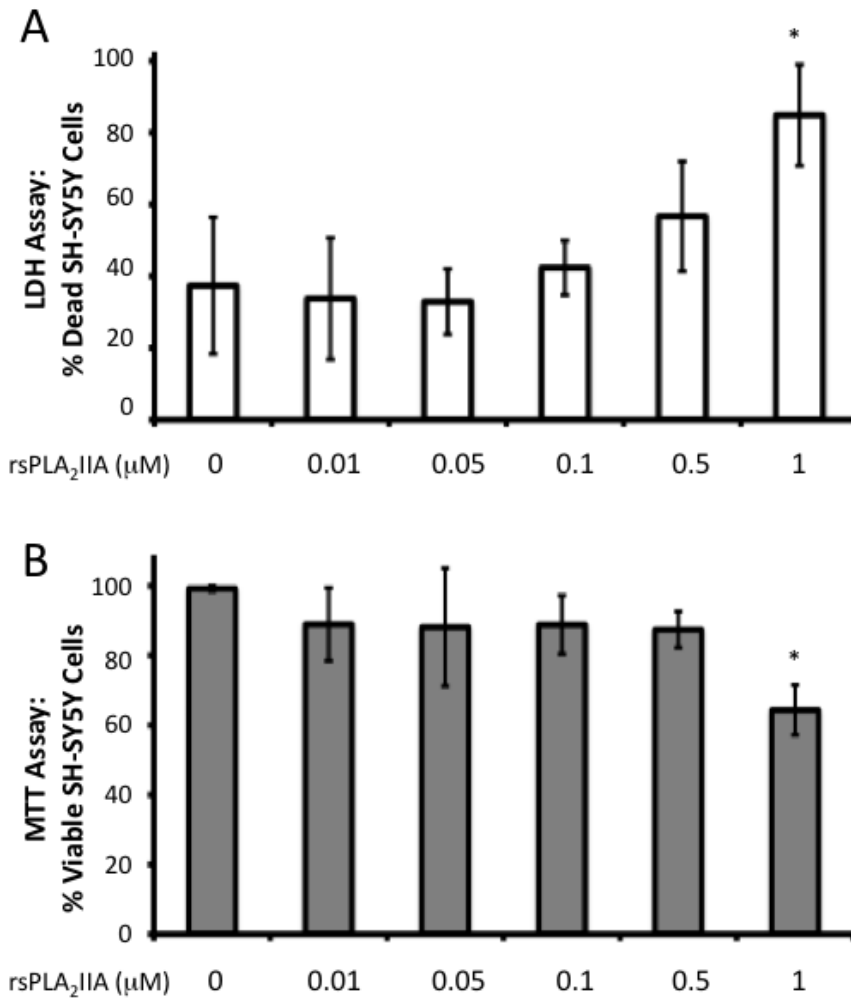


Figure 3.3: Human rsPLA₂IIA was toxic toward SH-SY5Y cells at 1 μM concentration. LDH (A) and MTT (B) assays were used to determine the effect of treating SH-SY5Y cells directly with various concentrations of rsPLA₂IIA compared to a medium only-treated control. (A) Cell death for each treatment is expressed as a percentage of a 100% lysed cell control. (B) Cell viability is expressed as a percentage of the values obtained from medium only-treated SH-SY5Y cells. Data from 6 independent experiments are presented as means. All values were compared using randomized block design ANOVA, followed by the Fisher's LSD test, where *P<0.05 if significantly different from the medium only treated control. Note that these experiments were performed in 96-well plates in order to conserve rsPLA₂IIA stock; therefore, a higher spontaneous cell death rate was observed for medium only treated SH-SY5Y cells.

Since both rsPLA₂IIA samples (from Prospec and University of Washington) were produced in bacteria, there was a possibility that the neurotoxicity observed was due to bacterial LPS contamination in the samples; therefore, the direct effect of LPS on SH-SY5Y cell viability was tested. Also, the cytotoxicity of human IFN- γ was tested to rule out the possibility that the cytotoxic effects of THP-1, U-373 MG, and human astrocyte supernatants were due to transfer of residual IFN- γ with supernatants from stimulated cell samples. Effects of LPS and IFN- γ on SH-SY5Y cell viability are shown in Figure 3.4. After 72 h incubation, only SH-SY5Y cells treated with the LPS concentration (1 μ g/ml) that is two fold higher than used to stimulate THP-1 cells showed significantly elevated LDH values as compared with the untreated control (Fig. 3.4.A); the MTT assay failed to detect significant toxic effects of LPS (Fig. 3.4.B). Human IFN- γ did not significantly affect SH-SY5Y viability according to both assays. Since the effects of both sPLA₂ types were observed at 1 μ M, LPS would only be responsible for the observed effects if the sPLA₂ samples have LPS contamination levels above 10 μ g/ml, which is very unlikely.

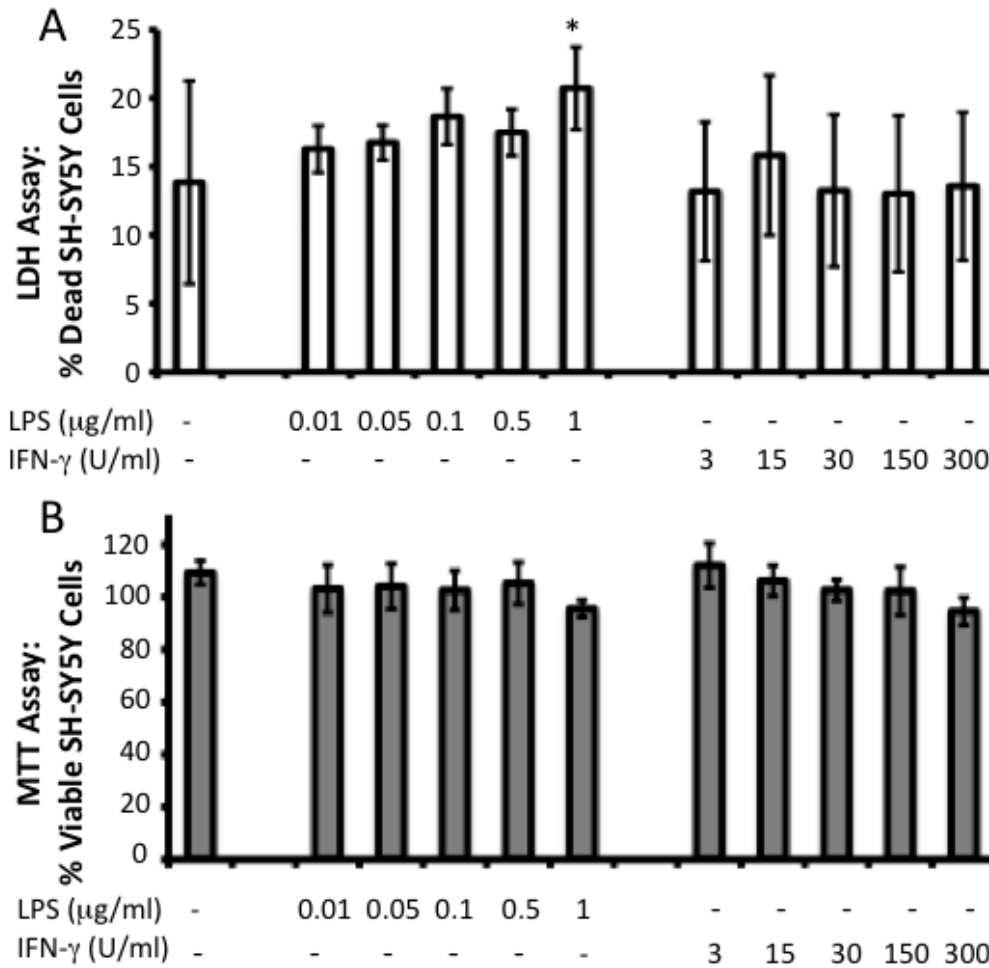


Figure 3.4: Neither bacterial LPS nor human IFN- γ exhibited significant cytotoxic effects toward SH-SY5Y cells at concentrations used for stimulation of human cell lines and astrocytes. LDH (A) and MTT (B) assays were used to determine the effect of treating SH-SY5Y cells directly with LPS (0.5 $\mu\text{g/ml}$) or IFN- γ (150 U/ml). (A) Cell death for each treatment is expressed as a percentage of a 100% lysed cell control. (B) Cell viability is expressed as a percentage of the values obtained for the medium only-treated SH-SY5Y cells. Data from 6 independent experiments are presented as means. All values were compared using randomized block design ANOVA, followed by the Fisher's LSD test, where * $P < 0.05$ if significantly different from the medium only treated control. Note that the 1 $\mu\text{g/ml}$ concentration of LPS that significantly elevated LDH levels is higher than the concentration used to stimulate THP-1 cells.

3.3 sPLA₂IIA mRNA Expression by Human Cell Lines and Astrocytes

Prior to mRNA extraction, THP-1 cells were stimulated with LPS (0.5 µg/ml) and IFN-γ (150 U/ml) for either 4, 24, or 48 h. U-373 MG cells were stimulated with IFN-γ (150 U/ml) for 24 h before mRNA collection, a time based on preliminary experiments that determined 24 h as an optimum stimulation period for sPLA₂IIA mRNA expression in astrocytes. Human astrocytes were also stimulated with IFN-γ; however, due to the limited number of human astrocytes available, mRNA was extracted from the cultures used for supernatant collection, which were stimulated for 48 h. Unstimulated cells of all three cell types were incubated in tissue culture medium only for 48 h before RNA extraction. Figure 3.5 shows that mRNA for both cyclophilin and G3PDH housekeeping genes were found in all samples studied. Increased expression of sPLA₂IIA mRNA-specific products was found in stimulated cell samples compared to unstimulated cell samples. For human astrocytes, only stimulated cells expressed sPLA₂IIA mRNA-specific products.

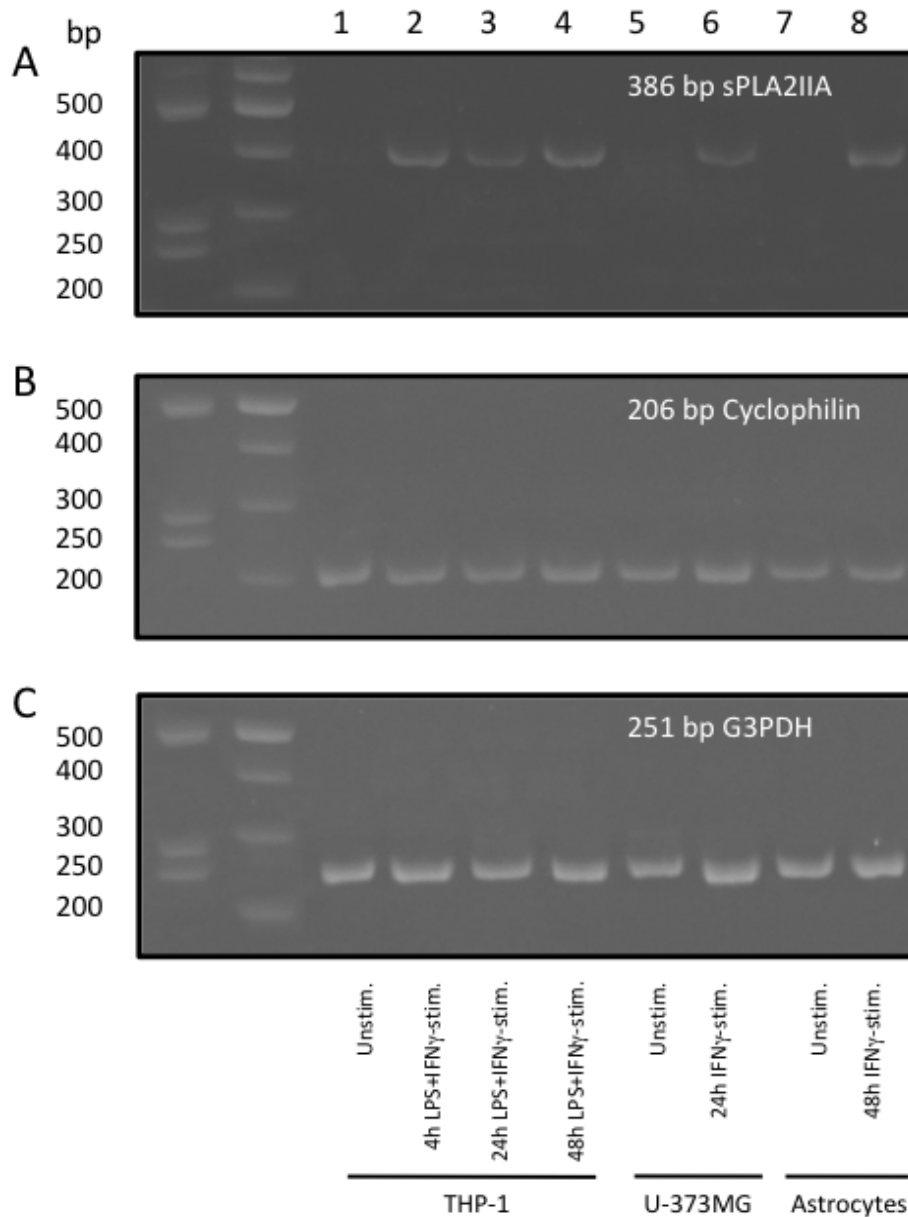


Figure 3.5: Stimulated cells expressed increased sPLA₂IIA mRNA compared to unstimulated cells. Total RNA samples extracted from stimulated and unstimulated THP-1 cells, U-373 MG cells and human astrocytes were amplified via RT-PCR using sPLA₂IIA (A), cyclophilin (B) and G3PDH (C) mRNA-specific primers. The PCR products were separated on polyacrylamide gels and visualized using SYBR safe dye. The mRNA expression patterns shown are representative of THP-1 and U-373 MG cell samples collected from 3 independent experiments, and human astrocytes prepared from 3 different surgical cases. Two different molecular weight ladders (1 kb and 100 bp) are shown in the left two lanes of the gel.

3.4 Concentrations of sPLA₂IIA in Glial Cell Supernatants

Supernatants from stimulated and unstimulated THP-1 cells, U-373 MG cells and human astrocytes were collected and analyzed for sPLA₂IIA protein concentration using a sPLA₂IIA-specific ELISA. Figure 3.6 shows that, in all three glial cell supernatants, sPLA₂IIA concentrations were significantly higher in stimulated samples versus unstimulated samples. The detection limit for the ELISA was 1.5 pM.

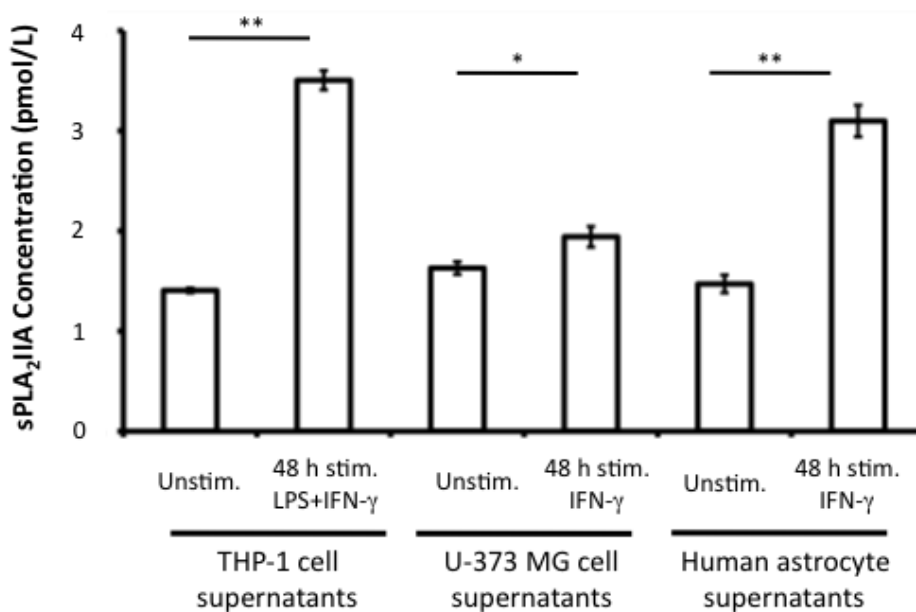


Figure 3.6: sPLA₂IIA protein concentrations were significantly higher in supernatants from stimulated compared to unstimulated human cell lines and astrocytes. Unstimulated cell supernatants (Unstim.) and 48 h stimulated cell supernatants (LPS+IFN-γ or IFN-γ alone respective to cell type), were collected from THP-1 cells, U-373 MG cells and primary human astrocytes and were analyzed for sPLA₂IIA concentrations using a sPLA₂IIA-specific ELISA. All sPLA₂IIA concentrations were determined using a calibration curve (see Methods). Data from 3-6 independent experiments are presented. Pairwise comparisons were made between stimulated and unstimulated samples respective of each cell type using Student's T-test for paired observations, showing significance where *P<0.05 and **P<0.01.

3.5 PLA₂ Enzymatic Activity in Cell Supernatants

Cell supernatants were collected from unstimulated and stimulated THP-1 cells, U-373 MG cells and human astrocytes and analyzed for total PLA₂ enzymatic activity using a fluorometric enzyme assay. No significant differences were found between PLA₂ enzymatic activities in stimulated compared unstimulated cell supernatants, regardless of cell type (Fig. 3.7).

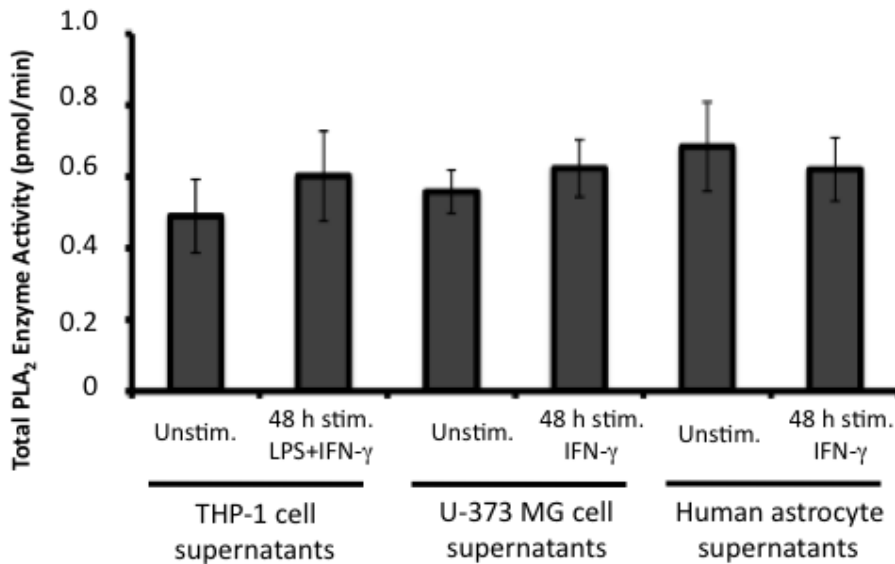


Figure 3.7: PLA₂ enzymatic activity measured in stimulated THP-1 cell, U-373 MG cell, and human astrocyte supernatants was not significantly different from respective unstimulated cell supernatants. Unstimulated (Unstim.) and 48 h stimulated cell supernatants (LPS+IFN- γ or IFN- γ alone respective to cell type) were collected from THP-1 cells, U-373 MG cells and primary human astrocytes, and were analyzed using a fluorometric sPLA₂ enzyme activity assay. Data from 3-5 independent experiments are presented as means. Pairwise comparisons were made between stimulated and unstimulated samples respective of each cell type using Student's T-test for paired observations. No statistical significance was found.

Before using the sPLA₂IIA-specific inhibitor RO032107, sPLA₂X-specific inhibitor RO092906 and control compound RO041709 in the cell culture models, they were first tested for inhibitory effects on 0.1 μ M rsPLA₂IIA enzymatic activity (Fig. 3.8).

1 μM of compound or DMSO solvent was incubated with 0.1 μM rsPLA₂IIA for 10 min before adding the 1-pyrenedecanoic acid substrate. After 10 min incubation, it was shown that the sPLA₂IIA-specific inhibitor RO032107 significantly reduced rsPLA₂IIA enzymatic activity compared to the DMSO solvent control. As expected, the sPLA₂X-specific inhibitor RO092906 and control compound RO041709 did not inhibit rsPLA₂IIA enzymatic activity.

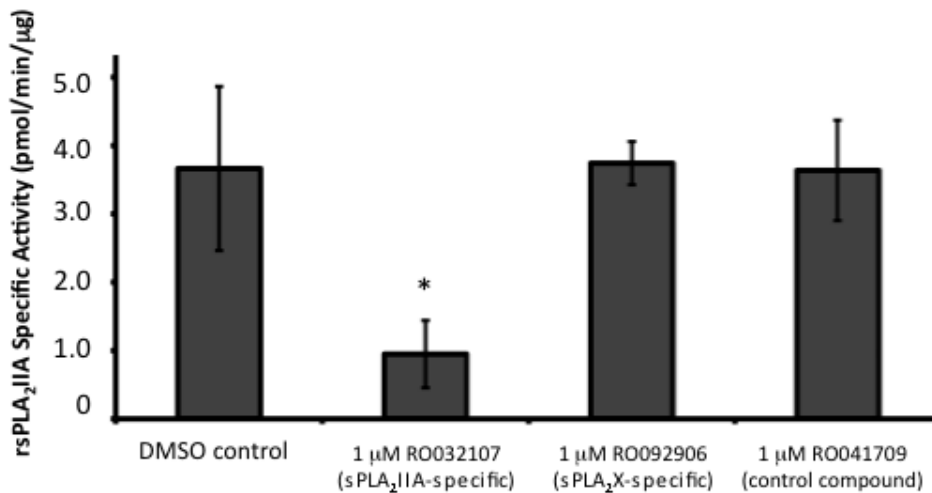


Figure 3.8: The sPLA₂IIA-specific inhibitor RO032107 significantly inhibited rsPLA₂IIA specific activity. 1 μM of RO032107, sPLA₂X-specific inhibitor RO092906 and control compound RO041709 were incubated with 0.1 μM rsPLA₂IIA for 10 min and then analyzed using a fluorometric PLA₂ enzyme activity assay. Data from 3 independent experiments are presented as means. All values were compared using randomized block design ANOVA, followed by Fisher's LSD test for multiple comparisons, where * $P < 0.05$ indicates a significant difference compared to DMSO control.

Figure 3.9 shows the effects of 10 μM RO032107 as well as the sPLA₂X-specific inhibitor RO092906 and control compound RO041709 on total PLA₂ activity in stimulated THP-1 cell supernatants. Compared with the DMSO solvent control, the sPLA₂IIA-specific inhibitor RO032107 was found to significantly inhibit PLA₂

enzymatic activity ($P=0.03$). As expected, control compound RO041709 did not significantly affect PLA₂ enzymatic activity when compared to the DMSO solvent control ($P=0.47$).

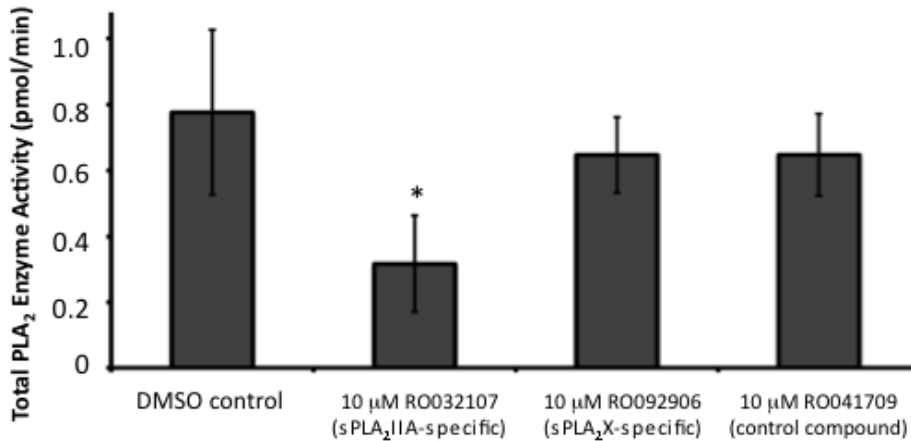


Figure 3.9: The sPLA₂IIA-specific inhibitor RO032107 significantly inhibited PLA₂ enzymatic activity in stimulated THP-1 cell supernatants. THP-1 cells were stimulated for 48 h with LPS (0.5 μg/ml) and IFN-γ (150 U/ml), after which their supernatants were collected, incubated with inhibitor or DMSO for 10 min, and analyzed using a fluorometric sPLA₂ enzyme activity assay. Data from 4 independent experiments are presented as means. All values were compared using randomized block design ANOVA, followed by Fisher's LSD test for multiple comparisons, where * $P<0.05$ indicates a significant difference compared to DMSO control.

In order to differentiate sPLA₂IIA enzymatic activity from total PLA₂ enzymatic activity, the sPLA₂IIA-specific inhibitor RO032107 was used on both stimulated and unstimulated cell supernatants for all three cell types (Fig. 3.10). Results from RO032107-treated supernatants were subtracted from values obtained in absence of the inhibitor in order to derive sPLA₂IIA-specific enzymatic activity; For example, enzymatic activity values from unstimulated THP-1 supernatant treated with RO032107 were subtracted from values obtained from DMSO-treated unstimulated THP-1 supernatants.

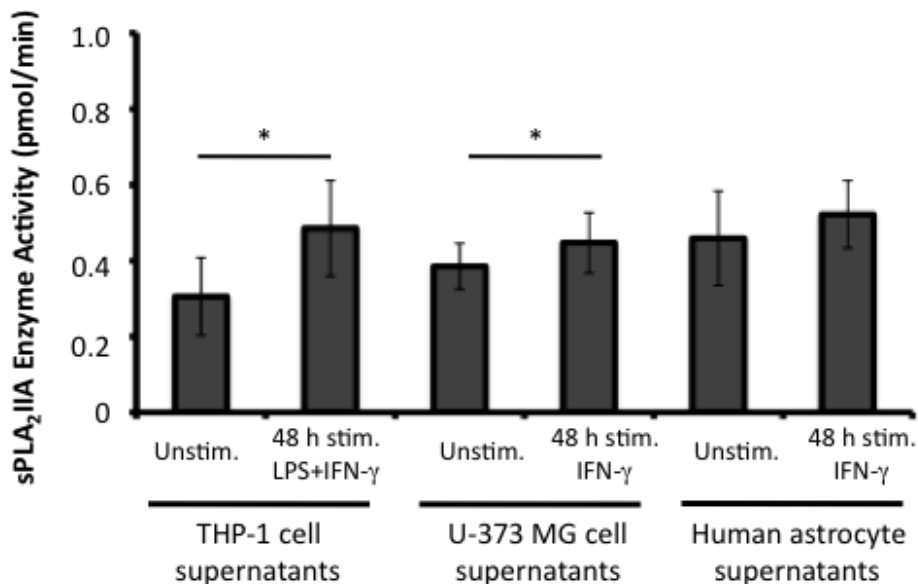


Figure 3.10: Calculated sPLA₂IIA enzymatic activity was significantly higher in supernatants of stimulated versus unstimulated THP-1 cell and U-373 MG supernatants, but not in human astrocyte supernatants. To derive sPLA₂IIA-specific activity, PLA₂ activity values (pmol/min) for RO032107-treated stimulated or unstimulated cell supernatants were subtracted from DMSO-treated stimulated or unstimulated supernatants, respectively. Data from 3-5 independent experiments are presented as means. Pairwise comparisons were made between stimulated and unstimulated samples respective of each cell type using Student's T-test for paired comparisons, where *P<0.05 was considered significant compared to corresponding unstimulated cells.

Figure 3.10 shows the calculated sPLA₂IIA-specific enzymatic activities in both unstimulated and stimulated supernatants from THP-1 cells, U-373 MG cells and human astrocytes. sPLA₂IIA enzymatic activity was significantly higher in stimulated compared to unstimulated THP-1 and U-373 MG cell supernatants (P=0.02 for both). There appeared to be an increase in the activity in human astrocyte supernatant compared with the respective unstimulated sample; however, in this case the increase did not reach statistical significance (P=0.80).

3.6 Effects of Specific sPLA₂ Inhibitors on Neurotoxicity of Stimulated Glial Cell Supernatants

The sPLA₂IIA-specific inhibitor RO032107 and its control compound RO041709 were used to attenuate the toxic effect of rsPLA₂IIA on SH-SY5Y cells. 10 µM of compound or DMSO was added 5 min after 1 µM rsPLA₂IIA was applied to SH-SY5Y cells. After 72 h, the death and viability of the SH-SY5Y cells were assessed using LDH and MTT assays, respectively. According to the LDH assay (Fig. 3.11.A), cell death resulting from DMSO only treatment was not significantly different from compound-treated samples (P=0.86 according to Fisher's LSD test for multiple comparisons); however, the MTT assay (Fig. 3.11.B) showed a visible increase in cell viability in SH-SY5Y cells treated with RO032107 compared to the DMSO control (P=0.06 according to Fisher's LSD test for multiple comparisons).

Next, the compounds RO032107, RO092906 and RO041709 were tested for their neuroprotective abilities by 1) incubating the compounds with stimulated THP-1 cell supernatants for 10 min before transfer to SH-SY5Y cells (Fig. 3.12), or 2) adding the compounds to SH-SY5Y cells immediately after the transfer of stimulated THP-1 cell supernatants (Fig. 3.13). Lower LDH values or higher MTT values compared to the DMSO solvent control would indicate reduced toxicity of supernatants.

The compounds showed no effect according to the LDH assay. The MTT revealed a modest trend towards reduced viability in samples treated with the control compound (Fig. 3.12.B). Direct addition of the compounds immediately after the transfer of stimulated THP-1 supernatant to SH-SY5Y cells also did not show any significant neuroprotective effects (Fig. 3.13). These findings indicate that either sPLA₂IIA induces neurotoxicity in a non-enzymatic manner or other PLA₂ isoforms may be involved.

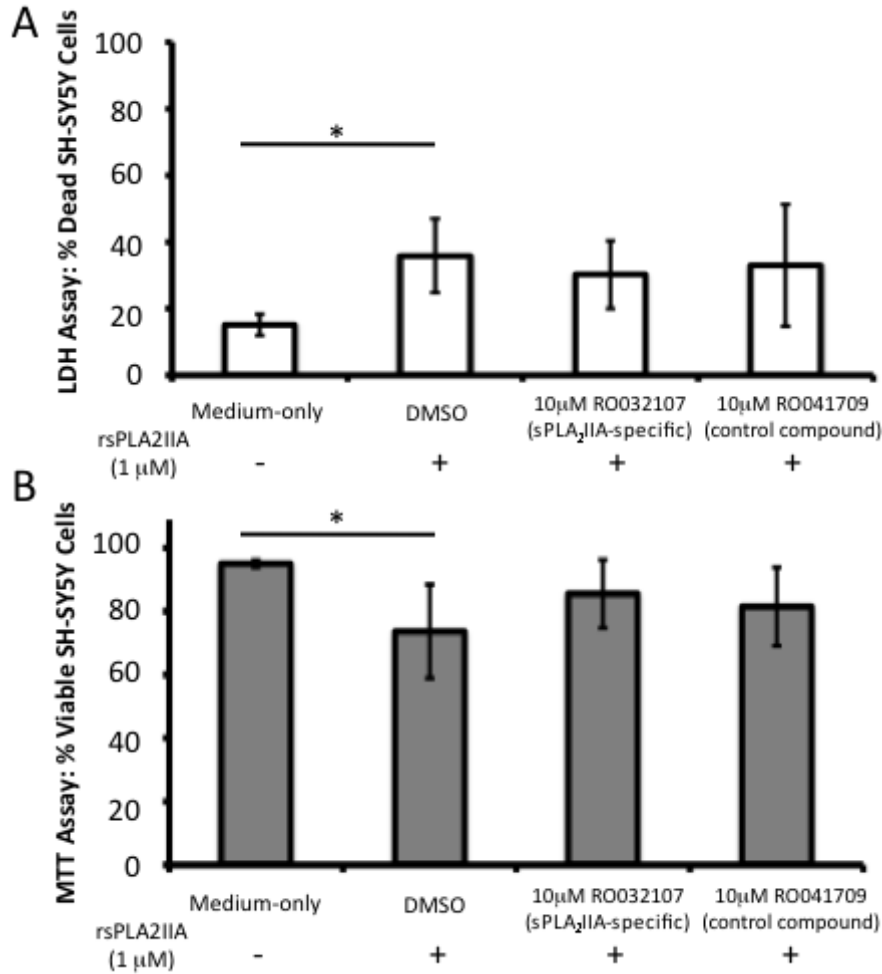


Figure 3.11: The sPLA₂IIA-specific inhibitor RO032107 and control compound RO041709 failed to significantly counteract rsPLA₂IIA-induced cytotoxicity toward SH-SY5Y cells. LDH (A) and MTT (B) assays were used to determine the effect of adding 1 μM rsPLA₂IIA and 10 μM compound or DMSO solvent to SH-SY5Y cells for 72 h. (A) The LDH assay was used to measure cell death for each treatment; the results are expressed as a percentage of a 100% lysed cell control. (B) The MTT assay was used to measure cell viability; the results are expressed as a percentage of the values obtained from medium-only treated SH-SY5Y cell control. Data from 3-5 independent experiments are presented as means. All values were compared using randomized block design ANOVA, followed by Fisher's LSD test for multiple comparisons, *P<0.05 indicates significant difference between the two samples.

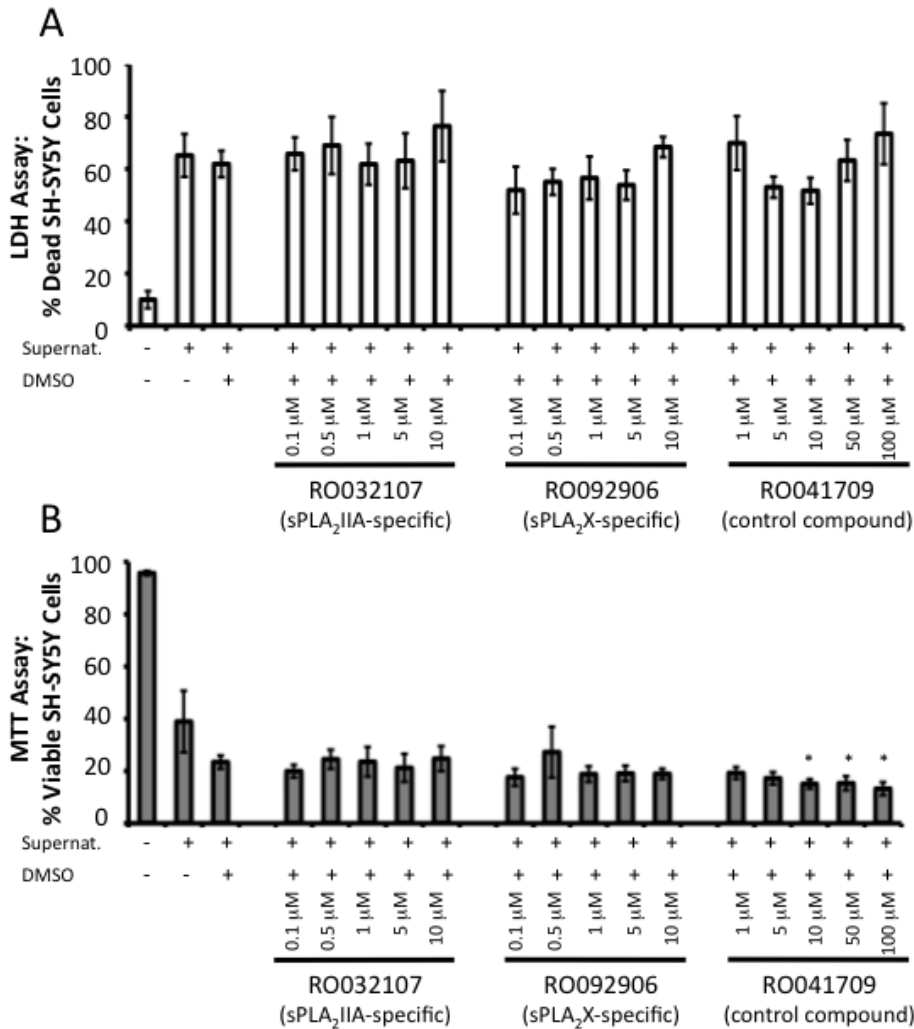


Figure 3.12: sPLA₂IIA- and sPLA₂X-specific inhibitors showed no significant effects on the cytotoxicity of supernatants from stimulated THP-1 cells. LDH (A) and MTT (B) assays were used to determine the effect of adding various concentrations of either sPLA₂IIA-specific inhibitor RO032107, sPLA₂X-specific inhibitor RO092906, or control compound RO041709 to the supernatants from LPS+IFN- γ -stimulated THP-1 cells 10 min before their transfer to SH-SY5Y cells. (A) The LDH assay was used to measure cell death for each treatment; the results are expressed as a percentage of a 100% lysed cell control. (B) The MTT assay was used to measure cell viability; the results are expressed as a percentage of the values obtained from medium-only treated SH-SY5Y cell control. Data from 5 independent experiments are presented as means. All values were compared using randomized block design ANOVA, followed by Fisher's LSD test for multiple comparisons, showing significance where *P<0.05 when compared to the DMSO control.

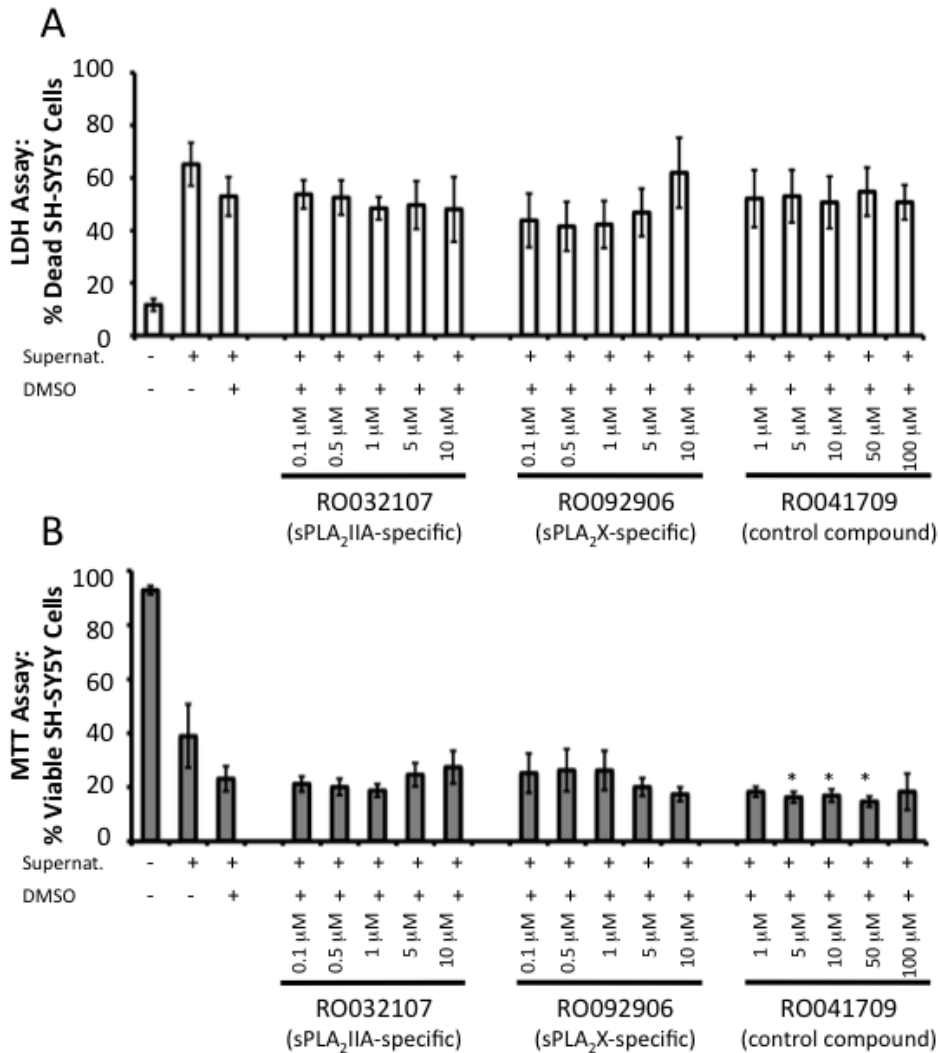


Figure 3.13: sPLA₂IIA- and sPLA₂X-specific inhibitors showed no neuroprotective effects. LDH (A) and MTT (B) assays were used to determine the effect of adding various concentrations of either sPLA₂IIA-specific inhibitor RO032107, sPLA₂X-specific inhibitor RO092906, or control compound RO041709 to SH-SY5Y cells immediately after transferring the supernatants from LPS+IFN- γ -stimulated THP-1 cells. (A) The LDH assay was used to measure cell death for each treatment; the results are expressed as a percentage of a 100% lysed cell control. (B) The MTT assay was used to measure cell viability; the results are expressed as a percentage of the values obtained from medium-only treated SH-SY5Y cell control. Data from 5 independent experiments are presented as means. All values were compared using randomized block design ANOVA, followed by the Fisher's LSD test, showing significance where *P<0.05 when compared to the DMSO control.

3.7 Removal of sPLA₂IIA from Cell Supernatants

Immunosorbent specific for sPLA₂IIA was used to remove the protein from supernatants of stimulated THP-1 cells, U-373 MG cells and human astrocytes before transferring the supernatants to SH-SY5Y cells. Figure 3.14 shows that the removal of sPLA₂IIA from stimulated THP-1 supernatants resulted in significantly increased SH-SY5Y viability as compared to the effect of either untreated supernatants from stimulated THP-1 cells or supernatants treated with Con A sepharose, which was used as a non-specific control. PGE₂-specific sorbent also caused significantly increased SH-SY5Y cell viability.

Effects of immunosorbents observed by the LDH and MTT assays (Fig. 3.14) were confirmed by the live/dead fluorescence assay (Fig. 3.15). Experiments using sPLA₂IIA-specific immunosorbents were repeated with stimulated THP-1 cell supernatants; SH-SY5Y cell viability was assessed using the live/dead fluorescence assay. Green cells represent live SH-SY5Y cells (examples indicated by the solid arrows in Fig. 3.15.A-D), while red cells represent dead cells (examples indicated by the dashed arrows in Fig. 3.15.A-D). Figure 3.15.E shows that the percentage of live SH-SY5Y cells for the sPLA₂IIA immunosorbent treated samples was significantly higher than for SH-SY5Y cells treated with stimulated THP-1 cell supernatants. Similarly, Figure 3.15.F shows that the percentage of dead SH-SY5Y cells for the sPLA₂IIA immunosorbent treated samples was significantly lower than values obtained from SH-SY5Y cells treated with stimulated THP-1 cell supernatants.

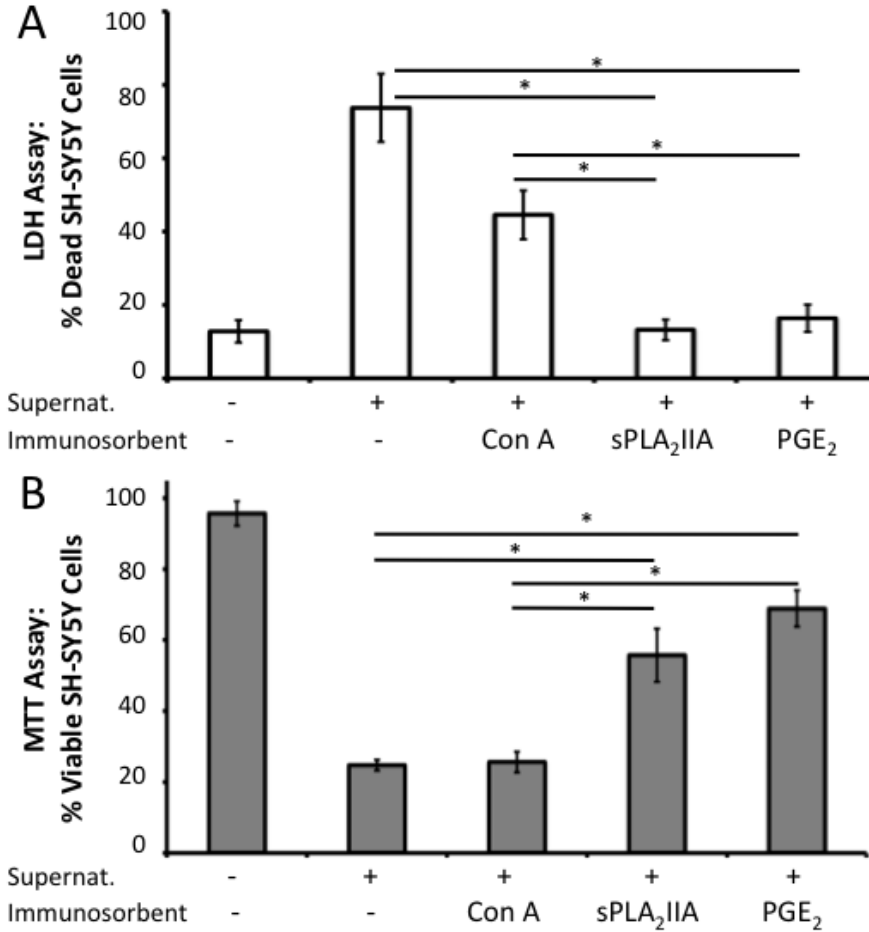


Figure 3.14: Immunosorbents specific for sPLA₂IIA and PGE₂ inhibited the cytotoxicity of THP-1 cell supernatants. LDH (A) and MTT (B) assays were used to determine the effect of treating neurotoxic THP-1 cell supernatants with sPLA₂IIA-, PGE₂- or Con A-specific immunosorbents. SH-SY5Y cells were exposed to either medium only (-/-), IFN- γ +LPS stimulated THP-1 cell supernatant, or IFN- γ +LPS-stimulated THP-1 cell supernatant treated with Con A-, sPLA₂IIA- or PGE₂-specific immunosorbents. (A) The LDH assay was used to measure cell death for each treatment; the results are expressed as a percentage of a 100% lysed cell control. (B) The MTT assay was used to measure cell viability; the results are expressed as a percentage of the values obtained from medium-only treated SH-SY5Y cell control. Data from 6 independent experiments are presented as means. All values were compared using randomized block design ANOVA, followed by Fisher's LSD test, *P<0.05 indicates significant difference between the two samples.

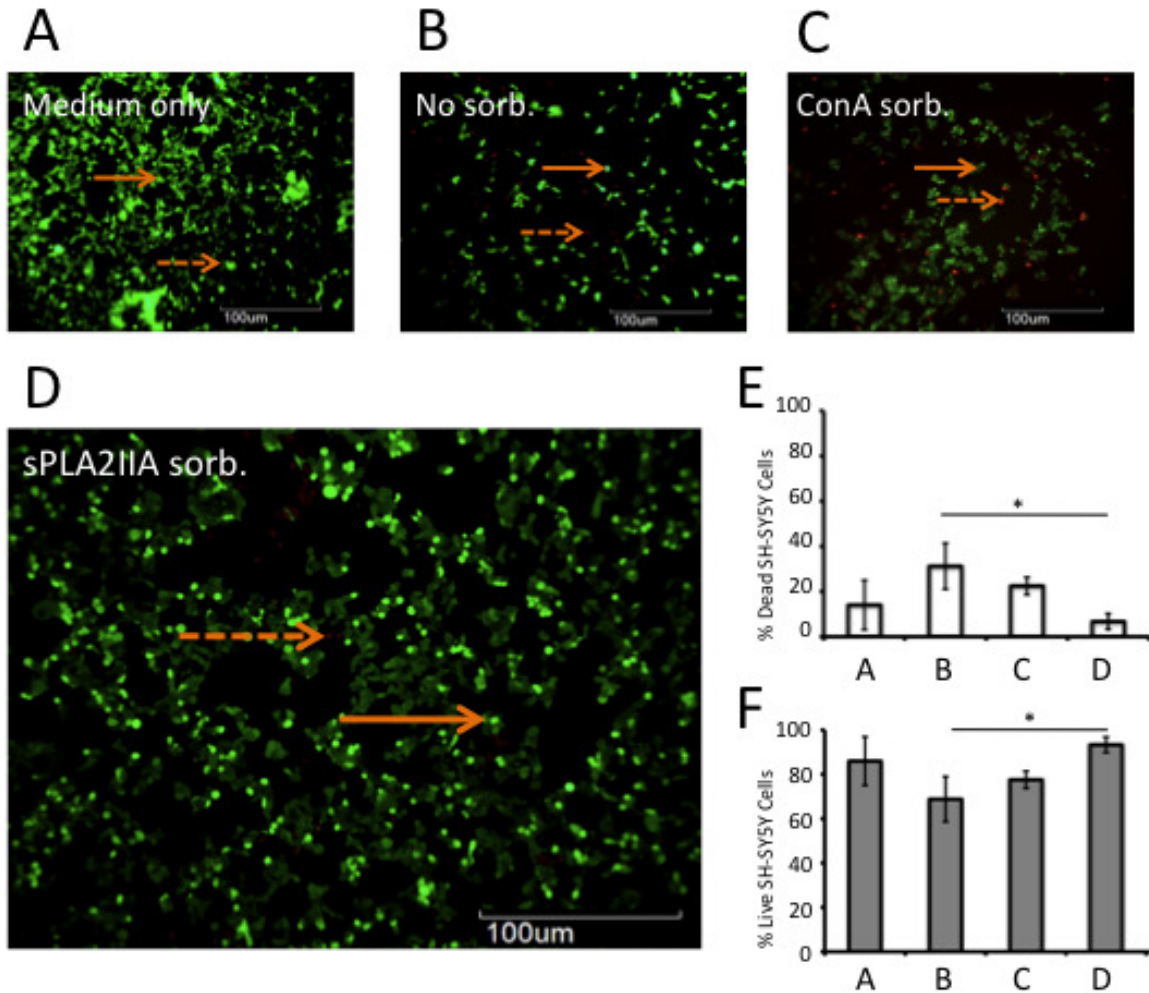


Figure 3.15: Live/Dead fluorescence assay images show that sPLA₂IIA immunosorbent treatment decreased stimulated THP-1 cell supernatant cytotoxicity toward SH-SY5Y cells. SH-SY5Y cells were exposed to either medium only (A), untreated IFN- γ +LPS-stimulated THP-1 cell supernatant (B), stimulated THP-1 cell supernatant treated with Con A (C) or sPLA₂IIA sorbent (D). After 72 h, SH-SY5Y cells were stained with Calcein AM and EthD-1 to differentiate green live cells (solid line arrow) from red dead cells (broken line arrow). (E) % live and (F) % dead SH-SY5Y cells are expressed as percentages of the total cell count for each treatment. Data presented in (E) and (F) are expressed as means from 3 independent experiments. All values were compared using randomized block design ANOVA, followed by Fisher's LSD test, where *P<0.05 indicates significant difference between the two samples.

Immunosorbent experiments were also repeated using supernatants from U-373 MG cells and human astrocytes that had been stimulated with IFN- γ (150 U/ml) for 48 h. Figure 3.16 shows the effect of sPLA₂IIA sorbent on the cytotoxicity of stimulated U-373 MG cell and human astrocyte supernatants. In both cases, the removal of sPLA₂IIA with a selective immunosorbent increased the viability of SH-SY5Y cells compared to untreated supernatants or Con A-treated supernatants.

3.8 Effects of Non-Specific PLA₂ Inhibitors and PGE₂ Receptor Antagonists on THP-1 Cytotoxicity Toward SH-SY5Y Cells

Since the sPLA₂IIA- and sPLA₂X-specific inhibitors showed no significant effects on the cytotoxicity of THP-1 cells (see Fig. 3.12 and 3.13), four non-specific PLA₂ inhibitors were tested to determine whether stimulated THP-1 cell supernatant toxicity was due to other PLA₂ isoforms. In addition, two PGE₂ receptor antagonists, that together targeted all four prostaglandin receptor types (EP receptors), were studied.

To test whether the compounds would affect stimulated THP-1 cytotoxicity, all six compounds were added to THP-1 cells immediately prior to stimulation with LPS and IFN- γ (Figure 3.17). A compound exhibiting anti-cytotoxic effects would reduce the cytotoxic effect of stimulated THP-1 cell supernatants on SH-SY5Y cells, as determined by the LDH and MTT assays. The PLA₂ inhibitor MAFP was found to be significantly toxic to THP-1 cells at 10 μ M according to the LDH assay (Fig. 3.17.A). BPPA, which is another PLA₂ inhibitor, was found to be significantly toxic to THP-1 cells at 10 μ M according to the MTT cell viability assay (Fig. 3.17.B); otherwise, both the non-specific

PLA₂ inhibitors and PGE₂ receptor antagonists did not exhibit significant toxicity toward THP-1 cells.

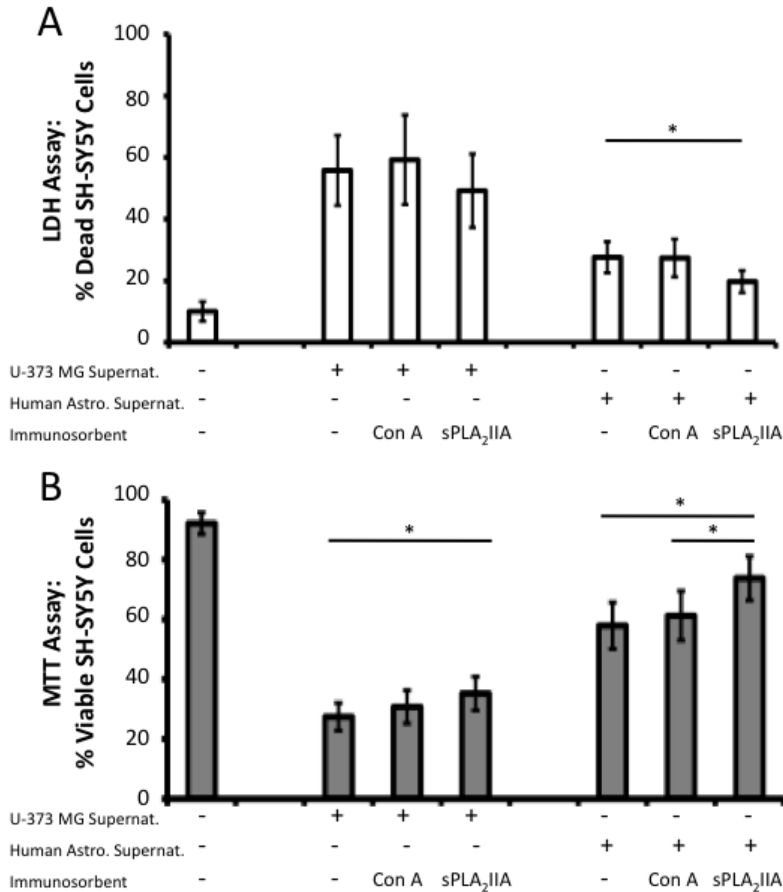


Figure 3.16: sPLA₂IIA-specific immunosorbent reduced cytotoxicity of stimulated U-373 MG cells and primary human astrocytes. LDH (A) and MTT (B) assays were used to determine the effect of treating neurotoxic U-373 MG and human astrocyte supernatants with sPLA₂IIA-specific sorbent. SH-SY5Y cells were exposed to either medium only, IFN- γ -stimulated U-373 MG cell supernatant, IFN- γ -stimulated human astrocyte supernatant, or either supernatant type treated with Con A- or sPLA₂IIA-specific immunosorbent. (A) Cell death for each treatment is expressed as a percentage of a 100% lysed cell control. (B) Cell viability is expressed as a percentage of values obtained from untreated SH-SY5Y cell samples. Data from 4-6 independent experiments are presented as means. All values were compared using randomized block design ANOVA, followed by Fisher's LSD test for multiple comparisons, where *P<0.05 indicates a significant difference between the two samples.

Figure 3.18 shows viability of SH-SY5Y cells 72 h after the transfer of THP-1 cell supernatants. No statistically significant anti-cytotoxic effects were observed; on the contrary, the cPLA₂/iPLA₂ inhibitor MAFP and the non-specific sPLA₂ inhibitor BPPA were found to enhance THP-1 cell cytotoxicity toward SH-SY5Y cells.

The non-specific PLA₂ inhibitors and PGE₂ receptor antagonists were also tested for direct neuroprotective properties. Each compound was added to supernatants from THP-1 cells that had been stimulated for 48 h with LPS and IFN- γ prior to their transfer to SH-SY5Y cells. Lower LDH values or higher MTT values as compared to the DMSO solvent control in Figure 3.19 would be considered to be neuroprotective effects. No statistically significant neuroprotective effects were observed; furthermore, the PLA₂ inhibitor OPHAO caused a significant, concentration-dependent decrease in SH-SY5Y cell viability. The inability of non-specific PLA₂ inhibitors and PGE₂ receptor antagonists to attenuate stimulated THP-1 cell toxicity indicates that the enzymatic function of sPLA₂IIA and other PLA₂ isoforms may not be important for their contribution to the toxicity of glial cell supernatants.

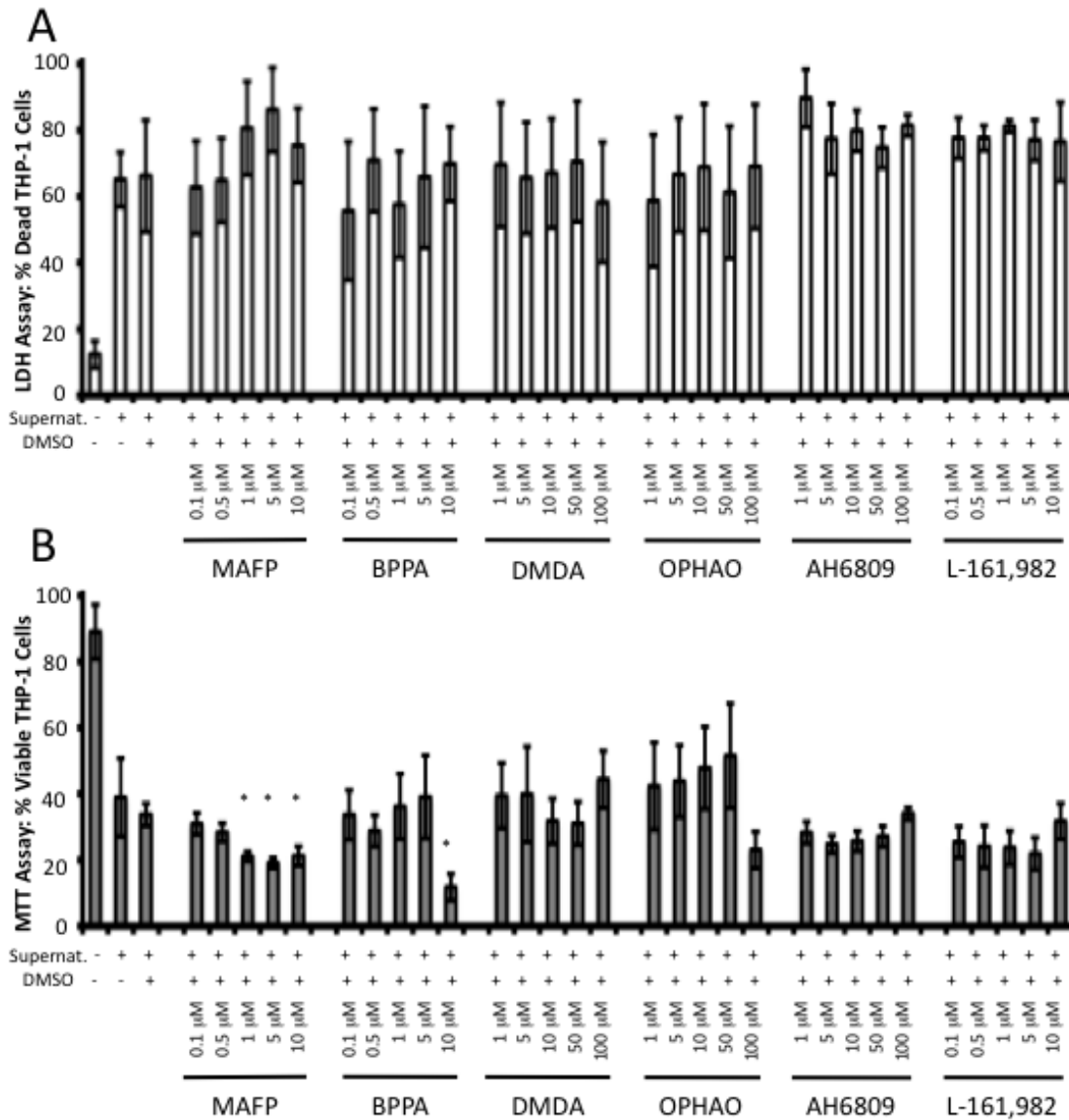


Figure 3.18: The PLA₂ inhibitors MAFP and BPPA increased stimulated THP-1 cell supernatant cytotoxicity toward SH-SY5Y cells. LDH (A) and MTT (B) assays were used to determine the effect of stimulated THP-1 supernatants treated with PLA₂ inhibitors MAFP, BPPA, DMDA, or OPHAO, or PGE₂ receptor antagonists AH6809 or L-161,982, on SH-SY5Y viability. (A) Cell death for each treatment is expressed as a percentage of a 100% lysed cell control. (B) Cell viability is expressed as a percentage of values obtained from untreated SH-SY5Y cell cultures. Data from 6 independent experiments are presented as means. All values were compared using randomized block design ANOVA, followed by Fisher's LSD test for multiple comparisons, where *P<0.05 if significantly different from the DMSO solvent control.

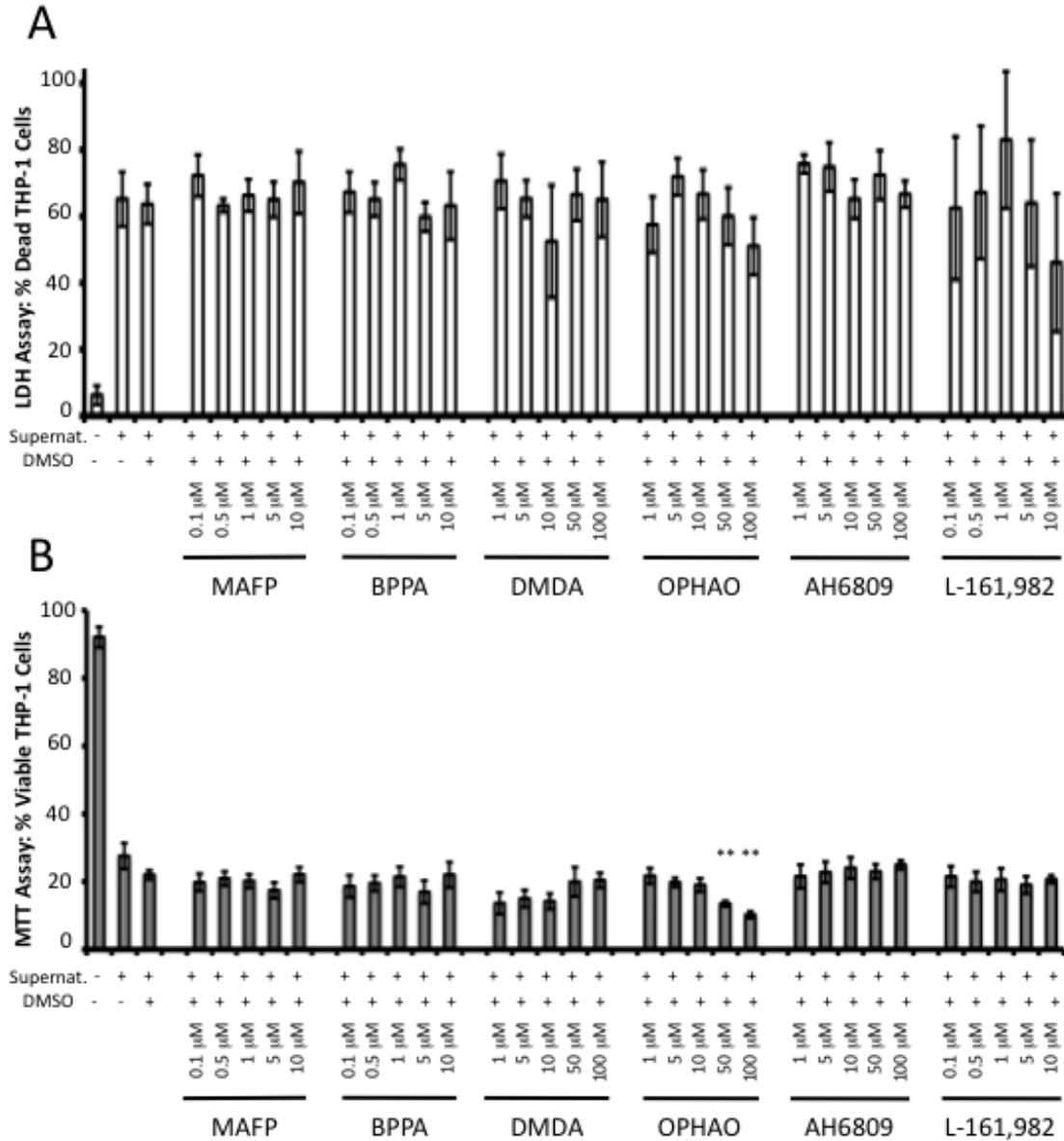


Figure 3.19: Non-specific PLA₂ inhibitors and PGE₂ receptor antagonists showed no direct neuroprotective effects. LDH (A) and MTT (B) assays were used to measure SH-SY5Y cell death and viability after 72 h incubation with THP-1 cell supernatants treated with either non-specific sPLA₂ inhibitors (MAFP, BPPA, DMDA or OPHAO) or with PGE₂ receptor antagonists (AH6809 or L-161,982). (A) Cell death for each treatment condition is expressed as a percentage of a 100% lysed cell control. (B) Cell viability is expressed as a percentage of values obtained from untreated SH-SY5Y cell samples. Data from 6 independent experiments are presented as means. All values were compared using randomized block design ANOVA, followed by the Fisher's LSD test, where **P<0.01 if significantly different from the DMSO solvent control.

3.9 Possible Mechanisms of sPLA₂IIA Toxicity

3.9.1 Effect of rsPLA₂IIA on H₂O₂-Induced Neurotoxicity

It has been shown that human sPLA₂IIA does not bind well to mammalian cell membranes (Lambeau and Gelb 2008); however, damage to cell membranes could potentially alter cell membrane composition, exposing glycerophospholipids with higher affinity to sPLA₂IIA interfacial binding sites. The effects of rsPLA₂IIA added to SH-SY5Y cells 5 min after the addition of 250 μ M H₂O₂ on SH-SY5Y cell viability was compared with the addition of either 1 μ M rsPLA₂IIA alone or 250 μ M H₂O₂ alone (Fig. 3.20). The LDH assay failed to detect any significant differences between any of the treatments (Fig. 3.20.A); however, the combined rsPLA₂IIA and H₂O₂ treatment resulted in a significant decrease in SH-SY5Y viability compared to both untreated SH-SY5Y cells and rsPLA₂IIA-only treated cells according to the MTT assay (Fig. 3.20.B).

In order to determine whether rsPLA₂IIA toxicity was enhanced by the effect of H₂O₂ on SH-SY5Y cells, the following calculations were performed. Average % viability from H₂O₂-alone treatment was subtracted from the average % viability from rsPLA₂IIA and H₂O₂ treatment to determine the % viability lost due to rsPLA₂IIA in the presence of H₂O₂. This difference was then compared to the difference obtained when the average % viability from rsPLA₂IIA-only treatment was subtracted from medium-only treatment to determine the % viability lost due to rsPLA₂IIA alone. According to paired Student's T-test, the % viability lost due to rsPLA₂IIA in the presence of H₂O₂ was not significantly different from the % viability lost due to rsPLA₂IIA alone (data not shown); therefore, the addition of H₂O₂ and rsPLA₂IIA resulted in additive, but not synergistic, toxicity toward SH-SY5Y cells.

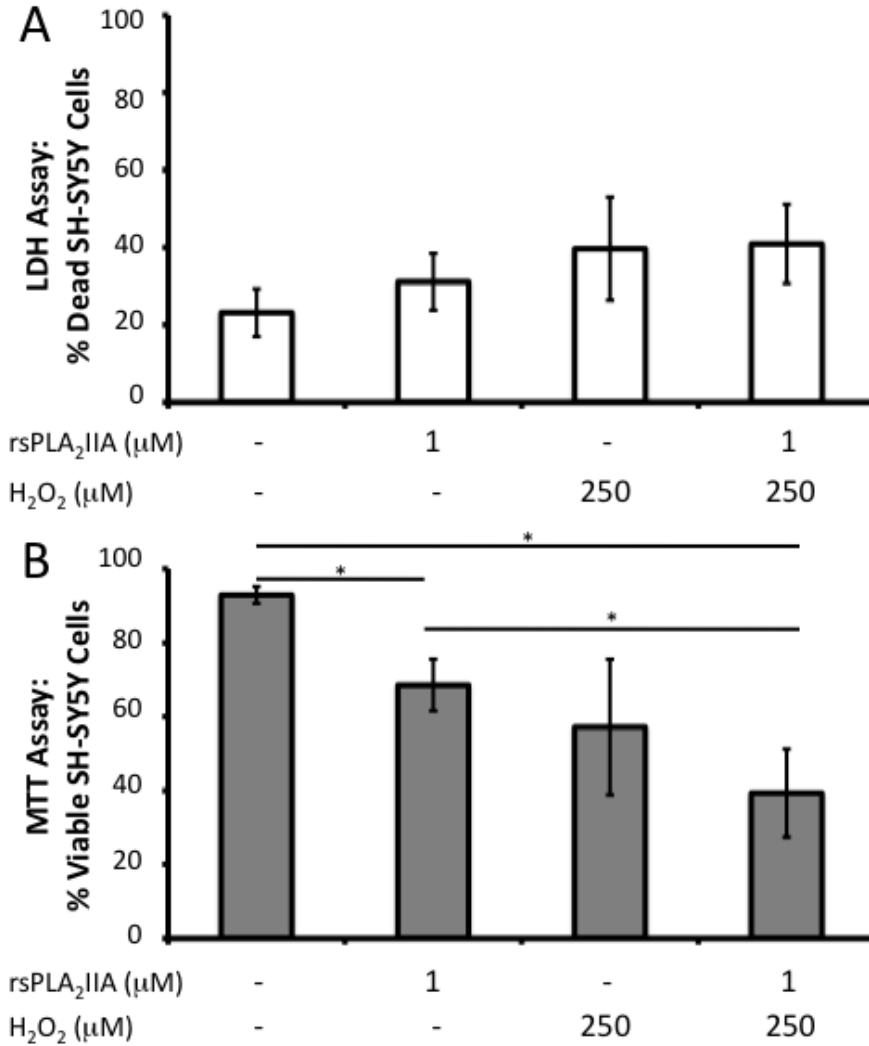


Figure 3.20: Decrease in SH-SY5Y cell viability due to H₂O₂ plus rsPLA₂IIA treatment was not significantly different from H₂O₂ only cytotoxicity. SH-SY5Y cell treatments included medium only, 1 μM rsPLA₂IIA, 250 μM H₂O₂, and 250 μM H₂O₂ plus 1 μM rsPLA₂IIA. (A) Cell death for each treatment is expressed as a percentage of a 100% lysed cell control. (B) Cell viability is expressed as a percentage of values obtained from untreated THP-1 cell samples. Data from 5 independent experiments are presented as means. All values were compared using randomized block design ANOVA, followed by Fisher's LSD test, where *P<0.05 indicates significant difference between the two samples.

3.9.2 Experiments with the PPAR α Antagonist MK886

Previous studies have shown that stimulation of mononuclear phagocytes with inflammatory mediators increases the production of sPLA₂IIA, which was suggested to occur via the activation of PPAR α (Beck *et al.* 2003). The PPAR α antagonist MK886 was therefore tested to determine whether antagonizing PPAR α would decrease the cytotoxic effects of stimulated THP-1 cell supernatants. THP-1 cells were treated with various concentrations of MK886 before stimulation with LPS (0.5 μ g/ml) and IFN- γ (150 U/ml). The LDH assay showed significant decreases in LDH activity at 5 and 10 μ M MK886 (Fig. 3.21.A); however, according to the MTT assay, MK886 reduced cell viability by approximately 30% as compared to the DMSO solvent control (Fig. 3.21.B).

The transfer of MK886-treated THP-1 supernatants to SH-SY5Y cells also resulted in a concentration-dependent decrease in both LDH (Fig. 3.21.A) and MTT (Fig. 3.21.B) values. MK886 caused severe loss of THP-1 cells at higher concentrations, which could be seen clearly upon microscopic examination. Since the LDH values in both Fig 3.21.A and 3.22.A were unexpectedly low, the MTT data in both figures appeared to be more reliable. The reduction of LDH activity measured at high MK886 concentrations could be due to denaturation of LDH or inhibition of its activity at low pH. No significant anti-cytotoxic effects of MK886 were observed, which suggests that sPLA₂IIA production may be induced by mechanisms other than PPAR α activation.

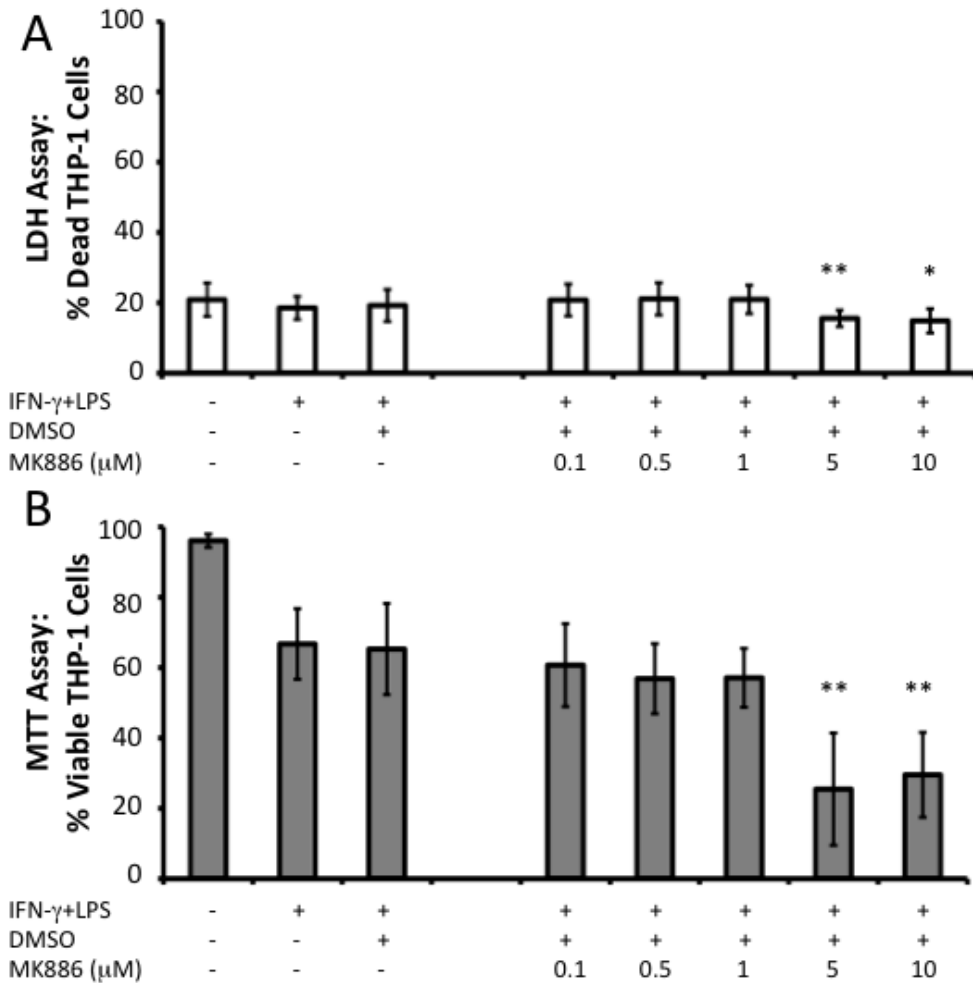


Figure 3.21: MK886 is toxic to THP-1 cells at concentrations above 1 μ M. LDH (A) and MTT (B) assays were used to determine the effect of treating THP-1 cells directly with the PPAR α receptor antagonist MK886 at various concentrations in the presence of the combination of LPS and IFN- γ . (A) Cell death for each treatment is expressed as a percentage of a 100% lysed cell control. (B) Cell viability is expressed as a percentage of values obtained from untreated THP-1 cell samples. Data from 5 independent experiments are presented as means. All values were compared using randomized block design ANOVA, followed by the Fisher's LSD test for multiple comparisons, where * P <0.05 and ** P <0.01 if significantly different from the DMSO solvent control.

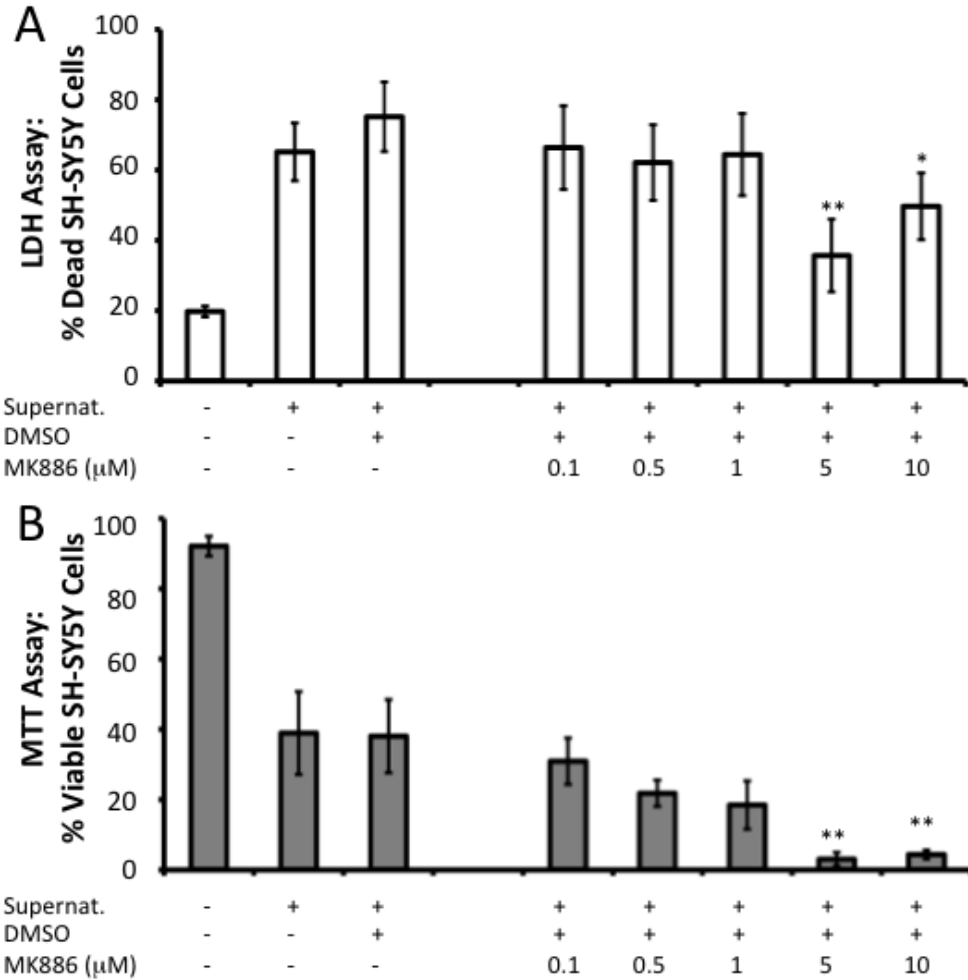


Figure 3.22: Supernatants from MK886-treated stimulated THP-1 cells were cytotoxic toward SH-SY5Y cells at high concentrations. LDH (A) and MTT (B) assays were used to determine the effect of MK886 on stimulated THP-1 cell cytotoxicity toward SH-SY5Y cells. (A) Cell death for each treatment is expressed as a percentage of a 100% lysed cell control. (B) Cell viability is expressed as a percentage of values obtained from untreated THP-1 cell samples. Data from 5 independent experiments are presented as means. All values were compared using randomized block design ANOVA, followed by Fisher's LSD test for multiple comparisons, where * $P < 0.05$ and ** $p < 0.01$ if significantly different from the DMSO solvent control.

3.9.3 Effects of the anti-TLR4/MD-2 Antibodies on sPLA₂IIA Toxicity Toward SH-SY5Y Cells

A non-enzymatic mechanism of sPLA₂IIA could involve TLR4 on neuronal plasma membrane, as TLR4 was found to interact with A β aggregates and cause neuronal apoptosis (Tang *et al.* 2008). To interfere with this complex, an anti-TLR4/MD-2 mAb was used. This mAb was either incubated with stimulated THP-1 supernatants before transfer to SH-SY5Y cells or directly applied to SH-SY5Y cells immediately after the transfer of stimulated THP-1 cell supernatants. After 72 h, the viability of SH-SY5Y cells was assessed by the LDH (Fig. 3.23.A) and MTT (Fig. 3.23.B) assays. Neither of the two methods of anti-TLR4/MD-2 mAb application resulted in significant neuroprotection, which indicates that sPLA₂IIA may be acting through other cell membrane receptors.

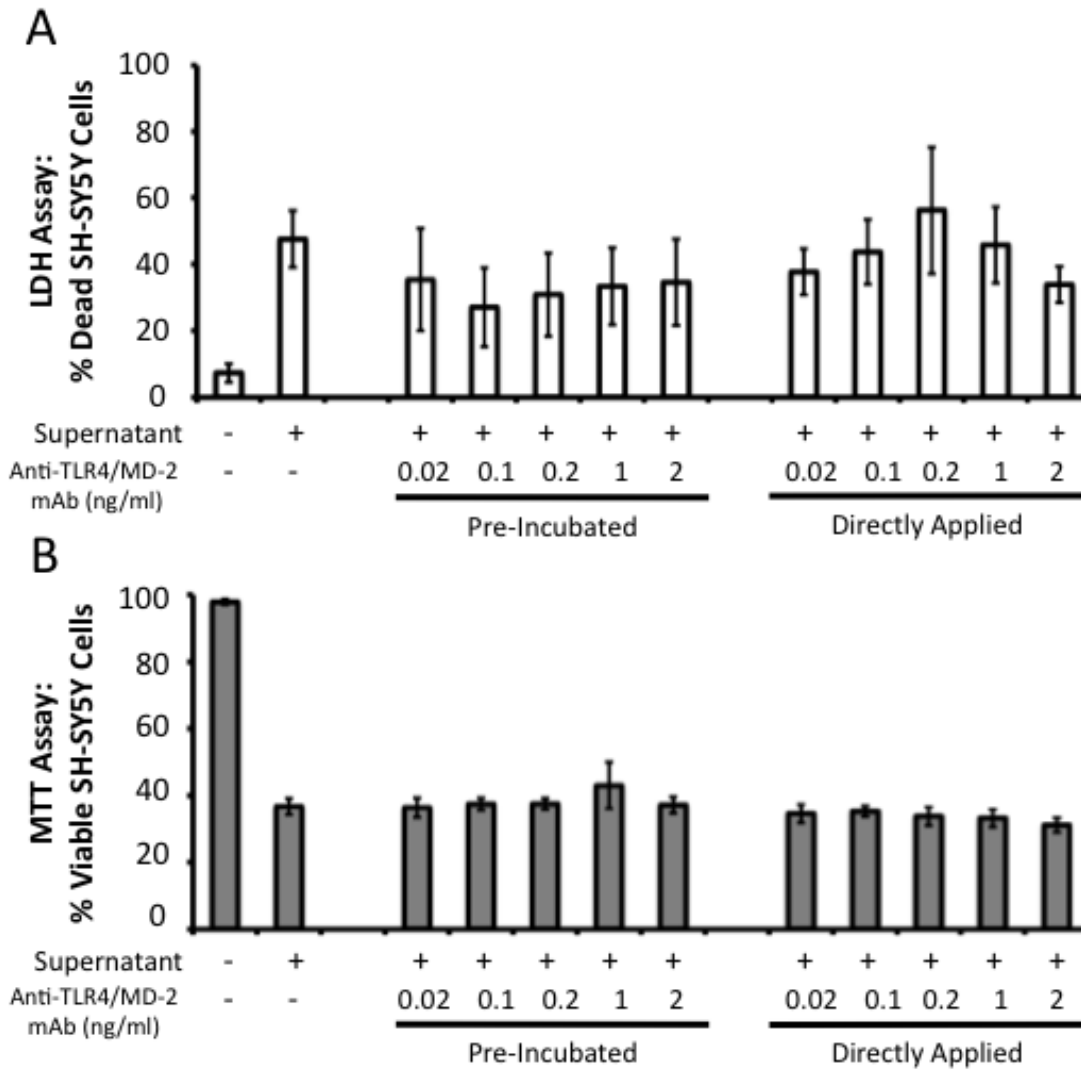


Figure 3.23: Anti-TLR4/MD-2 mAb does not protect SH-SY5Y cells from stimulated THP-1 supernatant toxicity. LDH (A) and MTT (B) assays were used to determine the effect of anti-TLR4/MD-2 mAb on THP-1 cytotoxicity toward SH-SY5Y cells using two methods. The anti-TLR4/MD-2 mAb was either incubated with stimulated THP-1 cell supernatants for 10 min before transfer to SH-SY5Y cells or added immediately after transfer. (A) Cell death for each treatment is expressed as a percentage of a 100% lysed cell control. (B) Cell viability is expressed as a percentage of values obtained from untreated THP-1 cell samples. Data from 5 independent experiments are presented as means. All values were compared using randomized block design ANOVA, followed by the Fisher's LSD test for multiple comparisons, no significant differences were observed.

4 Discussion

4.1 Neurotoxins Secreted by Stimulated Glial Cells

4.1.1 Stimulated Glial Cells Secrete Neurotoxic sPLA₂IIA

There are three main reasons why sPLA₂IIA was investigated in the context of neuroinflammation: 1) sPLA₂IIA has been implicated in chronic inflammation inherent to rheumatoid arthritis (Bidgood *et al.* 2000; Bryant *et al.* 2010; Jamal *et al.* 1998; Masuda *et al.* 2005) and atherosclerosis (Divchev and Schieffer 2008; Ghesquiere *et al.* 2005; Lambeau and Gelb 2008); 2) increased sPLA₂IIA mRNA concentrations have been observed in AD brains compared with non-dementia brains (Moses *et al.* 2006); and 3) exogenous sPLA₂IIA added to rat cortical neurons resulted in neuronal apoptosis (Chiricozzi *et al.* 2010; Yagami *et al.* 2002).

The results of this study support the central hypothesis that sPLA₂IIA is a neurotoxin secreted by stimulated glial cells. First, it was shown that stimulating microglia-like THP-1 cells with bacterial LPS and IFN- γ for 48 h resulted in secretions that were significantly toxic to neuron-like SH-SY5Y cells (Fig. 3.1), which was consistent with previously published studies (Hashioka *et al.* 2009; Klegeris and McGeer 2000). Second, using RT-PCR, it was found that sPLA₂IIA mRNA was expressed in stimulated but not unstimulated glial cells (Fig. 3.5), which has only been previously observed in the acute inflammation accompanying cerebral ischemia (Lin *et al.* 2004). These findings indicate that sPLA₂IIA mRNA is expressed in glial cells upon stimulation with pro-inflammatory factors. An ELISA specific for sPLA₂IIA was used to confirm that there was a significantly higher sPLA₂IIA protein concentration in stimulated compared to unstimulated glial cell supernatants (Fig. 3.6). These results suggest that

glial cells increase secretion of sPLA₂IIA upon stimulation with pro-inflammatory factors. Finally, we showed that at 1 μM, bee venom sPLA₂III and human rsPLA₂IIA induced significant neuronal death when added directly to human neuron-like SH-SY5Y cells (Fig. 3.2 for bee venom sPLA₂III and 3.3 for human rsPLA₂IIA), which validates findings from previous studies on sPLA₂IIA neurotoxicity (Mathisen *et al.* 2007; Yagami *et al.* 2002). Combined, these results indicate that, upon stimulation with pro-inflammatory factors, glial cells secrete neurotoxic sPLA₂IIA.

4.1.2 Comparison of sPLA₂IIA Protein Concentrations in Cell Culture Supernatants with Exogenous sPLA₂IIA Concentrations Required to Induce Neurotoxicity

Comparing Figures 3.3 and 3.6 reveals that there is a 500,000 times difference between the neurotoxic concentration of human rsPLA₂IIA (1 μM, Fig. 3.3) and the sPLA₂IIA protein concentration found in stimulated THP-1 cell supernatants (2 pM, Fig. 3.6). A possible explanation for this is that stimulated THP-1 cell supernatants contain a mixture of pro-inflammatory and cytotoxic mediators (Klegeris and McGeer 2000; Klegeris and McGeer 2003). Therefore, it is possible that the neurotoxicity of sPLA₂IIA is enhanced by the presence of these other mediators, which are not present when assessing the neurotoxicity of rsPLA₂IIA alone.

4.2 Inhibition of sPLA₂IIA Enzymatic Activity

It is still uncertain as to whether the secretion of sPLA₂IIA contributes to, or is a result of, neuroinflammation. This thesis included several experiments that were designed

to investigate the mechanism of sPLA₂IIA neurotoxicity. Recent studies on sPLA₂IIA suggest that, because of the net cationic charge of sPLA₂IIA, the actions of this protein are independent of its enzymatic activity; however, the effects of sPLA₂IIA-specific inhibitors have not been assessed in a neuroinflammatory model. It was therefore necessary to measure the effects of sPLA₂IIA-specific inhibition on stimulated glial cell models in order to determine whether sPLA₂IIA enzymatic activity significantly contributes to glial cell-mediated neurotoxicity.

4.2.1 sPLA₂IIA Enzymatic Activity is Significantly Higher in Stimulated than Unstimulated THP-1 and U-373 MG Cell Supernatants

Before specific inhibitors were tested on PLA₂ activity in stimulated THP-1 cell supernatants, the total PLA₂ and sPLA₂IIA-specific enzymatic activities were determined using a fluorescent enzymatic assay previously described by Radvanyi *et al.* (1989) and later modified by Pernas *et al.* (1991). Comparing total PLA₂ activities between stimulated and unstimulated supernatants of THP-1 cells, U-373 MG cells and astrocytes revealed no significant differences (Fig. 3.7), which indicates that not all extracellular PLA₂ groups are significantly affected by glial cell stimulation.

The sPLA₂IIA-specific inhibitor RO032107, sPLA₂X-specific inhibitor RO092906 and control compound RO041709 were used to determine whether sPLA₂IIA is enzymatically active in stimulated glial cell supernatants. The 50% maximal inhibitory concentrations (IC₅₀) for RO032107, RO092906 and RO042107 toward 0.5 nM rsPLA₂IIA-specific enzymatic activity have been estimated at 34 nM, >1600 nM and >900 nM, respectively (Oslund *et al.* 2008; Smart *et al.* 2004). Therefore, 1 μM of each compound was incubated with 0.1 μM rsPLA₂IIA for 10 min before measuring their

effects on sPLA₂IIA enzymatic activity using a fluorescent assay (Fig. 3.8). As expected, only the sPLA₂IIA-specific inhibitor RO032107 significantly inhibited rsPLA₂IIA activity compared to the DMSO control. This indicated that 1 μM RO032107 was sufficient to inhibit 0.1 μM rsPLA₂IIA enzymatic activity. Next, 10 μM of each of the compounds were incubated with 50 μL of stimulated THP-1 cell supernatants for 10 min before measuring their effects on sPLA₂IIA enzyme activity (Fig. 3.9). A concentration ten times higher was chosen due to the presence of high concentration of protein in tissue culture media that may cause non-specific binding and loss of activity of the inhibitors. Again, only the sPLA₂IIA-specific inhibitor RO032107 significantly inhibited sPLA₂IIA enzymatic activity.

Using RO032107 allowed for the distinction between sPLA₂IIA-specific enzymatic activity from total PLA₂ enzymatic activity in both stimulated and unstimulated glial cell supernatants. Though the total PLA₂ enzymatic activity was not significantly different in stimulated compared to unstimulated glial cell supernatants (Fig. 3.7), the observed sPLA₂IIA-specific activity was significantly higher in stimulated compared to unstimulated cell supernatants from both THP-1 and U-373 MG cells (Fig. 3.10). Stimulated astrocyte supernatant revealed higher sPLA₂IIA enzymatic activity compared to the unstimulated astrocyte supernatant, but the difference was not found to be statistically significant. These results indicate that there is sPLA₂IIA-specific activity in stimulated glial cell supernatants and that sPLA₂IIA enzymatic activity may play a role in stimulated glial cell toxicity toward SH-SY5Y cells.

4.2.2 sPLA₂IIA-Specific Inhibitor Failed to Protect SH-SY5Y Cells from rsPLA₂IIA Toxicity or Glial Cell-Induced Neurotoxicity

The sPLA₂IIA-specific inhibitor RO032107, sPLA₂X-specific inhibitor RO092906 and the control compound RO041709 were then tested using cell culture models. The first experiment involved direct addition of 1 μM rsPLA₂IIA to SH-SY5Y cells 5 min before adding 10 μM of RO032107, RO092906, RO041709 or DMSO solvent. The SH-SY5Y cells were then incubated for 72 h before being assessed for viability. Figure 3.11 shows that the compounds failed to inhibit rsPLA₂IIA-induced toxicity toward SH-SY5Y cells.

The same compounds were then used to determine whether sPLA₂IIA enzymatic activity contributed to stimulated THP-1 cell cytotoxicity toward SH-SY5Y cells. Compounds were either pre-incubated with stimulated THP-1 cell supernatants before transfer to SH-SY5Y cells, or were added immediately after the transfer of supernatants. Figure 3.12 shows that there was no significant reduction in THP-1 cell toxicity with any of the specific sPLA₂ inhibitors. There are several explanations for these findings: 1) sPLA₂IIA neurotoxicity could be due to a non-enzymatic mechanism (this explanation is supported by the fact that removing sPLA₂IIA from stimulated glial supernatant reduced their cytotoxicity); 2) other PLA₂ isoforms, which are not affected by the specific inhibitors, may be contributing to neurotoxicity (this explanation was ruled out by using non-specific PLA₂ inhibitors, which also did not affect the cytotoxicity of supernatants); or 3) other enzymes or toxins may be responsible for the effects observed.

There is evidence that L-type voltage-gated Ca²⁺ channel blockers and the non-steroidal anti-inflammatory compound S-2427 were successful at attenuating sPLA₂IIA-mediated neuronal apoptosis (Yagami *et al.* 2003, 2005). Because the sPLA₂IIA-specific

inhibitor RO032107 did not counter rsPLA₂IIA-induced neuronal death, it is possible that the Ca²⁺ channel blockers and S-2427 affected upstream or downstream events that countered the neurotoxic effect of sPLA₂IIA, rather than inhibiting its enzymatic activity. Lambeau and Gelb (2008) described this phenomenon as “non-specific inhibition”.

4.3 Removal of sPLA₂IIA and PGE₂ from Stimulated Glial Cell Supernatants Significantly Decreased Neuronal Death

Several studies have suggested that sPLA₂IIA mediates cPLA₂/COX-2-coupled production of pro-inflammatory eicosanoids, including PGE₂ (Beck *et al.* 2003; Bidgood *et al.* 2000; Bryant *et al.* 2010). It is therefore possible that sPLA₂IIA produced by stimulated glial cells provides feedback within a pathway that activates cPLA₂/COX-2 production of PGE₂. Whether PGE₂ is neuroprotective or neurotoxic in the context of AD is still under debate; however, the effects of PGE₂ are dependent on which of the four known EP receptors (EP₁₋₄; G-coupled protein receptors or GPCRs) it binds to (Wei *et al.* 2010). It has been shown that in AD, PGE₂ activation of EP₁, EP₂ or EP₄ receptors results in neuronal death, while EP₃ stimulation can result in neuroprotection (Wei *et al.* 2010).

The removal of sPLA₂IIA or PGE₂ from stimulated glial cell supernatants would prevent either mediator from potentially activating cell death pathways in neurons. sPLA₂IIA- and PGE₂-specific immunosorbents were used on stimulated glial cell supernatants to investigate the effect of removing sPLA₂IIA or PGE₂ from supernatants before their transfer to SH-SY5Y cells. Preliminary experiments established that the optimal incubation period of stimulated THP-1 cell supernatants with either sPLA₂IIA- or PGE₂-specific immunosorbents was 10 min at room temperature on a bench-top rocker.

The removal of sPLA₂IIA or PGE₂ from stimulated glial cell supernatant significantly reduced cytotoxicity of this supernatant toward SH-SY5Y cells (Fig. 3.14-16). Stimulated glial cell supernatants treated with sPLA₂IIA-specific immunosorbent were also tested for sPLA₂IIA content using the sPLA₂IIA-specific ELISA and it was confirmed that the sorbent effectively removed sPLA₂IIA from the supernatants (data not shown).

4.4 Non-Specific PLA₂ Inhibitors and PGE₂ Receptor Antagonists Failed to Protect SH-SY5Y Cells from Glial Cell-Induced Toxicity

Because cPLA₂ and iPLA₂ have shown higher affinities to mammalian cell membranes than sPLA₂ isoforms, the next set of experiments used non-specific PLA₂ inhibitors on stimulated THP-1 cells to determine whether the enzymatic activity of other PLA₂ isoforms were responsible for the neurotoxicity of glial cell supernatants. There was a significant decrease in stimulated THP-1 supernatant cytotoxicity toward SH-SY5Y cells as a result of removing PGE₂; therefore, further investigation of the effects of PGE₂ receptor antagonists on stimulated THP-1 cell cytotoxicity was warranted.

Four non-specific PLA₂ inhibitors (MAFP, BPPA, DMDA and OPHAO) and two PGE₂ receptor antagonists (AH6809 and L-161,982) were tested in the glia-induced neurotoxicity model by adding them both at the time of stimulation and directly after transfer of neurotoxic supernatants. MAFP has shown selectivity toward cPLA₂ and iPLA₂ isoforms and has an IC₅₀ of 0.5 μM (Lio *et al.* 1996). The sPLA₂ inhibitor BPPA, also known as S3319 from Sigma, rescued oligodendrocytes from H₂O₂-induced cell death at 1.25 μM (Titsworth *et al.* 2009). DMDA (IC₅₀ = 16 μM) was found to be selective toward the extracellular or sPLA₂ isoforms and was used in one of the first

studies suggesting differential roles between intracellular and extracellular PLA₂ isoforms (Lister *et al.* 1989). OPHAO is another sPLA₂ inhibitor, but its IC₅₀ has not yet been determined (Antonopoulou *et al.* 2008). AH6809 is known to antagonize receptors EP₁₋₃ (Abramovitz *et al.* 2000) while L-161,982 antagonizes the EP₄ receptor (Cherukuri *et al.* 2007).

When the compounds were added to THP-1 cells at the time of stimulation, MAFP (cPLA₂ and iPLA₂ inhibitor) and BPPA (sPLA₂ inhibitor) had significant cytotoxic effects on THP-1 cells (Fig. 3.17) and enhanced stimulated THP-1 cytotoxic effects on SH-SY5Y cells (Fig. 3.18). According to the MTT cell viability assay, the sPLA₂ inhibitor OPHAO showed significant neurotoxicity at higher concentrations when added to SH-SY5Y cells immediately after stimulated THP-1 cell supernatant transfer (Fig. 3.19.B), but this concentration-dependent trend was not reflected in the LDH assay results (Fig. 3.19.A).

Overall, the non-specific PLA₂ inhibitors did not protect SH-SY5Y cells from stimulated THP-1 cytotoxicity. Because the products of arachidonic acid formation can be either pro- or anti-inflammatory depending on the combinations of mediators, cell types and environment, it is possible that by inhibiting multiple forms of PLA₂ at once the beneficial pro-resolution pathways are also inhibited.

The lack of significant neuroprotective effects of PGE₂ receptor antagonists suggests that PGE₂ may not play a role in THP-1 cytotoxicity, which is opposite to what was predicted based on the results of using a PGE₂-specific immunosorbent on stimulated THP-1 supernatants (see Fig. 3.14) as well as studies suggesting the neurotoxicity of PGE₂ (Hanson *et al.* 2003). Since the PGE₂-specific immunosorbent was able to reduce

the toxicity of stimulated THP-1 supernatants toward SH-SY5Y cells, it was predicted that antagonizing all known PGE₂ receptors (EP₁₋₄) would result in an overall decrease in cytotoxicity of supernatants from stimulated THP-1 cells.

It can therefore be concluded that either: 1) PGE₂ is not involved in stimulated THP-1 cell cytotoxicity; 2) PGE₂ may be acting through mechanisms involving receptors other than EP₁₋₄; or 3) antagonizing the EP₃ receptor significantly prevented neuroprotection (Wei *et al.* 2010). In addition, there are other PG forms that are suspected to have pro-inflammatory and cytotoxic effects (Li *et al.* 2004; Yagami *et al.* 2002) and may have also been removed by the PGE₂ immunosorbent due to cross-reactivity of antibodies.

The neurotoxic effects of sPLA₂IIA on rat cortical neurons were suggested to involve the conversion of arachidonic acid to delta¹²-PGJ₂ (Li *et al.* 2004; Yagami *et al.* 2002); however, given that the sPLA₂IIA-specific inhibitor RO032107 did not significantly affect stimulated THP-1 cell cytotoxicity, sPLA₂IIA may not be the PLA₂ species responsible for producing significant quantities of arachidonic acid leading to the formation of either PGE₂ or delta¹²-PGJ₂. It is also unlikely that the PGE₂ immunosorbent bound to delta¹²-PGJ₂, since the specificity of the immunosorbent to other PG types was less than 0.1% according to the manufacturer, though delta¹²-PGJ₂ was not specifically tested (Cayman Chemical Company).

4.5 Non-Enzymatic Mechanisms of sPLA₂IIA Neurotoxicity

Since the specific inhibition of sPLA₂IIA enzymatic activity and the non-specific inhibition of PLA₂ enzymatic activity had no effect on THP-1 cell cytotoxicity, it is possible that sPLA₂IIA may induce neurotoxicity in a non-enzymatic manner. The non-enzymatic mechanism was investigated by using an immunosorbent specific for sPLA₂IIA to remove sPLA₂IIA protein from stimulated THP-1 cell supernatants. The removal of sPLA₂IIA significantly decreased stimulated THP-1 cell toxicity toward SH-SY5Y cells (Fig. 3.14 and 3.15). Using the sPLA₂IIA-specific immunosorbent on stimulated U-373 MG cell and stimulated human astrocyte supernatants also significantly decreased their toxicity toward SH-SY5Y cells (Fig 3.16). These results, combined with the observed lack of neuroprotection provided by the sPLA₂IIA-specific inhibitor RO032107, indicate that sPLA₂IIA does play a role in glial cell neurotoxicity and is acting in a non-enzymatic manner.

Other enzymes have also been investigated for their non-enzymatic activities. 17 β -hydroxysteroid dehydrogenase, which is another protein implicated in AD, has been found to contribute to the structural integrity of mitochondria in a manner independent of its enzymatic activity (Rauschenberger *et al.* 2009). Acetylcholinesterase is also secreted from neurons and has been suggested to induce Ca²⁺ entry into neurons in a non-hydrolytic manner, which may be remnant of a trophic-toxic mechanism in developing brains (Greenfield *et al.* 2008). In addition, Raveh *et al.* (2010) suggest that GPCR kinases not only phosphorylate GPCRs, but may competitively bind with and lure G-protein subunits away from the GPCR in order to deactivate the channel.

There are several lines of evidence that suggest that sPLA₂IIA may non-enzymatically interact with cell surface proteins. Adsorption to the cell membrane by sPLA₂IIA and its binding to surface proteins has been shown to activate cell signaling pathways leading to neuronal death (Kolko *et al.* 2002), increase monocytic cell proliferation (Saegusa *et al.* 2008), and signal macrophages to ingest and dispose of abnormal debris (Boilard *et al.* 2003). It is also possible that once sPLA₂IIA is bound to a receptor or cell membrane, the cell engulfs sPLA₂IIA, which then may hydrolyze anionic glycerophospholipids of the plasma membrane.

4.5.1 H₂O₂-Induced Neuronal Apoptosis Does Not Enhance rsPLA₂IIA Toxicity

It has been proposed that neurons undergoing apoptosis are more vulnerable to sPLA₂IIA adsorption and therefore likely to experience sPLA₂IIA-induced toxicity (Olson *et al.* 2010). During apoptosis, plasma membrane glycerophospholipids rearrange and bring anionic phosphatidylserine, which is normally located on the inner layer of the plasma membrane, to the outer membrane layer (Bezzine *et al.* 2002; Han *et al.* 2003). H₂O₂ has been shown to induce the liberation of arachidonic acid from murine mesangial cell membranes (Han *et al.* 2003) and cause apoptosis in rat cortical neurons 20 h after exposure to 25 μM H₂O₂ for 5 min (Hoyt *et al.* 1997); therefore, H₂O₂ was used to induce apoptosis prior to the addition of rsPLA₂IIA in order to assess whether pre-damage of SH-SY5Y cell membranes would enhance sPLA₂IIA neurotoxicity.

200 μM H₂O₂ incubated with primary astrocytes for 30 min maximally activated ERK in the MAPK cascade and arrested the cell cycle (Tournier *et al.* 1997). A shorter incubation period of 5 min and 250 μM H₂O₂ was used to treat SH-SY5Y cells. 1 μM

rsPLA₂IIA was then added to the SH-SY5Y cells. After 72 h, the SH-SY5Y cells were assessed for survival (Fig. 3.22). The pre-incubation of SH-SY5Y cells with H₂O₂ for 5 min before the addition of rsPLA₂IIA did not enhance rsPLA₂IIA-mediated neurotoxicity; rather, rsPLA₂IIA treatment caused the same percent reduction in cell viability when used alone and in combination with H₂O₂.

Further experiments with longer H₂O₂ pre-incubation times may be needed, as it is possible that 5 min incubation was not sufficient to induce the plasma membrane composition rearrangement required for increased sPLA₂IIA binding. In addition, it is possible that the rearrangement of the plasma membrane composition altered biochemical conformation of unidentified sPLA₂IIA receptors, which may have prevented sPLA₂IIA from binding to the sites and subsequently limited the effect of sPLA₂IIA non-enzymatic activity.

4.5.2 sPLA₂IIA Regulation Through PPAR α Cannot be Confirmed Due to Cytotoxicity of Receptor Antagonist MK886

Though non-specific PLA₂ inhibitors did not effectively attenuate stimulated THP-1 cell cytotoxicity, it was still possible that cPLA₂ α contributed to sPLA₂IIA regulation in THP-1 cells. It had been suggested that cPLA₂ α products activate PPAR α , which then up-regulates sPLA₂IIA transcription and expression (Beck *et al.* 2003; Han *et al.* 2003). A PPAR α antagonist was used to determine whether the antagonism of PPAR α would reduce sPLA₂IIA in THP-1 cell supernatants causing subsequent reduction of stimulated THP-1 cell cytotoxicity toward SH-SY5Y cells. MK886, a PPAR α antagonist, was added to THP-1 cells at the time of their stimulation. After 48 h,

THP-1 supernatants were transferred to SH-SY5Y cells, which were then incubated for another 72 h before being assessed for cell viability.

Concentrations of MK886 used in this study were selected based on experiments described by Kehrer *et al.* (2001). MK886 exhibited significant toxicity toward THP-1 cells at 5 and 10 μM , which were the two highest MK886 concentrations used (Fig. 3.20.B). Transferring stimulated THP-1 cell supernatants treated with 5 or 10 μM MK886 to SH-SY5Y cell cultures resulted in increased neuronal cell death (Fig. 3.21.B). Observation of both THP-1 cells and SH-SY5Y cells under microscope showed the absence of intact cells after treatment with 5 and 10 μM MK886. The LDH assay indicated low LDH activity in supernatants of cells treated with 5 or 10 μM MK886 despite the visual confirmation of cell death (Fig. 3.21.A). This suggests that any LDH present in THP-1 cells was either inhibited or denatured by MK886 at concentrations greater than 1 μM . Because of the cytotoxicity of MK886, it is inconclusive as to whether PPAR α antagonism would result in decreased THP-1 cell cytotoxicity toward SH-SY5Y cells. To find a definitive answer, another PPAR α receptor antagonist must be used.

4.5.3 Neuronal TLR4 Does Not Mediate sPLA₂IIA Neurotoxicity

Because several studies have demonstrated association of sPLA₂IIA with the nuclear factor kappa B (NF- κ B) and MAPK cell signaling pathways (Alaoui-El-Azher *et al.* 2002; Martin *et al.* 2009), it is possible that sPLA₂IIA may induce neuronal apoptosis by binding to toll-like receptor 4 (TLR4), which has been shown to activate both NF- κ B and MAPK pathways (Tang *et al.* 2008). An anti-TLR4/MD-2 mAb was either pre-incubated with stimulated THP-1 cell supernatants before transfer to SH-SY5Y cells or

added directly to SH-SY5Y cells immediately after transfer in order to disrupt the potential binding of sPLA₂IIA to TLR4 (Fig. 3.23). The results indicate that the anti-TLR4/MD-2 mAb was unsuccessful at attenuating stimulated THP-1 cell cytotoxicity toward SH-SY5Y cells. It is possible that the anti-TLR4/MD-2 complex mAb does not bind to TLR4 alone, or that it did not block the site that sPLA₂IIA binds to. It is also possible that sPLA₂IIA does not bind to TLR4. Mechanistic studies involving rsPLA₂IIA and TLR4 are warranted to investigate this potential relationship further by using another anti-TLR4 mAb to block the sPLA₂IIA-TLR4 interaction or by using immunoprecipitation technique.

5 Conclusions

5.1 Strengths and Limitations of this Study

Many previous studies have alluded to the involvement of sPLA₂IIA in the pathological events in rheumatoid arthritis (Bidgood *et al.* 2000; Bryant *et al.* 2010; Jamal *et al.* 1998; Masuda *et al.* 2005), atherosclerosis (Divchev and Schieffer 2008; Ghesquiere *et al.* 2005; Lambeau and Gelb 2008), cancer (Hernandez *et al.* 2010; Jiang *et al.* 2002; Martin *et al.* 2009; Mathisen *et al.* 2007; Mauchley *et al.* 2009) and neurodegeneration (Chiricozzi *et al.* 2010; Moses *et al.* 2006; Schaeffer *et al.* 2010; Wei *et al.* 2003; Yagami *et al.* 2002); however, the mechanisms of sPLA₂IIA action had not been addressed directly in the context of neuroinflammation. This thesis investigates the role of sPLA₂IIA in glial cell-mediated inflammation and neurotoxicity. The results of this thesis indicate that sPLA₂IIA acts in a manner independent of its enzymatic activity; therefore, future studies exploring the role of sPLA₂IIA in neuroinflammation should focus on its non-enzymatic activity, rather than its catalytic activity. The use of primary human astrocytes has also confirmed that both sPLA₂IIA mRNA and protein are up-regulated in IFN- γ stimulated astrocytes, which points to the potential detrimental role of activated astrocytes in neuroinflammation.

Several limitations were present throughout this thesis. The protein sequence that the sPLA₂IIA-specific mAb was raised against is proprietary and therefore it could not be confirmed if other proteins released from THP-1 cells were not also bound by the sPLA₂IIA-specific mAb used to prepare the immunosorbent. Since the sPLA₂IIA-specific mAb was used in both the ELISA and immunosorbent experiment, it is possible that results were confounded by other proteins that may express the same amino acid

sequence or epitopes similar to the one recognized by the sPLA₂IIA-specific mAb. In order to confirm these results, the ELISA and immunosorbent experiments must be repeated with sPLA₂IIA-specific mAbs from different companies.

Another limitation is that immortalized cell lines were used to model human microglia and neurons. It would strengthen the arguments made in this thesis to use primary human microglia and neurons in addition to the primary astrocytes used; however, as already mentioned in the introduction, opportunities to obtain human post-mortem brain tissue for microglia culture preparation are limited, and culturing primary human neurons is not currently possible.

5.2 Future Directions

Further studies on sPLA₂IIA and glial cell-mediated neurotoxicity will contribute to the overall understanding of neuroinflammation, which may in turn aid in the design of more specific anti-inflammatory drugs that can combat the underlying chronic inflammation inherent to neurodegenerative disorders. To increase the relevance of the *in vitro* experiments performed in this study, future work should use endogenous pro-inflammatory stimulants such as TNF- α and IL-1 β , as well as pathological stimulants such as A β (found in AD tissues) or α -syn (found in PD tissues). In addition, if possible, primary human microglia should be used to confirm the findings of this thesis. It would also be useful to determine protein concentrations of sPLA₂IIA in glial cells from humans with neurodegenerative disease or animal models of neurodegeneration.

One aspect of sPLA₂IIA neurotoxicity that was not addressed by the experiments

in this thesis is the role that sPLA₂IIA may play in glutamate-induced neurotoxicity. As mentioned, Ca²⁺ homeostasis may also be affected by the up-regulation of sPLA₂IIA; it has been demonstrated that sPLA₂IIA enhances Ca²⁺ intake into rat cortical neurons via the L-type voltage-gated Ca²⁺ channel (Yagami *et al.* 2003). Mitochondria purified from rat brain astrocytes, neuron-like PC-12 cells and U-251 astrocytoma cells were found to store sPLA₂IIA (Macchioni *et al.* 2004). It is critical to investigate what causes sPLA₂IIA to migrate to the mitochondria of neurons and the implications of the presence of sPLA₂IIA in neuronal mitochondria and intracellular Ca²⁺ stores (Macchioni *et al.* 2004; Mathisen *et al.* 2007; Yagami *et al.* 2003). It has already been shown that sPLA₂IIA does not interfere with Ca²⁺ homeostasis in the absence of glutamate (Macchioni *et al.* 2004); however, it would contribute to the overall understanding of neuronal excitotoxicity if the role of sPLA₂IIA is further investigated in glutamate-induced Ca²⁺ release from mitochondria.

The localization of sPLA₂IIA in mitochondria may be a result of prior internalization through binding with heparin sulfate proteoglycans or other cell surface receptors (Boilard *et al.* 2003; Macchioni *et al.* 2004). Future studies on sPLA₂IIA may test the effect of anti-integrin β3 mAb on the cytotoxicity of stimulated glial cells, and test whether this mAb would be neuroprotective by preventing sPLA₂IIA from binding with α5β3 integrin (Saegusa *et al.* 2008). In a similar manner, heparinase III and heparin could be used to prevent sPLA₂IIA from binding to heparin sulfate proteoglycans in order to investigate this particular binding mechanism. The identification of other potential sPLA₂IIA binding sites as well as compounds that block sPLA₂IIA from binding to

receptors that lead to cell death pathways may be beneficial in inhibiting sPLA₂IIA neurotoxicity.

5.3 Significance of Findings

The results of this study expand our knowledge of how sPLA₂IIA functions in inflammatory pathologies. Specifically, the experimental data in this study indicate that sPLA₂IIA transcription, expression and secretion are up-regulated in stimulated microglia-like cells as well as astrocytes, which causes death in neuron-like cells. Most importantly, sPLA₂IIA appears to contribute to neuronal death through a mechanism independent of its enzymatic activity; this observation is consistent with emerging evidence that sPLA₂IIA contributes to inflammatory processes in a non-enzymatic manner.

Though the sPLA₂IIA-specific inhibitor RO032107 was able to significantly reduce both rsPLA₂IIA enzymatic activity and sPLA₂IIA activity in stimulated THP-1 cell supernatants, the inhibitor did not reduce rsPLA₂IIA toxicity toward SH-SY5Y cells, nor did it attenuate stimulated THP-1 cell neurotoxicity. In addition, the removal of sPLA₂IIA significantly reduced the cytotoxicity of stimulated glial cell supernatants toward neuron-like SH-SY5Y cells, which confirms that sPLA₂IIA interacts with the neuronal membrane surface in order to initiate cell death. These results suggest that future studies on the role of sPLA₂IIA in glial cell-mediated neurotoxicity should focus on possible sPLA₂IIA binding sites on both neuronal and glial cell surfaces. Compounds that prevent sPLA₂IIA from binding to cell surface receptors may inhibit sPLA₂IIA-

mediated glial cell proliferation or neuronal cell death; therefore, such compounds could contribute to the resolution of chronic inflammation. Bringing an end to chronic inflammation can prevent further neurodegeneration, which may offer therapeutic relief and momentous hope to patients suffering from AD or PD.

References

1. Abramovitz M, Adam M, Boie Y, Carriere M, Denis D, Godbout C, Lamontagne S, Rochette C, Sawyer N, Tremblay NM *et al.* The utilization of recombinant prostanoid receptors to determine the affinities and selectivities of prostaglandins and related analogs. *Biochim Biophys Acta* 2000;1483(2):285-93.
2. Alaoui-El-Azher M, Wu Y, Havet N, Israel A, Lilienbaum A, Touqui L. Arachidonic acid differentially affects basal and lipopolysaccharide-induced sPLA(2)-IIA expression in alveolar macrophages through NF-kappaB and PPAR-gamma-dependent pathways. *Mol Pharmacol* 2002;61(4):786-94.
3. Aloisi F. Immune function of microglia. *Glia* 2001;36(2):165-79.
4. Antonopoulou G, Barbayianni E, Magrioti V, Cotton N, Stephens D, Constantinou-Kokotou V, Dennis EA, Kokotos G. Structure-activity relationships of natural and non-natural amino acid-based amide and 2-oxoamide inhibitors of human phospholipase A(2) enzymes. *Bioorg Med Chem* 2008;16(24):10257-69.
5. Aschner M, Allen JW, Kimelberg HK, LoPachin RM, Streit WJ. Glial cells in neurotoxicity development. *Annu Rev Pharmacol Toxicol* 1999;39:151-73.
6. Beck S, Lambeau G, Scholz-Pedretti K, Gelb MH, Janssen MJ, Edwards SH, Wilton DC, Pfeilschifter J, Kaszkin M. Potentiation of tumor necrosis factor alpha-induced secreted phospholipase A2 (sPLA2)-IIA expression in mesangial cells by an autocrine loop involving sPLA2 and peroxisome proliferator-activated receptor alpha activation. *J Biol Chem* 2003;278(32):29799-812.
7. Berg OG, Gelb MH, Tsai MD, Jain MK. Interfacial enzymology: the secreted phospholipase A(2)-paradigm. *Chem Rev* 2001;101(9):2613-54.
8. Bessis A, Bechade C, Bernard D, Roumier A. Microglial control of neuronal death and synaptic properties. *Glia* 2007;55(3):233-8.
9. Bezzine S, Bollinger JG, Singer AG, Veatch SL, Keller SL, Gelb MH. On the binding preference of human groups IIA and X phospholipases A2 for membranes with anionic phospholipids. *J Biol Chem* 2002;277(50):48523-34.
10. Bidgood MJ, Jamal OS, Cunningham AM, Brooks PM, Scott KF. Type IIA secretory phospholipase A2 up-regulates cyclooxygenase-2 and amplifies cytokine-mediated prostaglandin production in human rheumatoid synoviocytes. *J Immunol* 2000;165(5):2790-7.
11. Bird TD. Genetic aspects of Alzheimer disease. *Genet Med* 2008;10(4):231-9.
12. Birts CN, Barton CH, Wilton DC. A catalytically independent physiological function for human acute phase protein group IIA phospholipase A2: cellular uptake facilitates cell debris removal. *J Biol Chem* 2008;283(8):5034-45.

13. Birts CN, Barton CH, Wilton DC. Catalytic and non-catalytic functions of human IIA phospholipase A₂. *Trends Biochem Sci* 2009;35(1):28-35.
14. Block ML, Hong JS. Chronic microglial activation and progressive dopaminergic neurotoxicity. *Biochem Soc Trans* 2007;35(Pt 5):1127-32.
15. Block ML, Zecca L, Hong JS. Microglia-mediated neurotoxicity: uncovering the molecular mechanisms. *Nat Rev Neurosci* 2007;8:57-69.
16. Bobik A. Secretory phospholipase A₂ type IIA: a regulator of immune function in atherosclerosis? *Cardiovasc Res* 2009;81(1):9-10.
17. Boilard E, Bourgoin SG, Bernatchez C, Poubelle PE, Surette ME. Interaction of low molecular weight group IIA phospholipase A₂ with apoptotic human T cells: role of heparan sulfate proteoglycans. *FASEB J* 2003;17(9):1068-80.
18. Bozzo C, Lombardi G, Santoro C, Canonico PL. Involvement of beta(1) integrin in betaAP-induced apoptosis in human neuroblastoma cells. *Mol Cell Neurosci* 2004;25(1):1-8.
19. Bryant KJ, Bidgood MJ, Lei PW, Taberner M, Salom C, Kumar V, Lee L, Church WB, Courtenay B, Smart BP *et al.* A bifunctional role for group IIA secreted phospholipase A₂ in human rheumatoid fibroblast-like synoviocyte arachidonic acid metabolism. *J Biol Chem* 2010;286(4):2492-503.
20. Burke JE, Dennis EA. Phospholipase A₂ structure/function, mechanism, and signaling. *J Lipid Res* 2009;50 Suppl:S237-42.
21. Cameron B, Landreth GE. Inflammation, microglia, and Alzheimer's disease. *Neurobiol Dis*;37(3):503-9.
22. Casserly I, Topol E. Convergence of atherosclerosis and Alzheimer's disease: inflammation, cholesterol, and misfolded proteins. *Lancet* 2004;363(9415):1139-46.
23. Cherukuri DP, Chen XB, Goulet AC, Young RN, Han Y, Heimark RL, Regan JW, Meuillet E, Nelson MA. The EP4 receptor antagonist, L-161,982, blocks prostaglandin E₂-induced signal transduction and cell proliferation in HCA-7 colon cancer cells. *Exp Cell Res* 2007;313(14):2969-79.
24. Chiricozzi E, Fernandez-Fernandez S, Nardicchi V, Almeida A, Bolanos JP, Goracci G. Group IIA secretory phospholipase A₂ (GIIA) mediates apoptotic death during NMDA receptor activation in rat primary cortical neurons. *J Neurochem* 2010;112(6):1574-83.
25. Choy EH, Panayi GS. Cytokine pathways and joint inflammation in rheumatoid arthritis. *N Engl J Med* 2001;344(12):907-16.
26. Church WB, Inglis AS, Tseng A, Duell R, Lei PW, Bryant KJ, Scott KF. A novel approach to the design of inhibitors of human secreted phospholipase A₂ based on native peptide inhibition. *J Biol Chem* 2001;276(35):33156-64.

27. Ciesielski-Treska J, Ulrich G, Chasserot-Golaz S, Zwiller J, Revel MO, Aunis D, Bader MF. Mechanisms underlying neuronal death induced by chromogranin A-activated microglia. *J Biol Chem* 2001;276(16):13113-20.
28. Combs CK, Karlo JC, Kao SC, Landreth GE. beta-Amyloid stimulation of microglia and monocytes results in TNFalpha-dependent expression of inducible nitric oxide synthase and neuronal apoptosis. *J Neurosci* 2001;21(4):1179-88.
29. Coyle JT, Price DL, DeLong MR. Alzheimer's disease: a disorder of cortical cholinergic innervation. *Science* 1983;219(4589):1184-90.
30. Coyle JT, Puttfarcken P. Oxidative stress, glutamate, and neurodegenerative disorders. *Science* 1993;262(5134):689-95.
31. Cummings BS, McHowat J, Schnellmann RG. Phospholipase A(2)s in cell injury and death. *J Pharmacol Exp Ther* 2000;294(3):793-9.
32. Cummings JL. Alzheimer's Disease. *N Engl J Med* 2004;351(1):56-67.
33. Decker T, Lohmann-Matthes ML. A quick and simple method for the quantitation of lactate dehydrogenase release in measurements of cellular cytotoxicity and tumor necrosis factor (TNF) activity. *J Immunol Methods* 1988;115(1):61-9.
34. DeCoster MA, Lambeau G, Lazdunski M, Bazan NG. Secreted phospholipase A2 potentiates glutamate-induced calcium increase and cell death in primary neuronal cultures. *J Neurosci Res* 2002;67(5):634-45.
35. Dennis EA. Diversity of group types, regulation, and function of phospholipase A2. *J Biol Chem* 1994;269(18):13057-60.
36. Divchev D, Schieffer B. The secretory phospholipase A2 group IIA: a missing link between inflammation, activated renin-angiotensin system, and atherogenesis? *Vasc Health Risk Manag* 2008;4(3):597-604.
37. Dong Z, Liu Y, Scott KF, Levin L, Gaitonde K, Bracken RB, Burke B, Zhai QJ, Wang J, Oleksowicz L *et al*. Secretory phospholipase A2-IIa is involved in prostate cancer progression and may potentially serve as a biomarker for prostate cancer. *Carcinogenesis* 2010;31(11):1948-55.
38. Farooqui AA, Horrocks LA. Phospholipase A2-generated lipid mediators in the brain: the good, the bad, and the ugly. *Neuroscientist* 2006;12:245-61.
39. Flavin MP, Ho LT, Coughlin K. Neurotoxicity of soluble macrophage products in vitro--influence of dexamethasone. *Exp Neurol* 1997;145(2 Pt 1):462-70.
40. Flavin MP, Zhao G, Ho LT. Microglial tissue plasminogen activator (tPA) triggers neuronal apoptosis in vitro. *Glia* 2000;29(4):347-54.

41. Gan L, Ye S, Chu A, Anton K, Yi S, Vincent VA, von Schack D, Chin D, Murray J, Lohr S *et al.* Identification of cathepsin B as a mediator of neuronal death induced by Abeta-activated microglial cells using a functional genomics approach. *J Biol Chem* 2004;279(7):5565-72.
42. Ghesquiere SA, Gijbels MJ, Anthonsen M, van Gorp PJ, van der Made I, Johansen B, Hofker MH, de Winther MP. Macrophage-specific overexpression of group IIa sPLA2 increases atherosclerosis and enhances collagen deposition. *J Lipid Res* 2005;46(2):201-10.
43. Giulian D, Corpuz M, Chapman S, Mansouri M, Robertson C. Reactive mononuclear phagocytes release neurotoxins after ischemic and traumatic injury to the central nervous system. *J Neurosci Res* 1993;36(6):681-93.
44. Greenfield SA, Zimmermann M, Bond CE. Non-hydrolytic functions of acetylcholinesterase. The significance of C-terminal peptides. *FEBS J* 2008;275(4):604-11.
45. Han WK, Sapirstein A, Hung CC, Alessandrini A, Bonventre JV. Cross-talk between cytosolic phospholipase A2 alpha (cPLA2 alpha) and secretory phospholipase A2 (sPLA2) in hydrogen peroxide-induced arachidonic acid release in murine mesangial cells: sPLA2 regulates cPLA2 alpha activity that is responsible for arachidonic acid release. *J Biol Chem* 2003;278(26):24153-63.
46. Hansen MB, Nielsen SE, Berg K. Re-examination and further development of a precise and rapid dye method for measuring cell growth/cell kill. *J Immunol Methods* 1989;119(2):203-10.
47. Hanson AJ, Prasad JE, Nahreini P, Andreatta C, Kumar B, Yan XD, Prasad KN. Overexpression of amyloid precursor protein is associated with degeneration, decreased viability, and increased damage caused by neurotoxins (prostaglandins A1 and E2, hydrogen peroxide, and nitric oxide) in differentiated neuroblastoma cells. *J Neurosci Res* 2003;74(1):148-59.
48. Harris JE, Nuttall RK, Elkington PT, Green JA, Horncastle DE, Graeber MB, Edwards DR, Friedland JS. Monocyte-astrocyte networks regulate matrix metalloproteinase gene expression and secretion in central nervous system tuberculosis in vitro and in vivo. *J Immunol* 2007;178(2):1199-207.
49. Hashioka S, Klegeris A, Schwab C, McGeer PL. Interferon-gamma-dependent cytotoxic activation of human astrocytes and astrocytoma cells. *Neurobiol Aging* 2009.
50. Hernandez M, Martin R, Garcia-Cubillas M, Maeso-Hernandez P, Nieto M. Secreted PLA2 induces proliferation in astrocytoma through the EGF receptor: another inflammation-cancer link. *Neuro Oncol* 2010;12(12):1328.
51. Hickey WF. Basic principles of immunological surveillance of the normal central nervous system. *Glia* 2001;36(2):118-24.
52. Hirsch EC, Hunot S. Neuroinflammation in Parkinson's disease: a target for neuroprotection? *Lancet Neurol* 2009;8(4):382-97.

53. Hoyt KR, Gallagher AJ, Hastings TG, Reynolds JJ. Characterization of hydrogen peroxide toxicity in cultured rat forebrain neurons. *Neurochem Res* 1997;22(3):333-40.
54. Hu S, Chao CC, Khanna KV, Gekker G, Peterson PK, Molitor TW. Cytokine and free radical production by porcine microglia. *Clin Immunol Immunopathol* 1996;78(1):93-6.
55. Hume DA. The mononuclear phagocyte system. *Curr Opin Immunol* 2006;18(1):49-53.
56. Ibeas E, Fuentes L, Martin R, Hernández M, Nieto ML. Secreted phospholipase A2 type IIA as a mediator connecting innate and adaptive immunity: new role in atherosclerosis. *Cardiovasc Res* 2009;81:54-63.
57. Ibrahim Z, Busch J, Awwad M, Wagner R, Wells K, Cooper DK. Selected physiologic compatibilities and incompatibilities between human and porcine organ systems. *Xenotransplantation* 2006;13(6):488-99.
58. Ionescu VA, Villanueva EB, Hashioka S, Bahniwal M, Klegeris A. Cultured adult porcine astrocytes and microglia express functional interferon-gamma receptors and exhibit toxicity towards SH-SY5Y cells. *Brain Res Bull* 2011;84(3):244-51.
59. Jamal OS, Conaghan PG, Cunningham AM, Brooks PM, Munro VF, Scott KF. Increased expression of human type IIa secretory phospholipase A2 antigen in arthritic synovium. *Ann Rheum Dis* 1998;57(9):550-8.
60. Jensen MD, Sheng W, Simonyi A, Johnson GS, Sun AY, Sun GY. Involvement of oxidative pathways in cytokine-induced secretory phospholipase A2-IIA in astrocytes. *Neurochem Int* 2009;55(6):362-8.
61. Jiang J, Neubauer BL, Graff JR, Chedid M, Thomas JE, Roehm NW, Zhang S, Eckert GJ, Koch MO, Eble JN *et al.* Expression of group IIA secretory phospholipase A2 is elevated in prostatic intraepithelial neoplasia and adenocarcinoma. *Am J Pathol* 2002;160(2):667-71.
62. Kar S, Slowikowski SP, Westaway D, Mount HT. Interactions between beta-amyloid and central cholinergic neurons: implications for Alzheimer's disease. *J Psychiatry Neurosci* 2004;29(6):427-41.
63. Kehrer JP, Biswal SS, La E, Thuillier P, Datta K, Fischer SM, Vanden Heuvel JP. Inhibition of peroxisome-proliferator-activated receptor (PPAR)alpha by MK886. *Biochem J* 2001;356(Pt 3):899-906.
64. Kermer P, Liman J, Weishaupt JH, Bahr M. Neuronal apoptosis in neurodegenerative diseases: from basic research to clinical application. *Neurodegener Dis* 2004;1(1):9-19.
65. Kingham PJ, Pocock JM. Microglial secreted cathepsin B induces neuronal apoptosis. *J Neurochem* 2001;76(5):1475-84.
66. Klegeris A, McGeer PL. Interaction of various intracellular signaling mechanisms involved in mononuclear phagocyte toxicity toward neuronal cells. *J Leukoc Biol* 2000;67(1):127-33.

67. Klegeris A, McGeer PL. Toxicity of human monocytic THP-1 cells and microglia toward SH-SY5Y neuroblastoma Cells is reduced by inhibitors of 5-lipoxygenase and its activating protein FLAP. *J Leukoc Biol* 2003;73:369-78.
68. Klegeris A, Bissonnette CJ, McGeer PL. Modulation of human microglia and THP-1 cell toxicity by cytokines endogenous to the nervous system. *Neurobiol Aging* 2005a;26:673-82.
69. Klegeris A, McGeer PL. Chymotrypsin-like proteases contribute to human monocytic THP-1 cell as well as human microglial neurotoxicity. *Glia* 2005b;51(1):56-64.
70. Klegeris A, McGeer PL. Non-steroidal anti-inflammatory drugs (NSAIDs) and other anti-inflammatory agents in the treatment of neurodegenerative disease. *Curr Alzheimer Res* 2005;2(3):355-65.
71. Kolko M, de Turco EB, Diemer NH, Bazan NG. Secretory phospholipase A2-mediated neuronal cell death involves glutamate ionotropic receptors. *Neuroreport* 2002;13(15):1963-6.
72. Kuwata H, Yamamoto S, Miyazaki Y, Shimbara S, Nakatani Y, Suzuki H, Ueda N, Murakami M, Kudo I. Studies on a mechanism by which cytosolic phospholipase A2 regulates the expression and function of type IIA secretory phospholipase A2. *J Immunol* 2000;165(7):4024-31.
73. LaFerla FM, Green KM, Oddo S. Intracellular amyloid- β in Alzheimer's disease. *Nat Rev Neurosci* 2007;8(499-509).
74. Lambeau G, Lazdunski M, Barhanin J. Properties of receptors for neurotoxic phospholipases A2 in different tissues. *Neurochem Res* 1991;16(6):651-8.
75. Lambeau G, Ancian P, Nicolas JP, Beiboer SH, Moinier D, Verheij H, Lazdunski M. Structural elements of secretory phospholipases A2 involved in the binding to M-type receptors. *J Biol Chem* 1995;270(10):5534-40.
76. Lambeau G, Gelb MH. Biochemistry and physiology of mammalian secreted phospholipases A2. *Annu Rev Biochem* 2008;77:495-520.
77. Li Z, Jansen M, Ogburn K, Salvatierra L, Hunter L, Mathew S, Figueiredo-Pereira ME. Neurotoxic prostaglandin J2 enhances cyclooxygenase-2 expression in neuronal cells through the p38MAPK pathway: a death wish? *J Neurosci Res* 2004;78(6):824-36.
78. Lin TN, Wang Q, Simonyi A, Chen JJ, Cheung WM, He YY, Xu J, Sun AY, Hsu CY, Sun GY. Induction of secretory phospholipase A2 in reactive astrocytes in response to transient focal cerebral ischemia in the rat brain. *J Neurochem* 2004;90(3):637-45.
79. Lio YC, Reynolds LJ, Balsinde J, Dennis EA. Irreversible inhibition of Ca(2+)-independent phospholipase A2 by methyl arachidonyl fluorophosphonate. *Biochim Biophys Acta* 1996;1302(1):55-60.

80. Lister MD, Glaser KB, Ulevitch RJ, Dennis EA. Inhibition studies on the membrane-associated phospholipase A2 in vitro and prostaglandin E2 production in vivo of the macrophage-like P388D1 cell. Effects of manoilide, 7,7-dimethyl-5,8-eicosadienoic acid, and p-bromophenacyl bromide. *J Biol Chem* 1989;264(15):8520-8.
81. Macchioni L, Corazzi L, Nardicchi V, Mannucci R, Arcuri C, Porcellati S, Sposini T, Donato R, Goracci G. Rat brain cortex mitochondria release group II secretory phospholipase A(2) under reduced membrane potential. *J Biol Chem* 2004;279(36):37860-9.
82. Martin R, Hernandez M, Ibeas E, Fuentes L, Salicio V, Arnes M, Nieto ML. Secreted phospholipase A2-IIA modulates key regulators of proliferation on astrocytoma cells. *J Neurochem* 2009;111(4):988-99.
83. Massaad C, Paradon M, Jacques C, Salvat C, Bereziat G, Berenbaum F, Olivier JL. Induction of secreted type IIA phospholipase A2 gene transcription by interleukin-1beta. Role of C/EBP factors. *J Biol Chem* 2000;275(30):22686-94.
84. Masuda S, Murakami M, Komiyama K, Ishihara M, Ishikawa Y, Ishii T, Kudo I. Various secretory phospholipase A2 enzymes are expressed in rheumatoid arthritis and augment prostaglandin production in cultured synovial cells. *FEBS J* 2005;272(3):655-72.
85. Mathisen GH, Thorkildsen IH, Paulsen RE. Secretory PLA2-IIA and ROS generation in peripheral mitochondria are critical for neuronal death. *Brain Res* 2007;1153:43-51.
86. Mattson MP. Apoptosis in neurodegenerative disorders. *Nat Rev Mol Cell Biol* 2000;1(2):120-9.
87. Mauchley D, Meng X, Johnson T, Fullerton DA, Weyant MJ. Modulation of growth in human esophageal adenocarcinoma cells by group IIA secretory phospholipase A(2). *J Thorac Cardiovasc Surg* 2009;139(3):591-9; discussion 599.
88. McNaught KSP, Olanow CW. Protein aggregation in the pathogenesis of familial and sporadic Parkinson's disease. *Neurobiol Aging* 2006;27:530-45.
89. Miyake A, Yamamoto H, Takebayashi Y, Imai H, Honda K. The novel natural product YM-26567-1 [(+)-trans-4-(3-dodecanoyl-2,4,6-trihydroxyphenyl)-7-hydroxy-2-(4-hydroxyphenyl)chroman]: a competitive inhibitor of group II phospholipase A2. *J Pharmacol Exp Ther* 1992;263(3):1302-7.
90. Moore DJ, West AB, Dawson VL, Dawson TM. Molecular pathophysiology of Parkinson's disease. *Annual Rev Neurosci* 2005;28:57-87.
91. Moriguchi S, Mizoguchi Y, Tomimatsu Y, Hayashi Y, Kadowaki T, Kagamiishi Y, Katsube N, Yamamoto K, Inoue K, Watanabe S *et al*. Potentiation of NMDA receptor-mediated synaptic responses by microglia. *Brain Res Mol Brain Res* 2003;119(2):160-9.
92. Moses GS, Jensen MD, Lue LF, Walker DG, Sun AY, Simonyi A, Sun GY. Secretory PLA2-IIA: a new inflammatory factor for Alzheimer's disease. *J Neuroinflammation* [Internet]. 2006;3(28). Available from: <http://www.jneuroinflammation.com/content/3/1/28>

93. Mosmann T. Rapid colorimetric assay for cellular growth and survival: application to proliferation and cytotoxicity assays. *J Immunol Methods* 1983;65(1-2):55-63.
94. Mounier CM, Bon C, Kini RM. Anticoagulant venom and mammalian secreted phospholipases A(2): protein- versus phospholipid-dependent mechanism of action. *Haemostasis* 2001;31(3-6):279-87.
95. Murakami M, Kambe T, Shimbara S, Kudo I. Functional coupling between various phospholipase A2s and cyclooxygenases in immediate and delayed prostanoid biosynthetic pathways. *J Biol Chem* 1999;274(5):3103-15.
96. Nachlas MM, Margulies SI, Goldberg JD, Seligman AM. The determination of lactic dehydrogenase with a tetrazolium salt. *Anal Biochem* 1960;1:317-26.
97. Nakajima K, Kohsaka S. Microglia: activation and their significance in the central nervous system. *J Biochem* 2001;130(2):169-75.
98. Oka S, Arita H. Inflammatory factors stimulate expression of group II phospholipase A2 in rat cultured astrocytes. Two distinct pathways of the gene expression. *J Biol Chem* 1991;266(15):9956-60.
99. Olson ED, Nelson J, Griffith K, Nguyen T, Streeter M, Wilson-Ashworth HA, Gelb MH, Judd AM, Bell JD. Kinetic evaluation of cell membrane hydrolysis during apoptosis by human isoforms of secretory phospholipase A2. *J Biol Chem* 2010;285(14):10993-1002.
100. Oslund RC, Cermak N, Gelb MH. Highly specific and broadly potent inhibitors of mammalian secreted phospholipases A2. *J Med Chem* 2008;51(15):4708-14.
101. Oslund RC, Cermak N, Verlinde CL, Gelb MH. Simplified YM-26734 inhibitors of secreted phospholipase A2 group IIA. *Bioorg Med Chem Lett* 2008;18(20):5415-9.
102. Park KM, Trucillo M, Serban N, Cohen RA, Bolotina VM. Role of iPLA2 and store-operated channels in agonist-induced Ca²⁺ influx and constriction in cerebral, mesenteric, and carotid arteries. *Am J Physiol Heart Circ Physiol* 2008;294(3):H1183-7.
103. Parpura V, Haydon PG. Physiological astrocytic calcium levels stimulate glutamate release to modulate adjacent neurons. *Proc Natl Acad Sci U S A* 2000;97(15):8629-34.
104. Peilot H, Rosengren B, Bondjers G, Hurt-Camejo E. Interferon-gamma induces secretory group IIA phospholipase A2 in human arterial smooth muscle cells. Involvement of cell differentiation, STAT-3 activation, and modulation by other cytokines. *J Biol Chem* 2000;275(30):22895-904.
105. Pernas P, Masliah J, Olivier JL, Salvat C, Rybkine T, Bereziat G. Type II phospholipase A2 recombinant overexpression enhances stimulated arachidonic acid release. *Biochem Biophys Res Commun* 1991;178(3):1298-305.
106. Peuchen S, Bolanos JP, Heales SJ, Almeida A, Duchen MR, Clark JB. Interrelationships between astrocyte function, oxidative stress and antioxidant status within the central nervous system. *Prog Neurobiol* 1997;52(4):261-81.

107. Piek JJ, de Winter RJ. Type II secretory phospholipase A2: the emerging role of biochemical markers of plaque inflammation. *Eur Heart J* 2003;24(20):1804-6.
108. Pineau I, Lacroix S. Endogenous signals initiating inflammation in the injured nervous system. *Glia* 2009;57(4):351-61.
109. Pluckthun A, Dennis EA. Activation, aggregation, and product inhibition of cobra venom phospholipase A2 and comparison with other phospholipases. *J Biol Chem* 1985;260(20):11099-106.
110. Putz T, Ramoner R, Gander H, Rahm A, Bartsch G, Bernardo K, Ramsay S, Thurnher M. Bee venom secretory phospholipase A2 and phosphatidylinositol-homologues cooperatively disrupt membrane integrity, abrogate signal transduction and inhibit proliferation of renal cancer cells. *Cancer Immunol Immunother* 2007;56(5):627-40.
111. Radvanyi F, Jordan L, Russo-Marie F, Bon C. A sensitive and continuous fluorometric assay for phospholipase A2 using pyrene-labeled phospholipids in the presence of serum albumin. *Anal Biochem* 1989;177(1):103-9.
112. Rauschenberger K, Scholer K, Sass JO, Sauer S, Djuric Z, Rumig C, Wolf NI, Okun JG, Kolker S, Schwarz H *et al.* A non-enzymatic function of 17beta-hydroxysteroid dehydrogenase type 10 is required for mitochondrial integrity and cell survival. *EMBO Mol Med* 2009;2(2):51-62.
113. Raveh A, Cooper A, Guy-David L, Reuveny E. Nonenzymatic rapid control of GIRK channel function by a G protein-coupled receptor kinase. *Cell* 2010;143(5):750-60.
114. Rock RB, Gekker G, Hu S, Sheng WS, Cheeran M, Lokensgard JR, Peterson PK. Role of microglia in central nervous system infections. *Clin Microbiol Rev* 2004;17(4):942-64.
115. Rock KL. Pathobiology of inflammation to cell death. *Biol Blood Marrow Transplant* 2009;15(1 Suppl):137-8.
116. Saegusa J, Akakura N, Wu CY, Hoogland C, Ma Z, Lam KS, Liu FT, Takada YK, Takada Y. Pro-inflammatory secretory phospholipase A2 type IIA binds to integrins alphavbeta3 and alpha4beta1 and induces proliferation of monocytic cells in an integrin-dependent manner. *J Biol Chem* 2008;283(38):26107-15.
117. Sastre M, Klockgether T, Heneka MT. Contribution of inflammatory processes to Alzheimer's disease: molecular mechanisms. *International Journal of Developmental Neuroscience* 2006;24:167-76.
118. Schaeffer EL, da Silva ER, Novaes Bde A, Skaf HD, Gattaz WF. Differential roles of phospholipases A(2) in neuronal death and neurogenesis: implications for Alzheimer disease. *Prog Neuropsychopharmacol Biol Psychiatry* 2010;34(8):1381-9.
119. Smart BP, Pan YH, Weeks AK, Bollinger JG, Bahnson BJ, Gelb MH. Inhibition of the complete set of mammalian secreted phospholipases A(2) by indole analogues: a structure-guided study. *Bioorg Med Chem* 2004;12(7):1737-49.

120. Streit WJ, Mrak RE, Griffin WS. Microglia and neuroinflammation: a pathological perspective. *J Neuroinflammation* [Internet]. 2004;1(14). Available from: <http://www.jneuroinflammation.com/content/1/1/14>
121. Tang SC, Lathia JD, Selvaraj PK, Jo DG, Mughal MR, Cheng A, Siler DA, Markesbery WR, Arumugam TV, Mattson MP. Toll-like receptor-4 mediates neuronal apoptosis induced by amyloid beta-peptide and the membrane lipid peroxidation product 4-hydroxynonenal. *Exp Neurol* 2008;213(1):114-21.
122. Titsworth WL, Cheng X, Ke Y, Deng L, Burckardt KA, Pendleton C, Liu NK, Shao H, Cao QL, Xu XM. Differential expression of sPLA2 following spinal cord injury and a functional role for sPLA2-IIA in mediating oligodendrocyte death. *Glia* 2009;57(14):1521-37.
123. Tournier C, Thomas G, Pierre J, Jacquemin C, Pierre M, Saunier B. Mediation by arachidonic acid metabolites of the H₂O₂-induced stimulation of mitogen-activated protein kinases (extracellular-signal-regulated kinase and c-Jun NH₂-terminal kinase). *Eur J Biochem* 1997;244(2):587-95.
124. Town T, Nikolic V, Tan J. The microglial "activation" continuum: from innate to adaptive responses. *J Neuroinflammation* [Internet]. 2005;2:24. Available from: <http://www.jneuroinflammation.com/content/2/1/24>
125. Wagner B, Natarajan A, Grunau S, Kroismayr R, Wagner EF, Sibilica M. Neuronal survival depends on EGFR signaling in cortical but not midbrain astrocytes. *EMBO J* 2006;25(4):752-62.
126. Wang X, Chen S, Ma G, Ye M, Lu G. Involvement of proinflammatory factors, apoptosis, caspase-3 activation and Ca²⁺ disturbance in microglia activation-mediated dopaminergic cell degeneration. *Mech Ageing Dev* 2005;126(12):1241-54.
127. Wei LL, Shen YD, Zhang YC, Hu XY, Lu PL, Wang L, Chen W. Roles of the prostaglandin E₂ receptors EP subtypes in Alzheimer's disease. *Neurosci Bull* 2010;26(1):77-84.
128. Wei S, Ong WY, Thwin MM, Fong CW, Farooqui AA, Gopalakrishnakone P, Hong W. Group IIA secretory phospholipase A₂ stimulates exocytosis and neurotransmitter release in pheochromocytoma-12 cells and cultured rat hippocampal neurons. *Neuroscience* 2003;121(4):891-8.
129. Wu Y, Raymond B, Goossens PL, Njamkepo E, Guiso N, Paya M, Touqui L. Type-IIA secreted phospholipase A₂ is an endogenous antibiotic-like protein of the host. *Biochimie* 2010;92(6):583-7.
130. Xie HR, Hu LS, Li GY. SH-SY5Y human neuroblastoma cell line: in vitro cell model of dopaminergic neurons in Parkinson's disease. *Chin Med J (Engl)*;123(8):1086-92.

131. Yagami T, Ueda K, Asakura K, Hata S, Kuroda T, Sakaeda T, Takasu N, Tanaka K, Gemba T, Hori Y. Human group IIA secretory phospholipase A2 induces neuronal cell death via apoptosis. *Mol Pharmacol* 2002;61(1):114-26.
132. Yagami T, Ueda K, Asakura K, Nakazato H, Hata S, Kuroda T, Sakaeda T, Sakaguchi G, Itoh N, Hashimoto Y *et al.* Human group IIA secretory phospholipase A2 potentiates Ca²⁺ influx through L-type voltage-sensitive Ca²⁺ channels in cultured rat cortical neurons. *J Neurochem* 2003;85(3):749-58.
133. Yagami T, Ueda K, Hata S, Kuroda T, Itoh N, Sakaguchi G, Okamura N, Sakaeda T, Fujimoto M. S-2474, a novel nonsteroidal anti-inflammatory drug, rescues cortical neurons from human group IIA secretory phospholipase A(2)-induced apoptosis. *Neuropharmacology* 2005;49(2):174-84.
134. Zhang FX, Kirschning CJ, Mancinelli R, Xu XP, Jin Y, Faure E, Mantovani A, Rothe M, Muzio M, Arditi M. Bacterial lipopolysaccharide activates nuclear factor-kappaB through interleukin-1 signaling mediators in cultured human dermal endothelial cells and mononuclear phagocytes. *J Biol Chem* 1999;274(12):7611-4.

Appendices

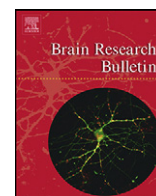
Appendix A: RNA Purity Values

Cell Type	µg/ml	Sample	260/280	260/230	230A	260A	280A	340A
THP-1	95.6	Unstimulated	2.03	2.09	0.083	0.169	0.086	0.005
		4h IFN- γ +LPS stimulated	2.07	2.13	0.064	0.126	0.065	0.009
		24h IFN- γ +LPS stimulated	2	2.09	0.046	0.096	0.048	0
		48h IFN- γ +LPS stimulated	1.71	2.11	0.023	0.048	0.028	0
U-373 MG	82.5	Unstimulated	2.15	2.25	0.033	0.073	0.034	0.001
		24h IFN- γ stimulated	2.38	2.47	0.017	0.041	0.017	0
Human Primary Astrocytes	17.8	Unstimulated	1.95	2.05	0.114	0.201	0.119	0.031
		48h IFN- γ stimulated	1.84	1.98	0.088	0.162	0.082	0.001

RNA sample purity was determined using an Eppendorf Biophotometer Plus spectrophotometer (see Methods for company information). RNA absorbs at 260 nm, while contaminants such as organic compounds, protein and particulates absorb at 230, 280 and >340 nm, respectively. The 260/280 ratio was used to determine RNA purity; a relatively pure RNA sample measures between 1.8-2.0 according to the manufacturer.

Appendix B: Publication

Ionescu VA, Villanueva EB, Hashioka S, Bahniwal M, Klegeris A. Cultured adult porcine astrocytes and microglia express functional interferon- γ receptors and exhibit toxicity towards SH-SY5Y cells. Brain Res Bull 2011;84(3):244-51.



Research report

Cultured adult porcine astrocytes and microglia express functional interferon- γ receptors and exhibit toxicity towards SH-SY5Y cells

Vlad A. Ionescu^a, Erika B. Villanueva^a, Sadayuki Hashioka^b, Manpreet Bahniwal^a, Andis Klegeris^{a,*}

^a Department of Biology, University of British Columbia Okanagan, 3333 University Way, Kelowna, BC, V1V 1V7 Canada

^b Kinsmen Laboratory of Neurological Research, University of British Columbia, Vancouver, BC, V6T 2A1 Canada

ARTICLE INFO

Article history:

Received 21 July 2010

Received in revised form

14 December 2010

Accepted 19 December 2010

Available online 24 December 2010

Keywords:

Aging

In vitro culture model

Neuroinflammation

Neurodegenerative diseases

Neurotoxicity

Pig glia

ABSTRACT

In vitro cultures of various glial cell types are common systems used to model neuroinflammatory processes associated with age-dependent human neurodegenerative diseases. Even though most researchers choose to use neonatal rodent brain tissues as the source of glial cells, there are significant variations in glial cell functions that are species and age dependent. It has been established that human and swine immune systems have a number of similarities, which suggests that cultured porcine microglia and astrocytes may be good surrogates for human glial cell types. Here we describe a method that could be used to prepare more than 90% pure microglia and astrocyte cultures derived from adult porcine tissues. We demonstrate that both microglia and astrocytes derived from adult porcine brains express functional interferon- γ receptors (IFN- γ -R) and CD14. They become toxic towards SH-SY5Y neuroblastoma cells when exposed to proinflammatory mediators. Upon such stimulation with lipopolysaccharide (LPS) and interferon- γ (IFN- γ), adult porcine microglia, but not astrocytes, secrete tumor necrosis factor- α (TNF- α) while both cell types do not secrete detectable levels of nitric oxide (NO). Comparison of our experimental data with previously published studies indicates that adult porcine glial cultures have certain functional characteristics that make them similar to human glial cells. Therefore adult porcine glial cells may be a useful model system for studies of human diseases associated with adulthood and advanced age. Adult porcine tissues are relatively easy to obtain in most countries and could be used as a reliable and inexpensive source of cultured cells.

Crown Copyright © 2010 Published by Elsevier Inc. All rights reserved.

1. Introduction

Considerable evidence suggests that neuroinflammatory processes play a significant role in a number of neurodegenerative disorders [16,18,28]. Data supporting this inflammatory hypothesis of neurodegeneration have been collected by analysing human post mortem tissue samples, studying transgenic animal models and culturing various cell types derived from the central nervous system of various animal species. It has become evident that microglia and astrocytes play a crucial role in the homeostasis of the nervous system; however, they also become actively involved in various pathological processes of the brain [6,46]. One of the best approaches for studying human microglia and astrocyte physiology

Abbreviations: DMEM-F12, Dulbecco's modified Eagle's medium–nutrient mixture F12 ham; ELISA, enzyme-linked immunosorbent assay; FBS, fetal bovine serum; GFAP, glial fibrillary acidic protein; IFN- γ , interferon- γ ; IFN- γ -R, interferon- γ receptors; IL, interleukin; LPS, lipopolysaccharide; MTT, 3-(4,5-dimethylthiazol-2-yl) 2,5-diphenyl tetrazolium bromide; NO, nitric oxide; PBS, phosphate-buffered saline; TNF- α , tumor necrosis factor- α .

* Corresponding author. Tel.: +1 250 807 9557; fax: +1 250 807 8005.

E-mail address: andis.klegeris@ubc.ca (A. Klegeris).

and pathology has been culturing these cells from either human post-mortem, surgical or fetal tissues [14,30,37]. However, due to ethical issues associated with such experiments and the limited availability of human tissues, there is a need for alternative model systems. The most commonly used surrogates for human glial cells have been cell lines derived mainly from humans or mice, as well as primary mouse or rat glial cells that are usually prepared from perinatal animals. The advantages of these culture systems include the fact that tissues are easily accessible and that the obtained cells are readily dividing, which allows significant numbers of cells to be harvested. Nevertheless, due to the existing interspecies differences in the case of rodent tissues as well as the alterations in oncogene expression and appearance of subclones in the case of cell lines, these culture systems are not ideal [1,3,45].

Pigs represent a species that might be a good model for human biomedical research in general, as well as an appropriate model for studies on immune and neuroinflammatory processes [44]. Of all the non-primate mammals, pigs have the physiology, anatomy and body size most similar to that of humans. The pig immune system is also very similar to humans and an intensive research effort has been directed towards the use of porcine organs for xenotransplantation in humans [12]. Various porcine cell types have

been cultured thus far, including peripheral blood lymphocytes [42], aortic and brain-derived endothelial cells [11,38], kidney cells [54] as well as myenteric and brain-derived neurons [2,5]. Several reports have already described porcine glial cell cultures, including mixed glial cultures prepared from one-day old animals [5,50], from which pure microglia and astrocyte cultures were extracted. Thus far, neonatal pigs have been the main source of microglia cultures studied [22,34,41,48–50].

To the best of our knowledge, only two reports have described adult porcine glial cells: Jeliaskova-Mecheva and Bobilya [25] described a porcine astrocyte/endothelial cell culture model that was prepared from 3 to 4 months old Yucatan miniature pigs, while Yang et al. [54] used adult pig retinal wholemounts to characterize microglia and other immune cells in this tissue by immunohistochemical staining; the latter study did not use cultured glial cells. Here we describe preparation of purified adult porcine microglia and astrocyte cell cultures and demonstrate that these cells express interferon- γ receptors (IFN- γ -R), CD14 and upon stimulation become cytotoxic to human neuronal SH-SY5Y cells.

2. Methods

2.1. Adult porcine glial cell cultures

Except during tissue extraction, all cells were cultured in Dulbecco's modified Eagle's medium–nutrient mixture F12 ham (DMEM-F12, HyClone, Logan, UT, USA, catalogue number 3026101) supplemented with either 5% or 10% heat-inactivated fetal bovine serum (FBS, HyClone, 3039603HI). For cell culture, the media was supplemented with an antibiotic/antimycotic solution at a final concentration of 100 U/ml penicillin G, 100 μ g/ml streptomycin and 0.25 μ g/ml amphotericin (1 \times antibiotics, HyClone, 3007901).

Intact heads from one year old land-raised Pietrain pigs were collected from a licensed local abattoir. Post-mortem delays varied between 3 and 5 h during which tissues were kept on ice. Brain tissues were excised under sterile conditions and placed into cold DMEM-high glucose (HyClone, 3024302) containing 5 \times antibiotics without FBS. Approximately 10 g of the cortical tissue was cut into small blocks, collected into a sterile Petri dish with DMEM-high glucose (0% FBS, 5 \times antibiotics); large blood vessels and the meninges were carefully removed. Following 3 washes with 10 ml of DMEM-high glucose (0% FBS, 5 \times antibiotics), a sterile razor blade was used to mechanically dissociate the brain tissue to a fine consistency (for approximately 2 min). The tissues were transferred into 50 ml tubes containing 45 ml of DMEM-high glucose (0% FBS, 5 \times antibiotics), 5 ml of 2.5% w/v trypsin solution (HyClone, 3003701) was added and tubes incubated at 37 $^{\circ}$ C for 30 min in a water bath with shaking. The tissues were treated with DNase 1 (40 Kunitz Units/ml, Sigma–Aldrich, St. Louis, MO, USA, D4263) for an additional 10 min, followed by further mechanical homogenization via repetitive pipetting using a sterile 10 ml serological pipette. The resulting mixture was split into two 50 ml tubes. DMEM-F12 (10% FBS, 1 \times antibiotics) was added to each tube to inhibit any residual trypsin and cells were centrifuged at 250 \times g for 10 min at 4 $^{\circ}$ C. The pellet was re-suspended in a total volume of 15 ml DMEM-F12 and the suspension was filtered through a sterile cell strainer (100 μ m, BD Falcon, Mississauga, ON, Canada, 352360). The filtrate was diluted with DMEM-F12 to reach the final volume of 30 ml and was carefully layered onto a Percoll density gradient solution prepared in 50 ml centrifuge tubes. The Percoll gradient was produced by gently layering 15 ml of 25% v/v Percoll (GE Healthcare, Piscataway, NJ, USA, 17-0891-01) isotonicity adjusted with phosphate buffered saline (PBS), onto 5 ml of 70% v/v Percoll. We were careful not to disturb the interface that appeared between the Percoll layers and the cell suspension. The resulting mixture was spun at 15,000 \times g for 10 min at 4 $^{\circ}$ C in a fixed-angle rotor. The upper cloudy layer, which contained the myelin and cell debris, was discarded. The cloudy interface layer containing the glial cells (2–3 ml) was carefully collected and diluted in 10 ml of DMEM-F12 (10% FBS, 1 \times antibiotics). Following a 10 min spin at 250 \times g to wash the residual Percoll, the resulting pellet containing the glial cells was re-suspended in DMEM-F12 (10% FBS, 1 \times antibiotics) and plated onto two 100 mm tissue culture-treated plates (Corning, Lowell, MA, 430167). Cell cultures were incubated in a designated CO₂ incubator (humidified 5% CO₂ and 95% air atmosphere) set at 39 $^{\circ}$ C, which is the normal body temperature for pigs.

Following 48 h incubation, the non-adherent cells and any residual debris were washed off with warm PBS with 1 \times antibiotics followed by the addition of fresh medium. The cell cultures reached confluence after 14–20 days incubation, after which the cultures were transferred to 75 cm² tissue culture flasks (Sarstedt, Montreal, Quebec, Canada, 831811002) as follows: the original media was removed and cells were trypsinized for 5 min using 5 ml of 0.25% w/v trypsin/EDTA solution (HyClone, 3004202). Cells were washed with 15 ml DMEM-F12 (10% FBS, 1 \times antibiotics), collected by centrifugation at 250 \times g for 10 min and re-suspended

in DMEM-F12 (10%FBS, 1 \times antibiotics) before being plated into tissue culture flasks.

After the mixed glial cell cultures became confluent again (typically 7–10 days), flasks were shaken at 200 rpm for 1 h at room temperature on an orbital shaker to remove the loosely adherent microglia cells. Microglia in the mixed glial culture supernatants were collected by centrifugation at 250 \times g for 10 min, re-suspended in DMEM-F12 (10% FBS, 1 \times antibiotics), and plated in 24-well plates for further experiments as described below. Microglia were harvested at one week intervals for up to three times. Typically, the yield of microglia was 0.25–0.4 million per 10 g of tissue sample from the initial two shakes. The third shaking generated at least four times less cells. For the isolation of astrocytes, confluent mixed glial cell cultures were first depleted of microglia by shaking. Astrocyte-enriched cultures were passaged at least twice over a period of 3 weeks before initiating the experiments; astrocytes were split by transferring 1/5th of cells into a new flask after cells had been detached by 0.25% w/v trypsin/EDTA solution. Astrocyte yield from one confluent 75 cm² tissue culture flasks was up to 2.5 million cells. Senescence in astrocyte-enriched cultures was detected in several cases after 6 or 7 passages as a significant decrease in cell growth rate associated with changes in cell morphology; therefore no experiments were performed with astrocytes-enriched cultures that were passaged more than 5 times. Cells in culture were observed with an inverted phase contrast microscope (Motic, Richmond, BC, Canada) and photographed using Motic 3000 digital camera.

2.2. Immunofluorescence light microscopy

For immunocytochemical assessment of culture purity, astrocytes and microglia were harvested as described above, plated on 4-well chambered slides (Lab-tek, Fisher Scientific, Ottawa, ON, Canada) at 5 \times 10⁵ cells/ml and allowed to adhere for 24 h. Cells were fixed with 4% buffered paraformaldehyde for 15 min, treated with a blocking solution containing 5% skim milk and/or 4% normal goat serum at room temperature for 1 h and incubated with primary antibodies at 4 $^{\circ}$ C overnight. Polyclonal rabbit anti-gliab fibrillary acidic protein (GFAP) antibodies (1:2,000 dilution; Dako, Denmark, Z0334) were used to stain astrocytes, and polyclonal rabbit anti-IBA-1 antibodies (1:200 dilution; Wako, Osaka, Japan, 019-19741) were used to stain microglia. Subsequently, the slides were washed in 50 mM Tris-HCl, pH 7.4, saline, 0.1% Triton X-100 (TBST) for 1 h and incubated at room temperature with Cy3-F(ab')₂ fragment conjugated sheep anti-rabbit IgG (1:2000 dilution, Sigma–Aldrich, C2306). 5 μ M bisbenzimidazole H33342 trihydrochloride (Hoechst H33342, Sigma–Aldrich, B2261) was used for nuclear counterstaining. Following 3 \times 20 min wash in TBST, the slides were coverslipped with ProLong Gold 8 anti-fade reagent (Invitrogen, Burlington, ON, Canada, P36930).

For double immunofluorescence staining, the monoclonal mouse antibody against IFN- γ -R2 (1:500 dilution; clone MMHGR-2, Fitzgerald Industries International, Concord, MA, USA, 10R-1145A) and the monoclonal mouse anti-CD14 antibody (1:100 dilution; clone RPA-M1, Zymed, San Francisco, CA, USA, 07-1403, now distributed by Invitrogen) were used combined with either the rabbit polyclonal antibody against GFAP (1:1000 dilution; Dako, Z0334) for the identification of astrocytes or with the rabbit polyclonal anti-IBA-1 antibodies (1:200 dilution; Wako, 019-19741) for the staining of microglia. The rabbit polyclonal anti-IFN- γ -R2 antibody (1:100 dilution; Abcam, Cambridge, MA, USA, ab77246) was also used combined with the mouse monoclonal anti-S100 beta antibody (S100B, 1:1000; Abcam, ab11178) for the identification of astrocytes. Cell cultures were then incubated at room temperature for 1 h with Alexa Fluor 488-conjugated goat anti-mouse IgG antibody (1:1000–1:500 dilutions; Invitrogen, A-10667) or Alexa Fluor 546-conjugated goat anti-rabbit IgG (1:1000–1:500; Invitrogen, A-11010). Hoechst 33258 (Sigma–Aldrich, B2883) was used for nuclear counterstaining. Cell cultures were examined under a fluorescence microscope (Olympus, BX-51, Tokyo, Japan), images were acquired with a digital Olympus DP71 camera and colocalized with ImagePro software (Improvision, Waltham, MA, USA). Negative controls for immunostaining were performed by omitting the primary antibody; no immunoreactivity was observed in these negative controls.

2.3. Glial cytotoxicity experiments

Cytotoxicity of porcine astrocytes and microglia towards human SH-SY5Y neuroblastoma cells (a gift from Dr. R. Ross, Fordham University, NY, USA) was assessed by methods previously established for analysis of human cell cytotoxicity [20,26]. SH-SY5Y cells were used without initial retinoic acid differentiation. Briefly, porcine astrocytes were seeded into 24-well tissue culture-treated plates (Corning, 3524) at a concentration of 6 \times 10⁵ cells/well in 0.8 ml of DMEM-F12 medium containing 5% FBS, while porcine microglia were used at 8 \times 10⁴ cells/well. Cells were allowed to adhere for 48 h, after which cell culture medium was removed and replaced with 0.8 ml of fresh medium. Bacterial lipopolysaccharide (LPS, 0.5 μ g/ml, >97% pure, from *Escherichia coli* 055:B5, Sigma–Aldrich, L6529) and recombinant porcine interferon- γ (IFN- γ , 0.1 μ g/ml, >97% pure, R&D Systems, Minneapolis, MN, USA, 985-PI) were used alone or in combination to stimulate glial cells. After 48 h incubation, 0.4 ml of cell-free supernatant was transferred to each well containing SH-SY5Y cells, which had been plated 24 h earlier at a concentration of 8 \times 10⁴ cells/well. After 72 h incubation, SH-SY5Y cell survival was assessed by the MTT assay and live/dead cell fluorescent staining.

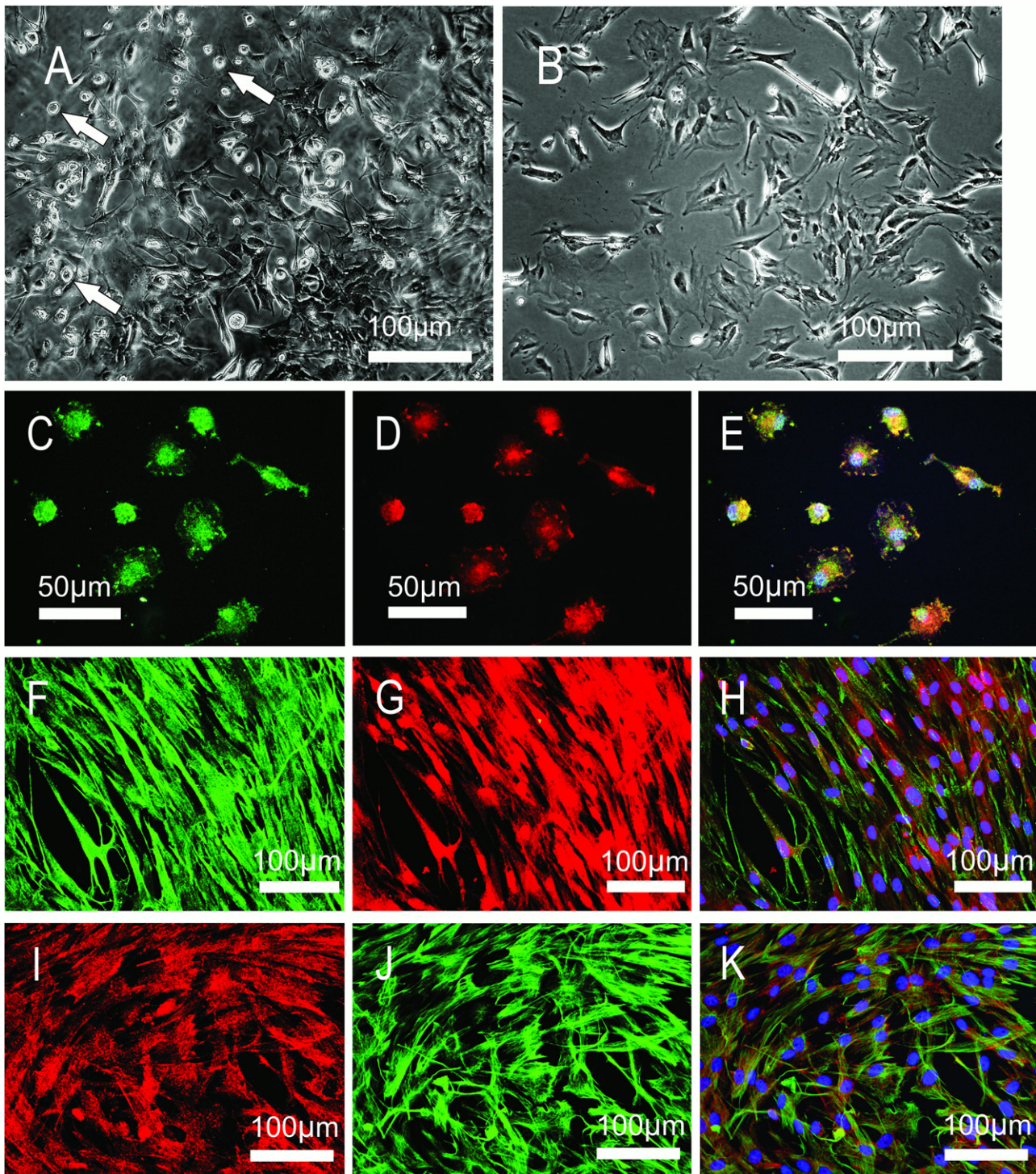


Fig. 1. Adult porcine glial cultures. (A, B) Phase contrast microscopy of mixed primary glial cell cultures (A) and astrocyte-enriched cultures (B). White arrows (A) indicate microglia cells that are loosely adherent on top of astrocyte monolayer. (C–E) Double immunofluorescence staining of IFN- γ -R and microglia-specific marker IBA-1 in microglia-enriched cultures. Cells were stained with a monoclonal IFN- γ -R specific antibody (C, green) and a polyclonal antibody against IBA-1 (D, red). The overlaid image shows that microglia cells are positive for IFN- γ -R (E). (F–K) Double immunofluorescence staining of IFN- γ -R and glial-specific markers in astrocyte-enriched cultures. Cells were stained with two different antibodies against IFN- γ -R (F, green; I, red) and either the polyclonal antibody against GFAP (G, red) or the monoclonal antibody against S100B (J, green), which are the markers of astrocytes. The merged images show that most of the IFN- γ -R-immunoreactive cells correspond to astrocytes (H, K). Cell nuclei were counterstained by Hoechst H33258 (E, H, K, blue). Photos are representative of cell cultures prepared from four different animals. Magnification bars in A, B, F–K = 100 μ m and in C–E = 50 μ m. See Section 2 for experimental details. (For interpretation of the references to colour in this figure legend, the reader is referred to the web version of the article.)

2.4. Measurement of cell viability

The MTT assay was performed as described previously [20,26]. This method is based on the ability of viable, but not dead cells, to convert the tetrazolium salt MTT (3-(4,5-dimethylthiazol-2-yl) 2,5-diphenyl tetrazolium bromide, Sigma–Aldrich,

M2128) to coloured formazan. SH-SY5Y cells were incubated with 0.5 mg/ml MTT at 37 °C for 1 h, the dark crystals formed were dissolved by adding an equal volume of SDS/DMF extraction buffer (20% sodium dodecyl sulphate, 50% N,N-dimethyl formamide, pH 4.7, both from Fisher Scientific) and optical densities at 570 nm were measured. The percent viable cells were calculated using values obtained from wells

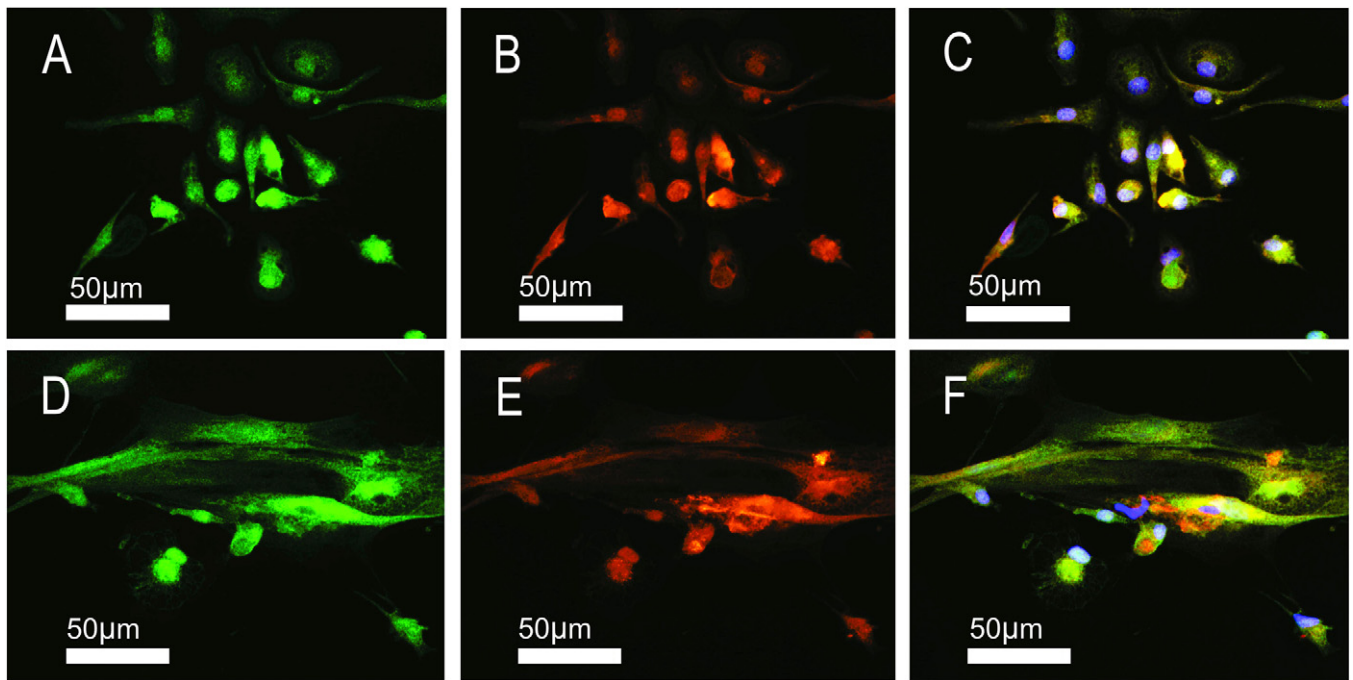


Fig. 2. Adult porcine microglia and astrocytes express CD14. (A–C) Double immunofluorescence staining of CD14 and microglia-specific marker IBA-1 in microglia-enriched cultures. Cells were stained with a monoclonal CD14 specific antibody (A, green) and a polyclonal antibody against IBA-1 (B, red). The overlaid image shows that microglia cells are positive for CD14 (C). (D–F) Double immunofluorescence staining of CD14 and astrocyte marker GFAP in astrocyte-enriched cultures. Cells were stained with a monoclonal CD14 specific antibody (D, green) and a polyclonal antibody against GFAP (E, red). The merged image shows that astrocytes are positive for CD14 (F). Photos are representative of cell cultures prepared from three different animals. Magnification bars = 50 μm . See Section 2 for experimental details. (For interpretation of the references to colour in this figure legend, the reader is referred to the web version of the article.)

exposed to cell culture medium only and wells containing cells lysed with 1% Triton X-100. In the case of porcine astrocytes, the MTT viability data were confirmed by Molecular Probes fluorescent live/dead assay, which was used to estimate the percentage of dead cells. A protocol supplied by the manufacturer of the kit (Invitrogen, L-3224) was followed. Viability of SH-SY5Y cells exposed to supernatants from porcine astrocytes was assayed by selecting 5 random fields of view of equal size in a total of 8 slides for each condition. The total number of cells in each field was counted after adding Calcein AM and EthD-1, which stain live and dead cells respectively. Cellular viability was expressed as the ratio of total viable cells to the total cell number in each field of view. Supernatants harvested from cultures prepared from 4 different animals were used for this study. Cell counts were performed in a blinded fashion.

2.5. Measurement of tumor necrosis factor (TNF)- α and nitrite concentrations

Porcine microglia and astrocytes were plated exactly as described in Section 2.3 for cytotoxicity experiments. LPS (0.5 $\mu\text{g}/\text{ml}$) and porcine IFN- γ (0.1 $\mu\text{g}/\text{ml}$) were used alone or in combination to stimulate glial cells. After 48 h incubation, culture supernatants from unstimulated and stimulated cells were collected and centrifuged at 5000 $\times g$ to remove cellular debris. 100 μl aliquots were used to measure TNF- α and nitrite concentrations. The TNF- α levels were measured using a commercially available enzyme-linked immunosorbent assay (ELISA) kit (Swine TNF- α Cytoset, BioSource International, Camarillo, CA, USA, CSC1753) according to manufacturer's instructions. The mean detection limit for the assay was 0.44 ng/ml.

The concentration of nitrite in tissue culture medium was measured as previously described [26] by mixing equal volumes (100 μl) of medium and Griess reagent (1% sulfanilamide, 0.1% N-1-naphthyl-ethylenediamine dihydrochloride, 2.5% phosphoric acid) and measuring absorbency at 550 nm.

2.6. Statistical analysis

Data are presented as means \pm standard error of the mean (SEM). Statistical evaluation of data was performed by Student's *t*-test or the randomized blocks design analysis of variance (ANOVA). Dunnett's post-hoc test was used for multiple comparisons.

3. Results

3.1. Phase contrast and immunofluorescence light microscopy

Phase contrast microscopy revealed that our extraction protocol produced mixed glial cell cultures, consisting of an astrocytic

monolayer and loosely adherent microglia (Fig. 1A, white arrows) on top. It was observed that shaking the plates dislodged microglia, resulting in a highly enriched microglia cell culture. This was confirmed by immunostaining of cultures prepared from three different animals, which showed that $94.6 \pm 2.9\%$ of cells released by shaking were IBA-1-positive microglia (Fig. 1D). Double immunostaining revealed that 100% of the IBA-1 positive microglia were also positive for IFN- γ -R (Fig. 1C–E) and CD14 (Fig. 2A–C). Further expansion of the primary mixed cell cultures combined with removal of microglia by shaking (as described in the methods section) resulted in highly purified astrocytic cell cultures (Fig. 1B, F–K); immunostaining of astrocyte-enriched cultures prepared from 4 different animals revealed that $98.3 \pm 1.1\%$ of cells were GFAP positive. Double immunofluorescence experiments showed that porcine astrocytes expressed IFN- γ -R (Fig. 1F–K) and CD14 (Fig. 2D–F). There were no noticeable differences in the intensity of microglia and astrocyte staining obtained using two different anti IFN- γ -R antibodies and the anti-CD14 antibody. Since 100% purity was not achieved for either microglia or astrocyte cultures, we confirmed by means of immunocytochemistry the presence of small number of astrocytes in microglia-enriched cultures and even smaller number of microglia in astrocyte-enriched cultures. Presence of contaminating oligodendrocytes also could not be ruled out.

3.2. Glial cytotoxicity assay

Stimulation of adult porcine microglia with both LPS and porcine IFN- γ resulted in microglia supernatants with significant toxicity towards human SH-SY5Y neuroblastoma cells (Fig. 3A). Stimulation of microglia with either LPS or IFN- γ alone, followed by the transfer of microglia cell-free supernatants to SH-SY5Y neuroblastoma cells, resulted in only moderate level of toxicity towards neuronal cells. However, when microglia stimulation was achieved with a combination of LPS and IFN- γ , only 38% of neuronal cells remained viable

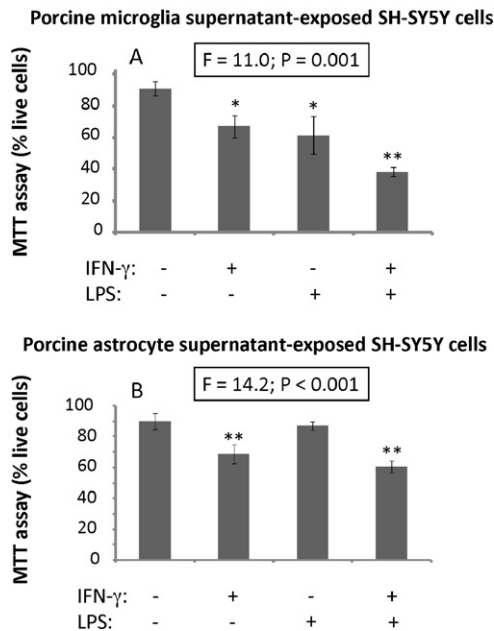


Fig. 3. Cell-free supernatants from stimulated porcine microglia and astrocyte cultures are toxic towards human neuroblastoma SH-SY5Y cells. Adult porcine microglia (A) and astrocyte (B) cultures were stimulated by LPS (0.5 $\mu\text{g/ml}$) and/or porcine IFN- γ (0.1 $\mu\text{g/ml}$) for 48 h. Subsequently, cell-free supernatants were removed and transferred to SH-SY5Y neuroblastoma cell cultures that had been plated 24 h earlier. Neuronal cell viability was measured 72 h later by the MTT assay. Cultures prepared from seven (A) and five (B) different animals were analysed. Randomized blocks design ANOVA was used to calculate F and P values; * $P < 0.01$, ** $P < 0.05$ significantly different from cell viability in cultures exposed to supernatants from unstimulated cells, Dunnett's post-hoc test.

following incubation with supernatants from stimulated porcine microglia.

We also demonstrated that stimulated porcine astrocytes showed significant toxicity towards the human SH-SY5Y neuroblastoma cells (Fig. 3B). IFN- γ alone induced adult porcine astrocyte cytotoxicity, while LPS alone failed to cause detectable levels of toxicity towards the neuronal cells. Furthermore, the combination of LPS and IFN- γ caused the toxicity similar to that observed by stimulation of astrocytes with IFN- γ alone.

We confirmed observations with porcine astrocytes using live/dead fluorescent dye assay. Counting of the SH-SY5Y cells in a blinded fashion revealed that cultures that had been exposed to supernatants from LPS and IFN- γ -stimulated astrocytes for 72 h had only a small, but statistically significant reduction of neuronal viability to $72.5 \pm 0.7\%$. The corresponding value in cultures exposed to supernatants from unstimulated cells was $89.1 \pm 1.0\%$ (data obtained from 4 independent experiments). The reduction in the total number of SH-SY5Y cells (live + dead) per field of view was much smaller in samples exposed to supernatants from stimulated astrocytes (54.7 ± 5.1 cells/field of view; Max = 68; Min = 46) compared to unstimulated cells (56.8 ± 14.5 cells/field of view; Max = 94; Min = 38). This difference was not significant ($P = 0.55$, Student's t -test, $N = 8$ slides for each condition). These observations indicate that the decreases in MTT signal and percent live cells in the cultures exposed to supernatants from stimulated astrocytes was at least partially due to the induction of SH-SY5Y cell death. Nonetheless, possible effects of astrocyte supernatants on SH-SY5Y cell proliferation rate cannot be completely ruled out.

Due to the possibility that the observed SH-SY5Y cell toxicity could be caused by either LPS or IFN- γ present in stimulated glial cell supernatants that were transferred to neuronal cells, we studied the direct effects of these proinflammatory mediators on SH-SY5Y cell viability. According to the MTT assay performed after

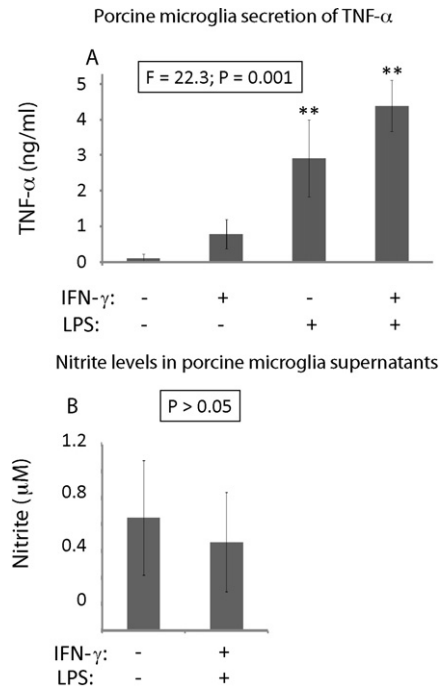


Fig. 4. LPS and IFN- γ treatment induces secretion of TNF- α by porcine microglia, while nitrite levels under the same experimental conditions remain unchanged. Adult porcine microglia cultures were stimulated by LPS (0.5 $\mu\text{g/ml}$) and/or porcine IFN- γ (0.1 $\mu\text{g/ml}$) for 48 h. TNF- α (A) and nitrite (B) concentrations in the cell-free supernatants were measured by ELISA and Griess reagents respectively. Cultures prepared from three different animals were analysed. Randomized blocks design ANOVA was used to calculate F and P values; ** $P < 0.01$, significantly different from unstimulated microglia samples, Dunnett's post-hoc test (A). No statistically significant changes in nitrite levels were detected according to the Student's t -test (B).

72 h incubation, neither LPS nor IFN- γ at the concentrations used to stimulate glial cells caused reduction of SH-SY5Y cell viability (data not shown).

3.3. Secretion of TNF- α and nitrite

Fig. 4A demonstrates that adult porcine microglia under the experimental conditions causing their cytotoxic response secrete detectable levels of TNF- α . The increase in TNF- α concentration was statistically significant when LPS alone or a combination of LPS and IFN- γ were used as stimuli. IFN- γ alone was a much weaker stimulus and no statistically significant increase in TNF- α secretion was observed in these samples. Adult porcine astrocytes stimulated under the experimental conditions causing their cytotoxic response did not respond with increased TNF- α secretion. Stimulation of these cells with 0.1 $\mu\text{g/ml}$ IFN- γ for 48 h did not increase TNF- α concentration in astrocyte-enriched culture supernatants; cultures prepared from four different animals were analysed (data not shown).

Measurement of nitrite levels in cell-free supernatants showed that neither microglia (Fig. 4B) nor astrocytes (data obtained from four different animals are not shown) prepared from adult porcine tissues responded to LPS and IFN- γ stimulation with increased nitric oxide (NO) production.

4. Discussion

We tried several different cell extraction techniques that have been described in the literature thus far for preparation of neonatal porcine and adult human astrocyte and microglia cultures. The extraction technique that yielded the best results for adult pig glial

culture preparation is described in Section 2 and represents a modified version of the previously described procedures reported for isolation of glia from new-born pigs [22,50] and adult human tissues [26,29,30]. We achieved the best results by first preparing mixed glial cell cultures, which were expanded *in vitro* to generate a monolayer of astrocytes with microglia growing loosely attached on top of the adherent astrocytes (Fig. 1A). Subsequently, purified microglia cultures were prepared by shaking the plates to dislodge the loosely adherent microglia cells. This method of preparation of microglia cell cultures is similar to the procedures used to prepare neonatal rodent [17] and porcine [50] microglia. Unlike neonatal rodent microglia, which divide and therefore can be harvested from mixed glial cultures for several weeks [15], adult porcine microglia had only limited capacity to proliferate; on average, we were able to harvest microglia only twice from each mixed glial cell culture. The third shaking generated at least four times less cells; therefore, adult porcine microglia cells were not dividing effectively under our *in vitro* cell culture conditions. We have previously observed that adult human microglia prepared from surgical and post-mortem specimens do not proliferate (unpublished observations), which has also been reported by other laboratories studying adult human microglia [32,36,52]. We were also unable to achieve a good yield of microglia cells using differential adhesion properties of microglia and astrocytes either with or without the use of Percoll gradients. These techniques have been commonly used to prepare adult human microglia cultures either from post-mortem or surgical specimens as well as from rodent brains [17,26,37]. Adult porcine astrocytes, similar to this cell type from all other species studied thus far, were actively dividing when transferred to *in vitro* cell culture environment. With continued passaging we were able to achieve highly enriched astrocyte cultures.

We also performed functional assays to assess the porcine glia. A number of studies have reported that stimulated human and rodent microglia become toxic to neuronal cells derived from various tissues (reviewed in [28,51]). Our study confirmed that adult porcine microglia, when stimulated with a combination of LPS and porcine IFN- γ , effectively induced human SH-SY5Y neuroblastoma cell death (Fig. 3A). Stimulation of porcine microglia with LPS or IFN- γ alone resulted in modest levels of toxicity towards neuronal cells. These data are very similar to our previously published observations where LPS and IFN- γ were used to induce neurotoxic response of human microglia derived from post-mortem and surgical samples [26,29].

Recently it was reported that human adult astrocytes and U-373 MG cells stimulated by IFN- γ become toxic to neuronal cells and that they do not respond to LPS stimulation [20]. We observed a very similar trend with cultured adult porcine astrocytes, which responded to IFN- γ stimulation by secreting neurotoxins while LPS alone treatment was ineffective (Fig. 3B). Porcine astrocytes caused considerably lower levels of SH-SY5Y cell death compared to microglia according to the MTT assay. Comparison of our experimental data with previously published observations demonstrated that adult porcine glial cells responded to LPS and IFN- γ stimulation in a manner similar to their human counterparts, even though the resulting toxicity levels (15–60% cell death) were considerably lower when compared to human and rodent microglia or astrocyte experiments, in which up to 90% neuronal cell death could be observed [4,20,26,31,35,53].

Studies on porcine glial cell neurotoxicity indicated that both microglia and astrocytes obtained from adult porcine tissues expressed functional IFN- γ -R. We confirmed the expression of the IFN- γ -R on both microglia and astrocytes by double immunofluorescence technique (Fig. 1). It was also apparent that the two porcine glial cell types responded differently to LPS treatment, which caused significant upregulation of microglia toxicity, but

had no effect on this parameter in astrocytes (Fig. 3). It has been established that LPS initiates its biological activities through a heteromeric receptor complex containing CD14, Toll-like receptor 4 (TLR4), and at least one other protein, MD-2 [10]. Since cultured porcine microglia and astrocytes expressed similar levels of CD14 (see Fig. 2), the inability of astrocytes to respond to LPS stimulation could stem from lower levels of TLR4 expression in astrocytes compared to microglia, which has already been reported for adult human [24] and murine [7] astrocytes. Differences existing in downstream signaling engaged by the LPS receptor complex in the two glial cell types, such as p38 mitogen-activated protein (MAP) kinase pathway [33], also cannot be ruled out.

A number of different substances have been suggested as possible glial neurotoxins. They include TNF- α , glutamate, L-cysteine, quinolinic acid, tissue plasminogen activator, cathepsin B, matrix metalloproteases, reactive oxygen and nitrogen species including NO and peroxynitrite (ONOO⁻); glial cells may also release a mixture of toxins in response to specific stimuli (for reviews see [28,51]). Here we studied secretion of two of these candidate molecules by adult porcine microglia and astrocytes under the cell culture conditions causing their cytotoxic response. We showed that porcine microglia responded to stimulation by LPS alone by secreting TNF- α . IFN- γ on its own did not cause significant secretion of TNF- α , but it had a synergistic effect when added to microglia cells in combination with LPS (Fig. 4A). Adult porcine astrocytes also did not respond to IFN- γ alone treatment by secreting TNF- α . Therefore, under our experimental conditions, the adult porcine glia neurotoxic responses did not correlate with the levels of TNF- α in cell culture supernatants. The ineffectiveness of IFN- γ and effectiveness of LPS alone to induce TNF- α secretion in porcine microglia cells is consistent with the previously published reports using rodent glial cells [9]. Interestingly, Lafortune et al. [30] have reported low levels of TNF- α mRNA in adult human astrocytes stimulated with LPS and IFN- γ compared to stimulated fetal human astrocytes and adult human microglia.

We were unable to detect increased nitrite levels in cell culture supernatants from either stimulated microglia or astrocytes, which indicated that the neuronal cell death observed under our cell culture conditions was not mediated by NO. The inability of adult porcine glial cells to secrete detectable levels of NO is similar to our previously published observations with human adult microglia, which did not produce NO under the same experimental conditions that were used in the current study [26]. Hu et al. [22] demonstrated earlier that, similar to human cells, neonatal porcine microglia did not respond to LPS and IFN- γ treatment with increased secretion of NO. Nitric oxide has been reported to be readily induced by these inflammatory mediators in rodent microglia and astrocytes [4,9,19,21]. It is possible that porcine glial cells may respond with NO production under different stimulatory conditions; thus a combination of interleukin (IL)-1 β , TNF- α and IFN- γ has been shown to induce NO production in human astrocytes [23].

Our study shows that adult porcine microglia toxicity is induced by LPS and IFN- γ , while only IFN- γ was able to trigger porcine astrocyte toxicity. This activation pattern was consistent with our previous studies on adult human microglia and astrocytes [20,26,29]. However, the induction of glial neurotoxicity, as well as the release of various pro-inflammatory mediators and neurotoxins, appears to be both species and stimulus dependent. For example, LPS alone induced TNF- α , IL-1 β and IL-6 secretion, while a combination of LPS and IFN- γ was required for induction of reactive oxygen species and neurotoxicity in both astrocytes and microglia prepared from newborn mice [39]. Microglia neurotoxicity induced by LPS and IFN- γ is well documented and has been attributed to a number of toxic species including superoxide anion, glutamate, NO, peroxynitrite, proteases, TNF- α and a combination of different toxins [4,27,43,53].

Astrocyte-induced neurotoxicity has been less studied. Two reports have demonstrated that human fetal astrocytes stimulated by a combination of IFN- γ and IL-1 β become neurotoxic [8,13]; application of specific inhibitors revealed involvement of TNF- α and NO as mediators of astrocytic toxicity, as well as partial involvement of glutamate and reactive oxygen species, which indicated that a mixture of several toxins was responsible for human fetal astrocyte neurotoxicity.

Due to the limited availability of human tissues, it is important to establish alternative model systems that could be used to study mechanisms of human diseases and to search for effective medicines. The porcine immune system has a number of characteristics that makes it similar to human [44]. Furthermore, in a previous report Hu et al. [22] demonstrated that new-born porcine microglia behave similar to human cells in terms of cytokine and NO production. Here we extended these observations by showing that porcine microglia and astrocytes prepared from adult animals could be induced to secrete neurotoxins in a manner that was similar to previously published observations with adult human glial cells. Use of adult cells could be advantageous for studies aimed at mechanisms of aging and age-associated neurodegenerative diseases since age-dependent differences in glial cell physiology have been documented for murine microglia [47], as well as rat [40] and human [30] astrocytes. Another advantage for choosing this source of tissues is availability of adult porcine tissues in most countries, and the fact that there is no need for costly animal care facilities to obtain such tissues. Therefore, the described method of culturing adult porcine glial cells could be a useful tool for neuroscience and neuroprotective drug discovery programs.

Conflict of interest

The authors declare that there are no conflicts of interest.

Acknowledgements

This work was supported by grants from the Natural Sciences and Engineering Research Council of Canada (A.K.), the Jack Brown and Family Alzheimer's Disease Research Foundation (A.K.) and the Pacific Alzheimer Research Foundation (S.H.). We thank staff of Inland Packers and Mr. Richard Yntema for providing us with the porcine tissues. We also thank Dr. Douglas Walker for helpful discussions on glial cell purification techniques and J. Madeira and J. Powell for technical assistance.

The study sponsors had no involvement in the study design; collection, analysis and interpretation of data; the writing of the manuscript; the decision to submit the manuscript for publication.

References

- [1] D.D. Allen, R. Caviedes, A.M. Cardenas, T. Shimahara, J. Segura-Aguilar, P.A. Caviedes, Cell lines as *in vitro* models for drug screening and toxicity studies, *Drug Dev. Ind. Pharm.* 8 (2005) 757–768.
- [2] M. Arciszewski, S. Pierzynowski, E. Ekblad, Lipopolysaccharide induces cell death in cultured porcine myenteric neurons, *Digest. Dis. Sci.* 9 (2005) 1661–1668.
- [3] J. Auwerx, The human leukemia cell line, THP-1: a multifaceted model for the study of monocyte-macrophage differentiation, *Experientia* 1 (1991) 22–31.
- [4] A. Bal-Price, G.C. Brown, Inflammatory neurodegeneration mediated by nitric oxide from activated glia-inhibiting neuronal respiration, causing glutamate release and excitotoxicity, *J. Neurosci.* 17 (2001) 6480–6491.
- [5] K. Barnes, A.J. Kenny, A.J. Turner, Localization of aminopeptidase N and dipeptidyl peptidase IV in pig striatum and in neuronal and glial cell cultures, *Eur. J. Neurosci.* 4 (1994) 531–537.
- [6] M.L. Block, L. Zecca, J.S. Hong, Microglia-mediated neurotoxicity: uncovering the molecular mechanisms, *Nat. Rev. Neurosci.* 1 (2007) 57–69.
- [7] C.C. Bowman, A. Rasley, S.L. Tranguch, I. Marriott, Cultured astrocytes express toll-like receptors for bacterial products, *Glia* 3 (2003) 281–291.
- [8] C.C. Chao, S. Hu, W.S. Sheng, D. Bu, M.I. Bukrinsky, P.K. Peterson, Cytokine-stimulated astrocytes damage human neurons via a nitric oxide mechanism, *Glia* 3 (1996) 276–284.
- [9] S.H. Choi, D.H. Choi, K.S. Song, K.H. Shin, B.G. Chun, Zaprinast, an inhibitor of cGMP-selective phosphodiesterases, enhances the secretion of TNF- α and IL-1 β and the expression of iNOS and MHC class II molecules in rat microglial cells, *J. Neurosci. Res.* 3 (2002) 411–421.
- [10] J. da Silva Correia, K. Soldau, U. Christen, P.S. Tobias, R.J. Ulevitch, Lipopolysaccharide is in close proximity to each of the proteins in its membrane receptor complex. Transfer from CD14 to TLR4 and MD-2, *J. Biol. Chem.* 24 (2001) 21129–21135.
- [11] M.A. Deli, C.S. Abraham, Y. Kataoka, M. Niwa, Permeability studies on *in vitro* blood–brain barrier models: physiology, pathology, and pharmacology, *Cell. Mol. Neurobiol.* 1 (2005) 59–127.
- [12] M.D. Dooldeniya, A.N. Warrens, Xenotransplantation: where are we today? *J. R. Soc. Med.* 3 (2003) 111–117.
- [13] M. Downen, T.D. Amaral, L.L. Hua, M.L. Zhao, S.C. Lee, Neuronal death in cytokine-activated primary human brain cell culture: role of tumor necrosis factor- α , *Glia* 2 (1999) 114–127.
- [14] R. Filipovic, N. Zecevic, Neuroprotective role of minocycline in co-cultures of human fetal neurons and microglia, *Exp. Neurol.* 1 (2008) 41–51.
- [15] A.M. Floden, C.K. Combs, Microglia repetitively isolated from *in vitro* mixed glial cultures retain their initial phenotype, *J. Neurosci. Methods* 2 (2007) 218–224.
- [16] H.M. Gao, J.S. Hong, Why neurodegenerative diseases are progressive: uncontrolled inflammation drives disease progression, *Trends Immunol.* 8 (2008) 357–365.
- [17] D. Giuliani, T.J. Baker, Characterization of ameboid microglia isolated from developing mammalian brain, *J. Neurosci.* 8 (1986) 2163–2178.
- [18] C.K. Glass, K. Saijo, B. Winner, M.C. Marchetto, F.H. Gage, Mechanisms underlying inflammation in neurodegeneration, *Cell* 6 (2010) 918–934.
- [19] G. Guo, N.R. Bhat, Hypoxia/reoxygenation differentially modulates NF- κ B activation and iNOS expression in astrocytes and microglia, *Antioxid. Redox Signal.* 5–6 (2006) 911–918.
- [20] S. Hashioka, A. Klegeris, C. Schwab, P.L. McGeer, Interferon- γ -dependent cytotoxic activation of human astrocytes and astrocytoma cells, *Neurobiol. Aging* 12 (2009) 1924–1935.
- [21] R.P. Hellendall, J.P. Ting, Differential regulation of cytokine-induced major histocompatibility complex class II expression and nitric oxide release in rat microglia and astrocytes by effectors of tyrosine kinase, protein kinase C, and cAMP, *J. Neuroimmunol.* 1–2 (1997) 19–29.
- [22] S. Hu, C.C. Chao, K.V. Khanna, G. Gekker, P.K. Peterson, T.W. Molitor, Cytokine and free radical production by porcine microglia, *Clin. Immunol. Immunopathol.* 1 (1996) 93–96.
- [23] S. Hu, W.S. Sheng, P.K. Peterson, C.C. Chao, Differential regulation by cytokines of human astrocyte nitric oxide production, *Glia* 4 (1995) 491–494.
- [24] C.S. Jack, N. Arbour, J. Manusow, V. Montgrain, M. Blain, E. McCrear, A. Shapiro, J.P. Antel, TLR signaling tailors innate immune responses in human microglia and astrocytes, *J. Immunol.* 7 (2005) 4320–4330.
- [25] V.V. Jeliakova-Mecheva, D.J. Bobilya, A porcine astrocyte/endothelial cell co-culture model of the blood–brain barrier, *Brain Res. Brain Res. Protoc.* 2 (2003) 91–98.
- [26] A. Klegeris, C.J. Bissonnette, P.L. McGeer, Modulation of human microglia and THP-1 cell toxicity by cytokines endogenous to the nervous system, *Neurobiol. Aging* 5 (2005) 673–682.
- [27] A. Klegeris, J. Li, T.K. Bammler, J. Jin, D. Zhu, D.T. Kashima, S. Pan, S. Hashioka, J. Maguire, P.L. McGeer, J. Zhang, Prolyl endopeptidase is revealed following SILAC analysis to be a novel mediator of human microglial and THP-1 cell neurotoxicity, *Glia* 6 (2008) 675–685.
- [28] A. Klegeris, P.L. McGeer, Non-steroidal anti-inflammatory drugs (NSAIDs) and other anti-inflammatory agents in the treatment of neurodegenerative disease, *Curr. Alzheimer Res.* 3 (2005) 355–365.
- [29] A. Klegeris, D.G. Walker, P.L. McGeer, Toxicity of human THP-1 monocytic cells towards neuron-like cells is reduced by non-steroidal anti-inflammatory drugs (NSAIDs), *Neuropharmacology* 7 (1999) 1017–1025.
- [30] L. LaFortune, J. Nalbantoglu, J.P. Antel, Expression of tumor necrosis factor α (TNF α) and interleukin 6 (IL-6) mRNA in adult human astrocytes: comparison with adult microglia and fetal astrocytes, *J. Neuropath. Exp. Neurol.* 5 (1996) 515–521.
- [31] W. Le, D. Rowe, W. Xie, I. Ortiz, Y. He, S.H. Appel, Microglial activation and dopaminergic cell injury: an *in vitro* model relevant to Parkinson's disease, *J. Neurosci.* 21 (2001) 8447–8455.
- [32] S.C. Lee, W. Liu, C.F. Brosnan, D.W. Dickson, GM-CSF promotes proliferation of human fetal and adult microglia in primary cultures, *Glia* 4 (1994) 309–318.
- [33] Y.B. Lee, J.W. Schrader, S.U. Kim, p38 Map kinase regulates TNF- α production in human astrocytes and microglia by multiple mechanisms, *Cytokine* 7 (2000) 874–880.
- [34] M.M. Lipovsky, G. Gekker, W.R. Anderson, T.W. Molitor, P.K. Peterson, A.I. Hoepelman, Phagocytosis of nonopsonized *Cryptococcus neoformans* by swine microglia involves CD14 receptors, *Clin. Immunol. Immunopathol.* 2 (1997) 208–211.
- [35] Y. Liu, L. Qin, G. Li, W. Zhang, L. An, B. Liu, J.S. Hong, Dextromethorphan protects dopaminergic neurons against inflammation-mediated degeneration through inhibition of microglial activation, *J. Pharmacol. Exp. Ther.* 1 (2003) 212–218.
- [36] L.F. Lue, L. Brachova, D.G. Walker, J. Rogers, Characterization of glial cultures from rapid autopsies of Alzheimer's and control patients, *Neurobiol. Aging* 3 (1996) 421–429.
- [37] L.F. Lue, D.G. Walker, J. Rogers, Modeling microglial activation in Alzheimer's disease with human postmortem microglial cultures, *Neurobiol. Aging* 6 (2001) 945–956.

- [38] B.T. Metzger, D.M. Barnes, J.D. Reed, Purple carrot (*Daucus carota* L.) polyacetylenes decrease lipopolysaccharide-induced expression of inflammatory proteins in macrophage and endothelial cells, *J. Agric. Food. Chem.* 10 (2008) 3554–3560.
- [39] T. Mizuno, R. Kuno, A. Nitta, T. Nabeshima, G. Zhang, J. Kawanokuchi, J. Wang, S. Jin, H. Takeuchi, A. Suzumura, Protective effects of nicergoline against neuronal cell death induced by activated microglia and astrocytes, *Brain Res.* 1–2 (2005) 78–85.
- [40] T. Nakagawa, J.P. Schwartz, Gene expression patterns in *in vivo* normal adult astrocytes compared with cultured neonatal and normal adult astrocytes, *Neurochem. Int.* 2–3 (2004) 203–242.
- [41] P.K. Peterson, G. Gekker, S. Hu, W.B. Anderson, M. Teichert, C.C. Chao, T.W. Molitor, Multinucleated giant cell formation of swine microglia induced by *Mycobacterium bovis*, *J. Infect. Dis.* 5 (1996) 1194–1201.
- [42] C. Pilon, F. Meurens, A. Dauba, H. Salmon, F. Velge-Roussel, Y. Lebranchu, C. Baron, Induction of porcine regulatory cells by mycophenolic acid-treated dendritic cells, *Transplant Proc.* 2 (2009) 700–702.
- [43] L. Qin, Y. Liu, T. Wang, S.J. Wei, M.L. Block, B. Wilson, B. Liu, J.S. Hong, NADPH oxidase mediates lipopolysaccharide-induced neurotoxicity and proinflammatory gene expression in activated microglia, *J. Biol. Chem.* 2 (2004) 1415–1421.
- [44] H.J. Rothkotter, E. Sowa, R. Pabst, The pig as a model of developmental immunology, *Human Exp. Toxicol.* 9–10 (2002) 533–536.
- [45] K. Sak, P. Illes, Neuronal and glial cell lines as model systems for studying P2Y receptor pharmacology, *Neurochem. Int.* 6 (2005) 401–412.
- [46] A.B. Salmina, Neuron–glia interactions as therapeutic targets in neurodegeneration, *J. Alzheimer Dis.* 3 (2009) 485–502.
- [47] M. Sawada, H. Sawada, T. Nagatsu, Effects of aging on neuroprotective and neurotoxic properties of microglia in neurodegenerative diseases, *Neurodegener. Dis.* 3–4 (2008) 254–256.
- [48] G. Sowa, G. Gekker, M.M. Lipovsky, S. Hu, C.C. Chao, T.W. Molitor, P.K. Peterson, Inhibition of swine microglial cell phagocytosis of *Cryptococcus neoformans* by femtomolar concentrations of morphine, *Biochem. Pharmacol.* 6 (1997) 823–828.
- [49] B.R. Tambuyzer, I. Lambrichts, M. Lenjou, E.J. Nouwen, Effects of the pig renal epithelial cell line LLC-PK1 and its conditioned medium on the phenotype of porcine microglia *in vitro*, *Eur. J. Cell Biol.* 4 (2007) 221–232.
- [50] B.R. Tambuyzer, E.J. Nouwen, Inhibition of microglia multinucleated giant cell formation and induction of differentiation by GM-CSF using a porcine *in vitro* model, *Cytokine* 4 (2005) 270–279.
- [51] L. Walter, H. Neumann, Role of microglia in neuronal degeneration and regeneration, *Semin. Immunopathol.* 4 (2009) 513–525.
- [52] K. Williams, A. Bar-Or, E. Ulvestad, A. Olivier, J.P. Antel, V.W. Yong, Biology of adult human microglia in culture: comparisons with peripheral blood monocytes and astrocytes, *J. Neuropathol. Exp. Neurol.* 5 (1992) 538–549.
- [53] Z. Xie, M. Wei, T.E. Morgan, P. Fabrizio, D. Han, C.E. Finch, V.D. Longo, Peroxynitrite mediates neurotoxicity of amyloid beta-peptide1–42- and lipopolysaccharide-activated microglia, *J. Neurosci.* 9 (2002) 3484–3492.
- [54] P. Yang, L. Chen, R. Zwart, A. Kijlstra, Immune cells in the porcine retina: distribution, characterization and morphological features, *Invest. Ophthalmol. Vis. Sci.* 5 (2002) 1488–1492.